MINISTRY OF NATIONAL EDUCATION

THE ANNALS OF "DUNAREA DE JOS" UNIVERSITY OF GALATI

Fascicle IX
METALLURGY AND MATERIALS SCIENCE

YEAR XXXVII (XLII)
June 2019, no. 2

ISSN 2668-4748; e-ISSN 2668-4756

2019
GALATI UNIVERSITY PRESS

EDITORIAL BOARD

EDITOR-IN-CHIEF

Prof. Marian BORDEI – "Dunarea de Jos" University of Galati, Romania

EXECUTIVE EDITOR

Assist. Prof. Marius BODOR – "Dunarea de Jos" University of Galati, Romania

SCIENTIFIC ADVISORY COMMITTEE

Assoc. Prof. Stefan BALTA – "Dunarea de Jos" University of Galati, Romania
Prof. Acad. Ion BOSTAN – Technical University of Moldova, the Republic of Moldova
Researcher Mihai BOTAN – The National Institute of Aerospace Research, Romania
Prof. Vasile BRATU – Valahia University of Targoviste, Romania
Prof. Francisco Manuel BRAZ FERNANDES – New University of Lisbon Caparica, Portugal
Prof. Bart Van der BRUGGEN – Katholieke Universiteit Leuven, Belgium
Prof. Acad. Valeriu CANTSER – Academy of the Republic of Moldova
Prof. Alexandru CHIRIAC – "Dunarea de Jos" University of Galati, Romania
Assoc. Prof. Stela CONSTANTINESCU – "Dunarea de Jos" University of Galati, Romania
Assoc. Prof. Viorel DRAGAN – "Dunarea de Jos" University of Galati, Romania
Prof. Valeriu DULGHERU – Technical University of Moldova, the Republic of Moldova
Prof. Jean Bernard GUILLOT – École Centrale Paris, France
Assoc. Prof. Gheorghe GURAU – "Dunarea de Jos" University of Galati, Romania
Prof. Philippe MARCUS – École Nationale Supérieure de Chimie de Paris, France
Prof. Rodrigo MARTINS – NOVA University of Lisbon, Portugal
Prof. Strul MOISA – Ben Gurion University of the Negev, Israel
Prof. Daniel MUNTEANU – "Transilvania" University of Brasov, Romania
Assist. Prof. Alina MURESAN – "Dunarea de Jos" University of Galati, Romania
Prof. Maria NICOLAE – Politehnica University Bucuresti, Romania
Prof. Florentina POTECASU – "Dunarea de Jos" University of Galati, Romania
Prof. Cristian PREDESCU – Politehnica University of Bucuresti, Romania
Prof. Tamara RADU – "Dunarea de Jos" University of Galati, Romania
Prof. Iulian RIPOSAN – Politehnica University of Bucuresti, Romania
Prof. Antonio de SAJA – University of Valladolid, Spain
Prof. Wolfgang SAND – Duisburg-Essen University Duisburg, Germany
Assist. Prof. Rafael M. SANTOS – University of Guelph, Canada
Prof. Ion SANDU – "Al. I. Cuza" University of Iasi, Romania
Prof. Mircea Horia TIEREAN – "Transilvania" University of Brasov, Romania
Prof. Elisabeta VASILESCU – "Dunarea de Jos" University of Galati, Romania
Prof. Ioan VIDA-SIMITI – Technical University of Cluj Napoca, Romania
Assoc. Prof. Petrica VIZUREANU – "Gheorghe Asachi" Technical University Iasi, Romania
Prof. François WENGER – École Centrale Paris, France

EDITING SECRETARY

Prof. Marian BORDEI – "Dunarea de Jos" University of Galati, Romania
Assist. Prof. Marius BODOR – "Dunarea de Jos" University of Galati, Romania
Assist. Prof. Eliza DANAILA – "Dunarea de Jos" University of Galati, Romania

THE ANNALS OF "DUNAREA DE JOS" UNIVERSITY OF GALATI
FASCICLE IX. METALLURGY AND MATERIALS SCIENCE
Nº. 2 - 2019, ISSN 2668-4748; e-ISSN 2668-4756
Volume DOI: https://doi.org/10.35219/mms.2019.2

Table of Contents

THE ANNALS OF "DUNAREA DE JOS" UNIVERSITY OF GALATI
FASCICLE IX. METALLURGY AND MATERIALS SCIENCE
Nº. 2 - 2019, ISSN 2668-4748; e-ISSN 2668-4756
Volume DOI: https://doi.org/10.35219/mms.2019.2

THE ANNALS OF "DUNAREA DE JOS" UNIVERSITY OF GALATI
FASCICLE IX. METALLURGY AND MATERIALS SCIENCE
N°. 2 - 2019, ISSN 2668-4748; e-ISSN 2668-4756
Article DOI: https://doi.org/10.35219/mms.2019.2.01

MICROSTRUCTURAL ANALYSIS OF THREE LAYER DEPOSITIONS WITH Ni AND Ti ON STEEL USING THE EDS METHOD

Manuela-Cristina PERJU*, Carmen NEJNERU, Catalin Andrei TUGUI, Dumitru Doru BURDUHOS-NERGIS, Dan-Gelu GALUSCA

Technical University "Gheorghe Asachi" of Iasi-Romania, Department of Technologies and Equipments for Materials Processing, Blvd. Mangeron, No. 51, 700050, Iasi, Romania
e-mail: * cryss_ela@yahoo.com

ABSTRACT

The ESD method (electro spark deposition) is used to cover through deposition the active parts of machines, working in heavy abrasive wear moist environment as well as in a dry environment. The paper proposes the use ESD method for Fe-C alloys for obtaining thin layers system with physical-mechanical properties improved comparing to base material. Due to polar effect, the predominant transfer of anode's material (electrode) towards cathode (piece) assures the forming of the superficial layer with well-determined physical - chemical properties. In addition, in multiple layers case the deposit of a supplementary layer emphasizes the diffusion of the first deposited layer by anchoring more the coating.

KEYWORDS: ESD method, microstructure, layer

1. Introduction

Nowadays, coating procedures on metallic surfaces are spreadingly used in industry for improving exploitation performances of the pieces and mechanic structures.

Going from these relevant aspects from industrial practice, the researches made in different countries such as Japan, China [1, 3, 4], Ireland [2] emphasized a series of knowledge that refer to technologies and studies with fundamental and experimental character which lead to improving superficial layers properties by using the impulse electric discharges method. It is seen that the main causes that produce the necessity of replacing some system parts in automotive industry are the destructions of surface layer through wear, fatigue and corrosion (ex. piston rings for Diesel engine).

Thus, the properties of the metallic materials were improved [5, 6], in order to raise deposited layer's adherence to basic material, in coating of composite materials by using impulse electric discharges.

Hardening technology with impulse electric discharge has known an explosive development due to special properties of wear resistance of the obtained layer. There were made researches [7] referring to the applicability of coating method with impulse electric discharges on metallic materials used in marine transport by improving corrosion resistance in seawater. Also, it was emphasized the influence of heat treatments on the characteristics of the deposited layers obtained with vibrating electrode on materials used for cutting tools [8].

Obtaining a thin layers system with special properties (wear resistance, corrosion resistance, impact resistance) requires a correct choice of the adding material in strict correlation with physical-mechanical properties of the base material [9-11]. Taking into account that the main objective is to improve the wear behaviour by deposition of hard layers, appears as necessary, in order to achieve the objective, the generation of a thin layers system: anchor layer with comparable properties to the support material, and the surface layer with required properties.

The technology involves a method of deposition and alloying and thin adherent layer, based on impulse electric discharge technology on one side, with a total of up to 3 layers of electrode material successor of nickel and titanium, which gives the parts processed a wide range of properties (mechanical strength, surface hardness corresponding compressive stresses and martensitic structure of complex carbide layer), which reduces the effects of wear, having positive effects on the life of the product

THE ANNALS OF "DUNAREA DE JOS" UNIVERSITY OF GALATI
FASCICLE IX. METALLURGY AND MATERIALS SCIENCE
N°. 2 - 2019, ISSN 2668-4748; e-ISSN 2668-4756
Article DOI: https://doi.org/10.35219/mms.2019.2.01

[12]. Durability of metal layers is the result of convolution of structural changes and thermo-mechanical fatigue.

2. Methods and materials

In order to obtain the thin layers, the ESD (electro spark deposition) method was used. This technology employs electricity stored in the capacitor to initiate an electrical spark between the cathode and the anode. The high temperature generated by the spark leads to the partial melting and mixing of the electrode and surface materials. Between two electric sparks, the amount of molten metal solidifies to form the surface layer. It must have a very good adhesion to the surface of the part and a good chemical and thermal compatibility with the substrate, as well as high qualities of resistance to wear and oxidation.

The deposition facility ELITRON 22 A [13], by ESD method, is the endowment of the laboratory Properties of metallic materials within the Faculty of Materials Science and Engineering in Iasi. The electrical diagram of the Elitron 22A type equipment is shown in Figure 1.

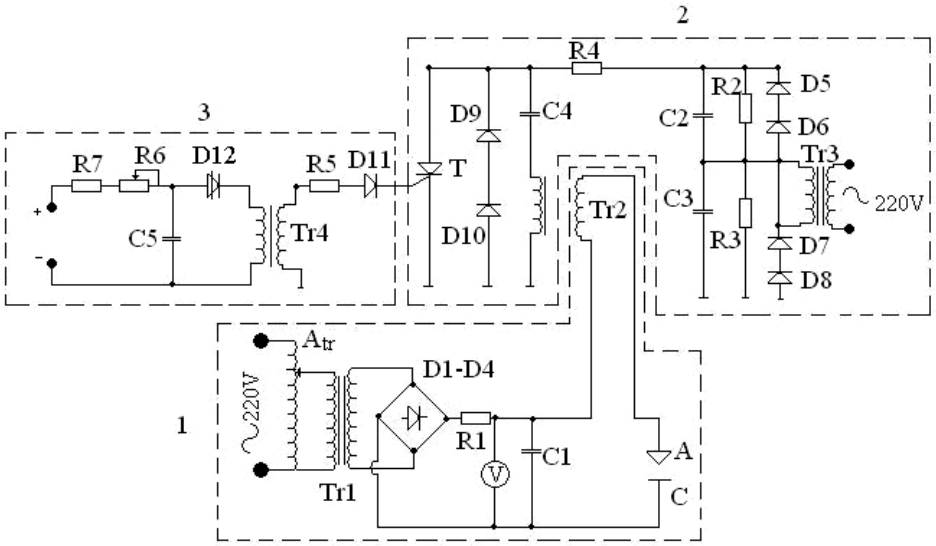

Fig. 1. *Electrical scheme of the deposition device, type Elitron 22A*

For the experiment, 42CrMo4 alloy weak steel base material, EN 10083-1 has been used, whose chemical composition was determined with the Foundry Master spectrometer [14]. It was chosen as the base material because the alloying elements, such as chromium and molybdenum, increase the quality, hardness, wear resistance, corrosion resistance and ensure good and stable mechanical properties at high temperatures.

Additive Ti and Ni electrodes were used as addition materials [15].

Table 1. *Chemical composition of 42CrMo4 alloy weak steel, %*

Element	Fe	C	Si	Mn	P	Cr	Mo	Ni	Al
Percent	95.7	0.477	0.185	0.331	0.023	1.20	0.193	1.36	0.239

The material of the electrodes strongly influences the alloying process by the ESD method, the influence being manifested both by the difficulty of deposition or by its ease and by the quality of the deposited surface (by quality understanding adhesion, roughness, layer thickness, presence of oxides, etc.).

3. Heterogeneous deposition with Ni/Ti/Ni

The Ni/Ti/Ni triple layer deposition creates relatively compact surfaces, with microdrops and microcracks due to the gases absorbed at the surface even from the liquid drop of the "droplets" deposited, Figure 2. It is observed that the splashes and craters due to the gases are especially characteristic of the deposition with nickel. The presence of the titanium in interstitial position creates the possibility of reducing this defect. EDX analysis shows by distribution, the massive presence of both titanium and as well as nickel, both having a very good coverage throughout the surface.

THE ANNALS OF "DUNAREA DE JOS" UNIVERSITY OF GALATI
FASCICLE IX. METALLURGY AND MATERIALS SCIENCE
Nº. 2 - 2019, ISSN 2668-4748; e-ISSN 2668-4756
Article DOI: https://doi.org/10.35219/mms.2019.2.01

The chemical analysis of the studied surface shows a presence of nickel of 27.99% by volume and titanium of 26.74% by volume, Figure 2b.

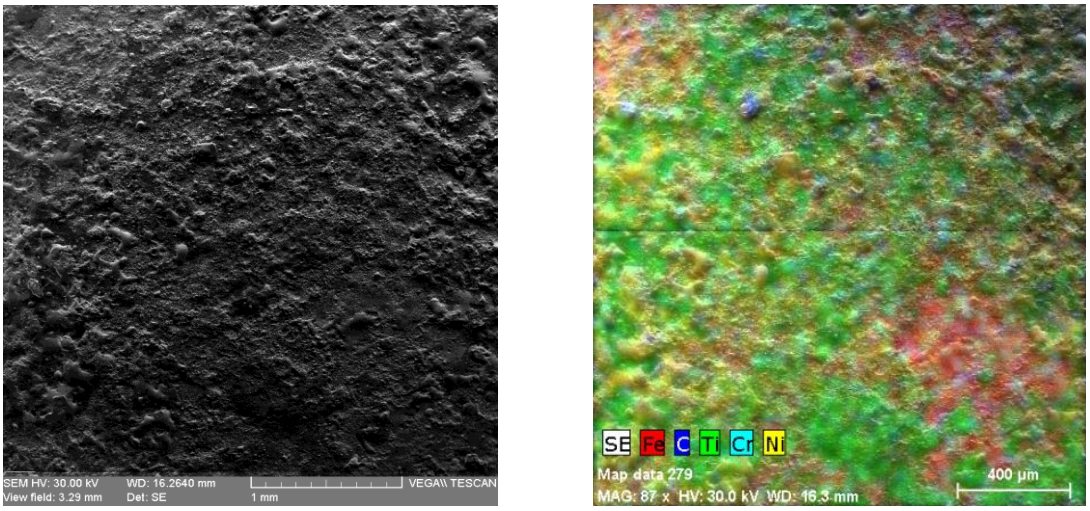

a) b)

Fig. 2. *Microstructures analysed at SEM; a) deposition with Ni / Ti / Ni on steel, SE, 1000X; b) EDX analysis for the distribution of the elements on the surface*

It is observed that the titanium has a high percentage even though it is an intermediate layer, due to its microalloying properties by dissolving in the metallic microbe.

4. Heterogeneous deposition with Ti/Ni/Ti

The Ti / Ni / Ti triple layer coating creates relatively smooth surfaces, with a slightly waved appearance due to superimposed molten "drops", with fine cracks and relatively few in number, with no obvious burns, no material overlaps, adhesions or other surface defects, Figure 3.

The effects of gas bubbles are no longer visible as in the Ni deposits a layer, which is due to the partial re-coating of the intermediate Ni layer in the coating. Surface EDX analysis shows by distribution a deposition with heavy Ti, Ni and Fe appearing on small areas by splashing and by microalloying the metal drop of the molten "drop", Figure 3b.

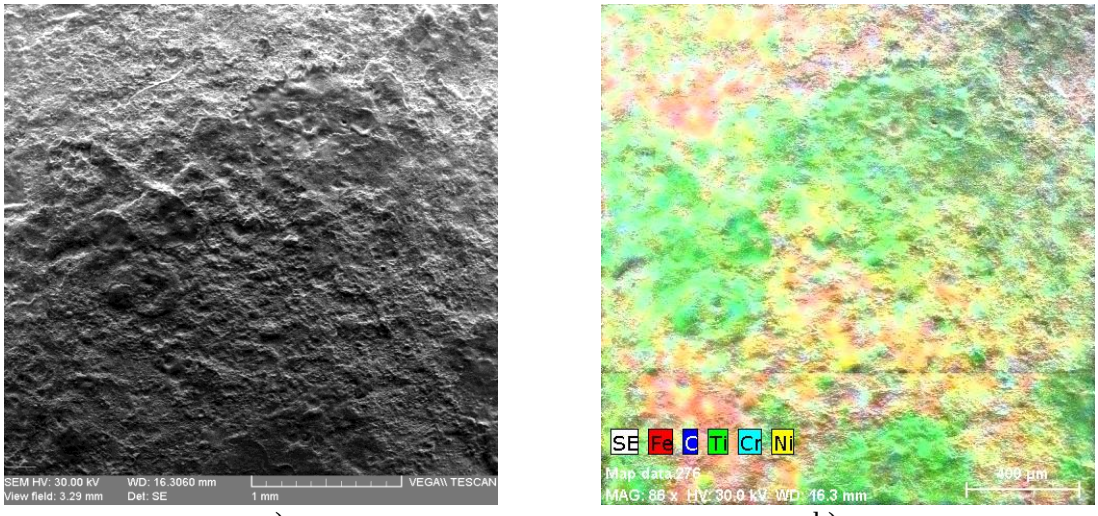

a) b)

Fig. 3. *Microstructures analysed at SEM; a) deposition with Ti/Ni/Ti on steel, SE, 1000X; b) EDX analysis for the distribution of the elements on the surface*

There is a presence of 30.43% by volume of iron, 28.94% by volume of titanium and 14.41% by volume of nickel. Also, a massive oxygen presence of 24.71% by volume is observed, due to surface oxidation because the deposition was done in ordinary atmosphere without protection.

5. Conclusions

The triple layers create compact deposits with a heavier microalloying, so that the layer grows, but not so much.

This is possible because there is an intermediate layer created from the melting of the support material with the additive material which generates very good mechanical properties (hardness, adhesion).

The thin layer hardened through impulse electric discharges method is splitted into an exterior layer with a strongly modified structure at the surface and an interior layer (diffusion layer) with the properties corresponding to basic material and added material.
The thin layers system hardened presents cracks that are advantageous to lubrication process (during exploitation) by protecting basic material of excessive wear.

Acknowledgment

This paper was realized with the support of COMPETE project nr. 9PFE/2018, financed by the Romanian Government.

References

[1]. Liu D., Gao W., Li Z., Zhang H., Hu Z., *Electro-spark deposition of Fe-based amorphous alloy coatings*, Materials Letters, 61, p. 165-167, 2007.
[2]. Hazar H., *Characterization of MoN coatings for pistons in a diesel engine*, Materials and Design, 31, p. 624-627, 2010.
[3]. Imamura S., Fukui H., Shibata A., Omori N., Setoyama M., *Properties and cutting performance of AlTiCrN/TiSiCN bilayer coatings deposited by cathodic-arc ion plating*, Surface & coatings technology, 4th International Conference on Metallurgical Coatings and Thin Films, San Diego, CA, USA, 2007.
[4]. Abboud J. H., Benyounis K. Y., Olabi A. G., Hashmi M. S. J., *Laser surface treatments of iron-based substrates for automotive application*, Journal of Materials Processing Technology, 182, p. 427-431, 2007.
[5]. Tamminen J., Sandstrom C.-E., Andersson P., *Influence of load on the tribological conditions in piston ring and cylinder liner contacts in a medium-speed diesel engine*, Tribology International, 39, p. 1643-1652, 2006.
[6]. Mikalsen R., Roskilly A. P., *A computational study of free-piston diesel engine combustion*, Applied Energy, 86, p. 1136-1143, 2009.
[7]. Perju M. C., Nejneru C., Vizureanu P., Stefanică R. G., *XPS Chemical Analysis for the Multilayer Deposition Wc/Tic/W on Gray Cast Iron Using Electric Impulse Discharge Method*, ModTech International Conference - New face of TMCR, Modern Technologies, Quality and Innovation - New face of TMCR, 24-26 May, Sinaia, Romania, 2012.
[8]. Perju M. C., Nejneru C., Vizureanu P., Axinte M., *The Surface Modification of Low Alloy Steel with Ni Electrode by Electrospark Deposition Method*, Metalurgia International, vol. XVIII, 5, p. 174-177, 2013.
[9]. Wang Y., Ma H., Li X., *Interface behavior of tungsten coating on stainless steel by electro spark deposition*, MATEC Web of Conferences, 35, 01006, 2015.
[10]. Peterkin S., *Electro-Spark Deposition Machine Design, Physical Controls and Parameter Effects*, A thesis presented to the University of Waterloo, Ontario, Canada, 2016.
[11]. Radek N., Pietraszek J., Szczotok A., *Properties of anti-wear electro-spark deposited coatings, technical transactions mechanics*, 4, p. 113-118, 2016.
[12]. Vizureanu P., Perju M. C., Achiţei D. C., Nejneru C., *Advanced Electro-Spark Deposition Process on Metallic Alloys*, Capitol 3, Advanced Surface Engineering Research, Published: November 14th, DOI: 10.5772/intechopen.75772, ISBN: 978-1-78984-340-8, 2018.
[13]. ***, *Instalaţie Elitron 22*, Academia de Ştiinţe, Republica Moldova, Chişinău, 1992.
[14]. Perju M. C., Nejneru C., Vizureanu P., Axinte M., *The surface modification of low alloy steel with Ni electrode by electrospark deposition method*, Metalurgia International, vol. XVIII, 5, p. 174-176, 2013.
[15]. Lărgeanu A. E., Nejneru C., Găluşcă D. G., Perju M. C., Axinte M., *Comparative morfology unipuls deposition with nichel and titanium electrodes using the impulse discharge method*, Buletinul Institutului Politehnic, Iaşi, Fasc.3, Tomul LV(LIX), ISSN 1453-1690, p. 45-50, 2009.

THE ANNALS OF "DUNAREA DE JOS" UNIVERSITY OF GALATI
FASCICLE IX. METALLURGY AND MATERIALS SCIENCE
N°. 2 - 2019, ISSN 2668-4748; e-ISSN 2668-4756
Article DOI: https://doi.org/10.35219/mms.2019.2.02

SAFETY ENVIRONMENTAL ASSESSMENT IN THE BLAST FURNACE SECTION

Adrian VASILIU
"Dunarea de Jos" University of Galati, Romania
e-mail: avasiliu@ugal.ro

ABSTRACT

Assessing the safety climate used as a practical means to a relevant determinant problem regarding the safety and health in the work in the organization. The instruments applied are collected through questionnaires, group discussions or interviews and observations. The aim of the study is to determine a working climate at a steel section of elaboration (furnace) and a climatic definition of administration (management, health communication and safety).

KEYWORDS: blast furnace section, safety climate, occupational management

1. Introduction

The steel industry is one of the industrial activities, quite complex, with production costs, and high professional risks. This is how global trends of implementation in production technologies, raw materials, characterized by efficiency and performance have occurred and are currently manifesting, with the ultimate goal of reducing specific fuel consumption and energy losses, which will affect as little as possible the environment and which does not lead to occupational accidents and diseases. As the number of people in charge increased, the number and importance of managerial functions increased, and the structure organized to make the managerial act more efficient, bears the name of managerial organization.

The term "safety climate" has been used as a multi-domain factor, having an important role in the safety of the work environment, and represents the interaction between the safety climate and the security behaviour [3].

The climate of safety measures and describes the common perception of the employees on how to manage safety in a working environment in a certain period. Depending on priorities such as production and quality, perceptions provide an index to prioritize safety within an organization. The study of the safety climate has been presented as an important index in the health and safety problems of the working environments and the corrective actions thereof have a considerable effect on the efficiency of the work of the workers and the successful control over the accidents in the working environment [3].

Security behaviour is considered as another important index in the health and safety problems of the working environment, and it has an instrument for implementing and reforming the results of the effects of creating efficiency in the functioning of the employees and the successful control of accidents that could have environments for work [3].

2. Objectives

The aim of the study is to determine the climate and safety profile in a steel section for the development of the first fusion furnace and to define the safety climate (management, communication for health and safety at work, safety priority). Ten aspects of safety aspects are evaluated, including the relationship of the organization and the manager's commitment, the role of the process leader, the role of the staff, the effect of the colleague, the competence of the worker, the risky behaviour, the obstacles in the safety behaviour, the work permit and the incident and pseudo incidents report in the section. ovens. The result indicated that there is a significant difference in the safety climate between the different working groups.

3. Theoretical considerations

A Quality Management System (SMC) is a system through which an organization intends to eliminate or at least reduce non-conformities to the technical specifications, the respective industrial standards, in the most efficient and effective way possible. In other words, a SMC represents a set of

THE ANNALS OF "DUNAREA DE JOS" UNIVERSITY OF GALATI
FASCICLE IX. METALLURGY AND MATERIALS SCIENCE
N°. 2 - 2019, ISSN 2668-4748; e-ISSN 2668-4756
Article DOI: https://doi.org/10.35219/mms.2019.2.02

policies, processes and procedures necessary for planning and execution in the area of basic activities.
The Likert scale is an ordinal scale, which is used to evaluate multiple rating statements between a "total agreement" and a "total disagree". The number of steps of the ladder is one and the same for all statements about the phenomenon (five steps). For the processing and interpretation of the data of the 5 levels (Table 1) of the scale will be assigned scores [2].

Table 1. *Assessing the importance of values*

Question evaluation	Disagree Total	Disagree	No Agreement / Disagree	Agreement	Agreement Total
Scores	-2	-1	0	+1	+2

After completing the questionnaire, each article can be analysed separately or, in some cases, responses to an article can be summed to create a score for a group of articles. Therefore, the Likert scale is often called summative scale. The score obtained by the subject is calculated by making the algebraic sum [4].

Data processing is performed in the same way as in the case of Semantic Differential. The average scores for each statement are calculated on a scale from (-2) total disagreement to (2) total agreement.

The total score represents the arithmetic mean of the calculated scores:

$$S_i = \frac{1}{n}\sum x_i \qquad (1)$$

where:
x_1, x_2..., x_m is the possible values of characteristic X (scale of values of characteristic X);

The relative frequencies, expressed as a percentage, are also called percentage frequencies. They are calculated according to the formula [4]:

$$f_i = \frac{n_i}{n} \cdot 100 \ [\%] \qquad (2)$$

where:
f_i is the relative frequency of a value [%];
n - number of subjects investigated;
n_1, n_2...n_i - number of subjects, corresponding to the investigated feature.

The cumulative frequency is the percentage of individuals that do find up to or below a step (value) of the scale. She is calculated according to the formula [4]:

$$F_i = \frac{n_1 + n_2 + n_3 + \cdots + n_i}{n} \cdot 100 \ \ [\%]$$

$$F_i = f_1 + f_2 + f_3 + \cdots + f_i \qquad (3)$$

where:
F_i is the cumulative frequency [%];

The score obtained by the subject is calculated by making the algebraic sum. Frequency distributions can also be represented graphically, in form of bar charts, circular charts, radar, etc.

The values of the studied characteristics, collected from the analysed subjects, represent some statistical data (concrete sizes, determined by counting, measuring, etc.), which are grouped in the so-called databases.

4. Material and methods

The security climate can be measured in several ways, depending on the needs and capacity of an organization. The tool can be used to examine the climate or safety situation in an organization.

For this reason, the data are obtained through three separate and independent sources (questionnaire, face-to-face interviews and group discussions, observation) and are used in the evaluation [5, 6].

Qualitative methods can be classified as follows:

- questionnaire is defined as a list of questions addressed to employees, made up in order to obtain, based on the answers given, information on a problem.
- observation - online collection of information on events, phenomena, objects, persons, etc.;
- interview - discussion that involves the use of an interview guide, unstructured or semi-structured, applied to individuals, with manoeuvring possibilities.

The issues of safety aspects are evaluated, including the relationship of the organization and the manager's commitment, the role of the trial leader, the role of the staff, the effect of the colleague, the competence of the worker, the obstacles in the safety behaviour, the work permit and the incident report and the pseudo incidents in the furnace section.

The questionnaire was established based on documentation, to measure the credibility or validity of the content (Table 2).

After completing the questionnaire, each element (question) is analysed separately. Although

THE ANNALS OF "DUNAREA DE JOS" UNIVERSITY OF GALATI
FASCICLE IX. METALLURGY AND MATERIALS SCIENCE
N°. 2 - 2019, ISSN 2668-4748; e-ISSN 2668-4756
Article DOI: https://doi.org/10.35219/mms.2019.2.02

there is an ordered relationship by category sets, there is no indication of real differences between categories.

Table 2

The question ??
What is the safety climate in the manager's commitment?
What is the safety climate for the benefit of the worker?
Which is the priority of the safety climate?
What is the safety climate in the operating instructions?
What is the safety climate in a supportive environment?
What is the safety climate in worker participation?
What is the safety climate as an individual priority?
What is the safe climate in the work environment?
What is the safety climate in the communication of health?
What is the safety climate in managing change?
What is the safety climate in the training of employees?
What is the safe climate in safe behavior?
What is the safety climate in common values?
What is the adaptation of the safety climate to the system?
What is the safety climate in accidents and accidents?
What is the safe climate in the perception of risk?
What is the safety climate in the management style?

5. Working method

The research is on one of the steel industries in ArcelorMittal Galati blast furnace 5 (Vu= 2700 m^3) to determine the safety climate and provide a profile, [1].

In total, 57 subjects were asked to complete the questionnaire (all worked in the blast furnace section).

Their age ranged from 27-48 years and their working age, from 10-24 years. Of these, 88% are married, a total of 25 subunits, 20 subjects have general and secondary education, and 12 have higher education. The results are presented below (Table 3).

The processing is necessary for the creation of databases of personal data interviewed (Table 2) and average scores (weighted average) and frequencies relative to the relationship (1) are calculated.

1. Management

Table 3. *Calculation for question no. 1*

What is the safety climate in the manager's commitment?					
Scores	-2	-1	0	+1	+2
Respondents	2	4	2	15	34

Formula of calculation, score 1(57 subjects):

$$S_1 = \frac{-2 \cdot 2 - 1 \cdot 4 + 0 \cdot 2 + 1 \cdot 15 + 2 \cdot 34}{57} \approx 1{,}315$$

2. Marketing

Table 4. *Calculation for question no. 2*

Which is the priority of the safety climate?					
Scores	-2	-1	0	+1	+2
Respondents	2	1	7	15	32

Formula of calculation score 2 (57 subjects):

$$S_2 = \frac{-2 \cdot 2 - 1 \cdot 1 + 0 \cdot 7 + 1 \cdot 15 + 2 \cdot 32}{57} \approx 1{,}263$$

3. Education

Table 5. *Calculation for question no. 3*

What is the priority of the safety climate in education??					
Scores	-2	-1	0	+1	+2
Respondents	4	1	6	3	43

Formula of calculation, score 1(57 subjects):

$$S_3 = \frac{-2 \cdot 4 - 1 \cdot 1 + 0 \cdot 6 + 1 \cdot 3 + 2 \cdot 43}{57} \approx 1{,}403$$

4. Safety instructions

Table 6. *Calculation for question no. 4*

What is the safety climate in the operating instructions?					
Scores	-2	-1	0	+1	+2
Respondents	1	3	5	15	33

Formula of calculation, score 1(57 subjects):

$$S_4 = \frac{-2 \cdot 1 - 1 \cdot 3 + 0 \cdot 5 + 1 \cdot 15 + 2 \cdot 33}{57} \approx 1{,}333$$

5. Costs

Table 7. *Calculation for question no. 5*

What is the safety climate in a supportive environment?					
Scores	-2	-1	0	+1	+2
Respondents	2	2	1	10	42

THE ANNALS OF "DUNAREA DE JOS" UNIVERSITY OF GALATI
FASCICLE IX. METALLURGY AND MATERIALS SCIENCE
N°. 2 - 2019, ISSN 2668-4748; e-ISSN 2668-4756
Article DOI: https://doi.org/10.35219/mms.2019.2.02

Formula of calculation, score 1(57 subjects):

$$S_5 = \frac{-2\cdot 2 - 1\cdot 2 + 0\cdot 1 + 1\cdot 10 + 2\cdot 42}{57} \approx 1{,}543$$

6. Participation

Table 8. *Calculation for question no. 6*

What is the safety climate in worker participation?					
Scores	-2	-1	0	+1	+2
Respondents	2	4	1	19	31

Formula of calculation, score 1(57 subjects):

$$S_6 = \frac{-2\cdot 2 - 1\cdot 4 + 0\cdot 1 + 1\cdot 19 + 2\cdot 31}{57} \approx 1{,}280$$

7. Individual priority and insecurity

Table 9. *Calculation for question no. 7*

What is the safety climate as an individual priority?					
Scores	-2	-1	0	+1	+2
Respondents	0	1	2	3	51

Formula of calculation, score 1(57 subjects):

$$S_7 = \frac{-2\cdot 0 - 1\cdot 1 + 0\cdot 2 + 1\cdot 3 + 2\cdot 51}{57} \approx 1{,}824$$

8. Individual perception of risk

Table 10. *Calculation for question no. 8*

What is the safety climate in perception of risk?					
Scores	-2	-1	0	+1	+2
Respondents	1	6	6	19	25

Formula of calculation, score 1(57 subjects):

$$S_8 = \frac{-2\cdot 1 - 1\cdot 6 + 0\cdot 6 + 1\cdot 19 + 2\cdot 25}{57} \approx 1{,}070$$

9. Working environment

Table 11. *Calculation for question no. 9*

What is the safety climate in a supportive environment?					
Scores	-2	-1	0	+1	+2
Respondents	4	3	1	16	33

Formula of calculation, score 1(57 subjects):

$$S_9 = \frac{-2\cdot 4 - 1\cdot 3 + 0\cdot 1 + 1\cdot 16 + 2\cdot 33}{57} \approx 1{,}245$$

10. Common values

Table 12. *Calculation for question no. 10*

What is the safety climate in common values?					
Scores	-2	-1	0	+1	+2
Respondents	4	8	3	20	18

Formula of calculation, score 1(57 subjects):

$$S_{10} = \frac{-2\cdot 4 - 1\cdot 8 + 0\cdot 3 + 1\cdot 20 + 2\cdot 18}{57} \approx 0{,}701$$

11. Management of change

Table 13. Calculation for question no. 11

What is the safety climate in management of change?					
Scores	-2	-1	0	+1	+2
Respondents	2	4	2	15	34

Formula of calculation, score 1(57 subjects):

$$S_{11} = \frac{-2\cdot 2 - 1\cdot 4 + 0\cdot 2 + 1\cdot 15 + 2\cdot 34}{57} = 0{,}719$$

12. Public perception

Table 14. Calculation for question no. 12

What is the safety climate in the Public perception?					
Scores	-2	-1	0	+1	+2
Respondents	6	6	2	24	19

Formula of calculation, score 1(57 subjects):

$$S_{12} = \frac{-2\cdot 6 - 1\cdot 6 + 0\cdot 2 + 1\cdot 24 + 2\cdot 19}{57} \approx 0{,}771$$

13. Competence and certification

Table 15. Calculation for question no. 13

What is the climate in the competence and certification?					
Scores	-2	-1	0	+1	+2
Respondents	5	2	2	28	20

Formula of calculation, score 1(57 subjects):

$$S_{13} = \frac{-2\cdot 5 - 1\cdot 2 + 0\cdot 2 + 1\cdot 28 + 2\cdot 20}{57} \approx 0{,}982$$

THE ANNALS OF "DUNAREA DE JOS" UNIVERSITY OF GALATI
FASCICLE IX. METALLURGY AND MATERIALS SCIENCE
N°. 2 - 2019, ISSN 2668-4748; e-ISSN 2668-4756
Article DOI: https://doi.org/10.35219/mms.2019.2.02

14. Cooperation

Table 16. Calculation for question no. 14

What is the safety climate in the communication of health?					
Scores	-2	-1	0	+1	+2
Respondents	9	12	6	15	16

Formula of calculation, score 1(57 subjects):

$$S_{14} = \frac{-2 \cdot 9 - 1 \cdot 12 + 0 \cdot 6 + 1 \cdot 15 + 2 \cdot 16}{57} \approx 0{,}298$$

15. Safe behavior

Table 17. Calculation for question no. 15

What is the adaptation of the safety climate to the system?					
Scores	-2	-1	0	+1	+2
Respondents	2	6	6	22	21

Formula of calculation, score 1(57 subjects):

$$S_{15} = \frac{-2 \cdot 2 - 1 \cdot 6 + 0 \cdot 6 + 1 \cdot 22 + 2 \cdot 21}{57} \approx 0{,}947$$

16. Incidents and accidents

Table 18. Calculation for question no. 16

What is the safety climate in accidents and accidents?					
Scores	-2	-1	0	+1	+2
Respondents	8	11	6	22	10

Formula of calculation, score 1(57 subjects):

$$S_{16} = \frac{-2 \cdot 8 - 1 \cdot 11 + 0 \cdot 6 + 1 \cdot 22 + 2 \cdot 10}{57} \approx 0{,}263$$

17. Implementation of the safety system

Table 19. Calculation for question no. 17

What is the safety climate in the management style??					
Scores	-2	-1	0	+1	+2
Respondents	3	3	1	18	32

Formula of calculation, score 1(57 subjects):

$$S_{17} = \frac{-2 \cdot 3 - 1 \cdot 3 + 0 \cdot 1 + 1 \cdot 18 + 2 \cdot 32}{57} \approx 1{,}280$$

The average score values for each statement are presented in the table below: - average scores calculated on a scale of -2 (Total disagreement) to 2 (Total agreement). The results are presented in the Table 20:

Table 20

No.	The field of evaluation	Method of evaluation	Average value
1	Management	Checklist	1.315
2	Marketing	Checklist	1.263
3	Education	Checklist	1.403
4	Safety instructions	Checklist	1.333
5	Costs	Checklist	1.543
6	Participation	Checklist	1.280
7	Individual priority and insecurity	Checklist	1.842
8	Individual perception of risk	Checklist	1.070
9	Working environment	Checklist	1.245
10	Common values	Checklist	0.701
11	Management of change	Checklist	0.719
12	Public perception	Checklist	0.771
13	Competence and certification	Checklist	0.982
14	Cooperation	Checklist	0.298
15	Safe behavior	Checklist	0.947
16	Incidents and accidents	Checklist	0.263
17	Implementation the safety system	Checklist	1.280

The average score values for each statement are presented in the table below: - average scores calculated on a scale of -2 (Total disagreement) to 2 (Total agreement).

The data that is arranged in columns or rows in a worksheet can be graphically represented in a radar chart. Radar diagrams compare the aggregate values of several data series.

The total score: Based on the calculated scores, determining the total score middle, as the arithmetic mean of the scores of the n (n = 17) characteristics:

$$S_T = \frac{1}{n}\sum_{1=1}^{n} S_i = \frac{17{,}536}{17} \cdot = \mathbf{1{,}03153}$$

THE ANNALS OF "DUNAREA DE JOS" UNIVERSITY OF GALATI
FASCICLE IX. METALLURGY AND MATERIALS SCIENCE
N°. 2 - 2019, ISSN 2668-4748; e-ISSN 2668-4756
Article DOI: https://doi.org/10.35219/mms.2019.2.02

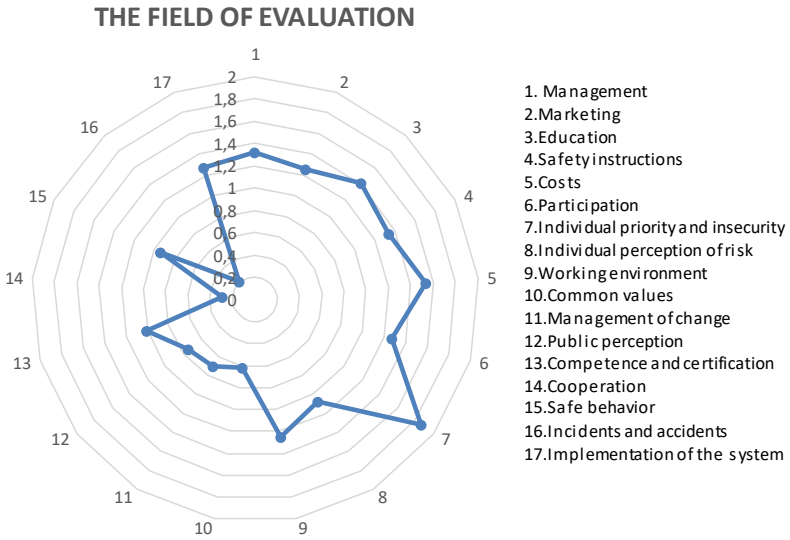

Fig. 1. *Graphic diagram of the safety climate profile*

6. Conclusions

Management's decision regarding safety issues, conducting proactive activities regarding incidents, immediate reform of safety issues, lead to the creation of a safe and healthy work climate (overall average score ST = 1.03153). Research has shown that the safety climate is on average in the industry.

1. The employees criticized the concerns regarding the non-observance of the safety instructions from some employees;

2. On the other hand, in 7 areas, they are below the average of evaluation, namely, areas of incidents and accidents (≈ 0.263), cooperation (≈ 0.298) common values (≈ 0.701) change management (≈ 0.719) and leadership style (0.771) which need to be further analysed and urgent measures taken to address the shortcomings;

3. On the opposite side, based on the analysis, it turns out that there are very well-developed areas, such as, individual priority (1.824), costs (1.543), education and training (1.403) and management (1.315);

4. The rest of the analysed areas (7) are above average;

5. As measures the interest of the services responsible for the safety on behalf of the employees and of the management is proposed;

6. Research has shown that the safety climate is on average in the industry. In some areas of the security climate, such as the commitment of management, communication, security priority, security regulations, support environment, participation, individual priority, individual perception of risk, working environment, achievement of the safety climate are approximately in average. In other areas, including common values, change management, leadership style, competence and training, cooperation, safe behaviour, incidents and accidents, the score is poor.

References

[1]. ***, *Documentation of ArcelorMittal Galati*.
[2]. ***, *Likert Scale*, http://en.wikipedia.org.
[3]. **Adrian Vasiliu**, *Occupational health and safety management*, Electronic course, UGAL Galati, 2018.
[4]. **Oleg Bulgaru**, *Statistical applications in sociological research*, Course support, ISBN 978-9975-71-XXX-X, USM, Chisinau, 2018.
[5]. ***, *OSH: 2001 - Guiding principles for occupational safety and health management systems*.
[6]. ***, *OHSAS 18002: Implementation guide of OHSAS 18001*, Likert Scale, http://en.wikipedia.org.

THE ANNALS OF "DUNAREA DE JOS" UNIVERSITY OF GALATI
FASCICLE IX. METALLURGY AND MATERIALS SCIENCE
N°. 2 - 2019, ISSN 2668-4748; e-ISSN 2668-4756
Article DOI: https://doi.org/10.35219/mms.2019.2.03

USE OF TAGUCHI METHODS IN DESIGNING AN EXPERIMENTAL MODEL OF WIND TURBINE WITH VERTICAL AXIS WITH CURVED SHEET BLADES

Nelu CAZACU
"Dunarea de Jos" University of Galati, Romania
e-mail: nelu.cazacu@ugal.ro

ABSTRACT

Increasing the efficiency of the conversion of electricity into light energy (UV LEDs) has made possible a new stage in the development of vertical axis wind turbines by compensating for the small wind energy conversion efficiency (14.81%). The work is based on the use of Taguchi methods (TM) in increasing the efficiency of a wind turbine with vertical axis blades made of deformed aluminium foil. Experiments were carried out in the wind tunnel to confirm the models selected by the QE procedure.

KEYWORDS: Taguchi methods, TM, VAWT, microWT

1. Introduction

Over time, wind turbines have undergone continuous development. Wind energy (WE) is among the first forms of energy that have been used by humans, along with solar energy [1]. The last 150 years have marked a continuous development of wind turbines in the two important directions: water pumping and electricity generation [2].

Today, many wind turbines are destined for the production of complementary electricity (RES) and in decentralized systems (out grid) [2]. This is also possible due to the evolution of the electrical and electronic equipment of domestic utility towards the reduction of the energy consumption which has attracted the decrease of the consumed currents and the decrease of the working voltages. For example, the microprocessors that are used today usually use 3.3V less than 5V or 12V. Also, the lighting systems have evolved in order to increase the conversion efficiency by using LEDs so that for the same lighting the energy required decreases and makes it possible to use RES for local lighting. But overall, energy consumption has increased due to the increase in the number of people living in modern comfort.

In other words, alternative energy sources (RES) such as solar or wind energy (WE) can be used separately or in combination to charge a battery when it is sunny or blowing so that during the night the stored energy will discharge to the LED- the lighting of a lighting system. The system can be independent or complementary to the consumption from the mains [2].

The paper aims to optimize with the help of Taguchi Methods (TM) the shape and dimensions of the blades of a VAWT, intended to obtain electricity from wind energy. Because drag force VAWTs are not only driven by the resistive force, it is possible to use this gate to look for constructive variants that use other forces that are involved in the rotational motion and which increase the conversion efficiency over the Betz limit of these (14.81%) [3]. Simple structures from accessible materials are preferred that reduce the costs of implementation by focusing on VAWT design.

$$E = \frac{1}{1} m v^2 \tag{1}$$

The volume flow and the mass flow are:

$$\dot{V} = A \cdot v \tag{2}$$

$$\dot{m} = \rho \cdot A \cdot v \tag{3}$$

The power of wind is:

$$P = \frac{1}{2} \rho \cdot A \cdot v^3 \tag{4}$$

For VAWT, like "S-rotor" the Betz limit is 4/27 (14.81%) [3]. The drag force (3) is:

THE ANNALS OF "DUNAREA DE JOS" UNIVERSITY OF GALATI
FASCICLE IX. METALLURGY AND MATERIALS SCIENCE
N°. 2 - 2019, ISSN 2668-4748; e-ISSN 2668-4756
Article DOI: https://doi.org/10.35219/mms.2019.2.03

$$D = C_D \frac{1}{2}\rho(v-u)^2 A \quad (5)$$

And the power to each blade is:

$$p = Du = C_D \frac{1}{2}\rho v^3(1-\lambda)^2\lambda \quad (6)$$

The proposed conceptual model considers a wind turbine with a vertical axis, which the blades are made of sheet and which is brought to its semi-cylindrical shape. You can use 2...6 blades of different width and with different seating angles.

For experiments, a part of the Taguchi concepts is used (TM).

Taguchi concepts. Three concepts are important to understand Taguchi's approach and method. Product variability is present for all products. Variability is determined by different factors that are located at producer and also to consumer.

Robust Quality (RQ) [4]. This method calls for making products and processes that are quality robust. Quality robust products are products that can be produced uniformly and consistently in a variety of adverse manufacturing and environmental conditions. The basic idea is to remove the effects of adverse condition instead of removing the causes. Taguchi suggest that removing the effects is often chapter that removing the causes and more effective in producing a robust product.

Notation:
E - energy, J
v - wind speed, m/s
m - mass of air, kg
ρ - air density, kg/m³
u - tip blade speed, m/s
$\dot{V}$ *- volumic debit m³/h*
$\dot{m}$ *- mass debit, kg/m³*
A - swept aria, m²
p - wind power, W
ρ - air density, kg/m³
n - rotation speed, rpm
C_D *- drag coefficient*
λ *- specific speed*

Abbreviations:
WE - Wind Energy
RES - Renewable Energy Sources
microWT - micro Wind Turbine
TM - Taguchi Methods
QE - Quality Engineering
VAWT - Vertical Axis Wind Turbine
HAWT - Horizontal Axis Wind Turbine
QLF - Quality Loss Function
RQ - Robust Quality
LED - Light Emitting Diode

Quality Loss Function (QLF) [4]. Taguchi has also defined what he calls a quality loss function. A quality loss functions (QLF) identifies all costs connected with poor quality and shows these costs increase as the product moves away from being exactly what the customer wants. These costs include not just the cost to the customer in terms of satisfaction but also warranty and service costs; internal inspections, repairs, and scrap costs; and costs that can best described as cost to society.

Experiments with orthogonal array [4, 5]. One of the most important elements of TM is the use of partial-factorial experiments, based by orthogonal matrices.

2. Experimental conditions

The maximum wind speed in the open wind tunnel on which the experiments were performed is 9 m/s. The other factors have the value range according to the limits imposed on the realization of the experimental model (EM).

The maximum area of the model in cross-section is 10% of the area of the working section of the wind tunnel. the order of the factors is according to the degree of knowledge of the investigated phenomenon [6-8]. Other details regarding the experimentation conditions:

- The maximum section of the wind tunnel measuring area is 0.25 m², which leads to a maximum section of the experimental model (EM) of 10%, respectively 0.025 m²;
- The maximum diameter of the model should not exceed 0.178 m;
- The objective function is the speed of the model n (rot/min, rpm) which must be as high as possible;
- The blades are made of sheet metal and have the dimensions 0.225 m x 0.07 m, respectively, 0.225 m x 0.035 m, and 0.225 m x 0.0175 m;
- The number of blades is 2, 3 or 6;
- There is no other task than rubbing in the bearings (peaks).

The existing wind tunnel offers conditions for experimenting with the behaviour of the aerodynamic profiles having the following characteristics: wind speed 0…9 m/s, measuring section: 0.5 m x 0.5 m (0.25 m²), electronic balance (drag force), and balance two-point electronics (Lift and Drag). LC6000 anemometer was used for wind speed measurement. An Atmel 328U microprocessor-based data acquisition system was used for data acquisition [10].

THE ANNALS OF "DUNAREA DE JOS" UNIVERSITY OF GALATI
FASCICLE IX. METALLURGY AND MATERIALS SCIENCE
N°. 2 - 2019, ISSN 2668-4748; e-ISSN 2668-4756
Article DOI: https://doi.org/10.35219/mms.2019.2.03

3. Experimental models (EM)

They were made after selecting the level of the factors and were updated for each experiment, by changing the blades and adjusting the positioning angles. In Fig. 1, Fig. 2 and Fig. 3 the models used in experiments 3, 6 and 9 are shown. A detail for fixing the blades is shown in Fig. 4.

Fig. 1. *Experimental model for experiment no. 3*

Fig. 2. *Experimental model for experiment no. 6*

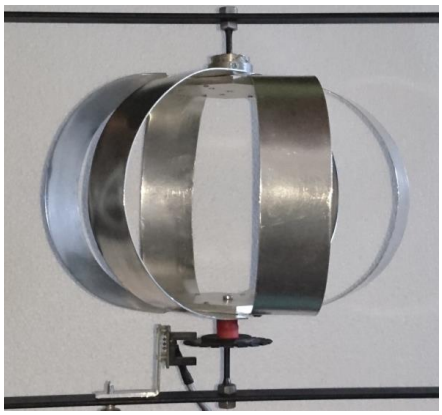

Fig. 3. *Experimental model for experiment no. 9*

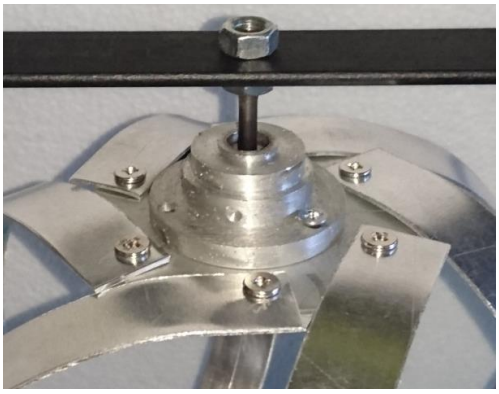

Fig. 4. *Detail with fixing the blades*

Table 1. *Factors influencing the experiment*

n.o.	factor	m.u.	range of values
1	wind speed	m/s	0… 9
2	number of blades	m2	2…6
3	blade width	m	0…0,1
4	settlement angle	grd	0 … 90
5	air temperature	°C	- 35 … + 45
6	air pressurelui	Pa	9050…1080hPa
7	air relative humidity	%	30…80
8	etc.		

Table 2. *Factors that are considered in the experiment*

symbol	Factor	m.u	levels		
			1	2	3
A	wind speed	m/s	5	7	9,5
B	number of blades	-	2	3	6
C	blade width	m	0,070	0,035	0,0175
D	settlement angle	grd.	30	45	60

Table 3. *Orthogonal array experiment (standardized L9)*

experiment	factors			
	A	B	C	D
1	1	1	1	1
2	1	2	2	2
3	1	3	3	3
4	2	1	2	3
5	2	2	3	1
6	2	3	1	2
7	3	1	3	2
8	3	2	1	3
9	3	3	2	1

THE ANNALS OF "DUNAREA DE JOS" UNIVERSITY OF GALATI
FASCICLE IX. METALLURGY AND MATERIALS SCIENCE
Nº. 2 - 2019, ISSN 2668-4748; e-ISSN 2668-4756
Article DOI: https://doi.org/10.35219/mms.2019.2.03

Table 4. *Experimental matrix*

experiment	specified factors and levels			
	A	B	C	D
m.u.	m/s	-	m	grd.
1	5	2	0,070	30
2	5	3	0,035	45
3	5	6	0,0175	60
4	7	2	0,035	60
5	7	3	0,0175	30
6	7	6	0,070	45
7	9,5	2	0,0175	45
8	9,5	3	0,070	60
9	9,5	6	0,035	30

Table 5. *The measured results of the target function and the conversion into dB*

experiment	EM rotation speed	target function
u.m.	rpm	dB
1	0	-40.00
2	0	-40.00
3	0	-40.00
4	0	-40.00
5	0	-40.00
6	165	22.17
7	0	-40.00
8	126	21.00
9	66	18.20

Table 6. *Calculating the average effect of the level of each factor*

the average effect of each level	relation	value, dB
m_{A1}=	$1/3(n_1+n_2+n_3)$=	-40.00
m_{A2}=	$1/3(n_4+n_5+n_6)$=	-19.28
m_{A3}=	$1/3(n_7+n_8+n_9)$=	-0.27
m_{B1}=	$1/3(n_1+n_4+n_7)$=	-40.00
m_{B2}=	$1/3(n_2+n_5+n_8)$=	-19.67
m_{B3}=	$1/3(n_3+n_6+n_9)$=	0.12
m_{C1}=	$1/3(n_1+n_6+n_8)$=	1.06
m_{C2}=	$1/3(n_2+n_4+n_9)$=	-20.60
m_{C3}=	$1/3(n_3+n_5+n_7)$=	-40.00
m_{D1}=	$1/3(n_1+n_5+n_9)$=	-20.60
m_{D2}=	$1/3(n_2+n_6+n_7)$=	-19.28
m_{D3}=	$1/3(n_3+n_4+n_8)$=	-19.67
	average=	-19.85

Table 7. *The average effect of the level of each factor*

	factor	levels			
		UM	1	2	3
A	wind speed	dB	-40	-19.28	**-0.27**
B	number of blades	dB	-40	-19.67	**0.12**
C	blade width	dB	**1.0595**	-20.60	-40.00
D	settlement angle	dB	-20.6	**-19.28**	-19.67
				m	-19.85

4. Experimental regimes

The experiments were performed following an L9 orthogonal matrix with nine experiments [4, 5]. The factors considered with notable influence are shown in Table 1 and the selected ones (A, B, C and D) are shown in Table 2. Also, in Table 2 the levels selected for the experiment, for each factor are shown.

The orthogonal matrix L9 [5] used in the experiments is shown in the Table 3 and the updating of this matrix with the factor levels and its transformation into the matrix after which the experiments were actually performed is shown in Table 4. For each experiment the levels of the considered factors were respected, which is one of the difficulties of using orthogonal matrices: from one experiment to another it is possible that all the factors can be reset.

In order to calculate the objective function with the relation:

$$\eta = 10 \log n \qquad (7)$$

We considered the speed at a reasonable value of 0.0001 rpm. The objective function is in the "Larger the better" category because it wants the highest value, respectively the highest rotational speed for the experimental model (EM).

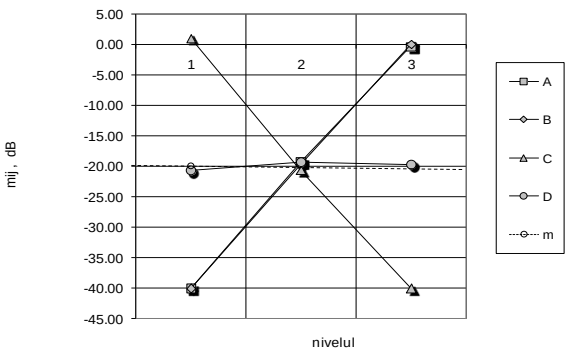

Fig. 5. *Allure of the influence of each factor*

THE ANNALS OF "DUNAREA DE JOS" UNIVERSITY OF GALATI
FASCICLE IX. METALLURGY AND MATERIALS SCIENCE
No. 2 - 2019, ISSN 2668-4748; e-ISSN 2668-4756
Article DOI: https://doi.org/10.35219/mms.2019.2.03

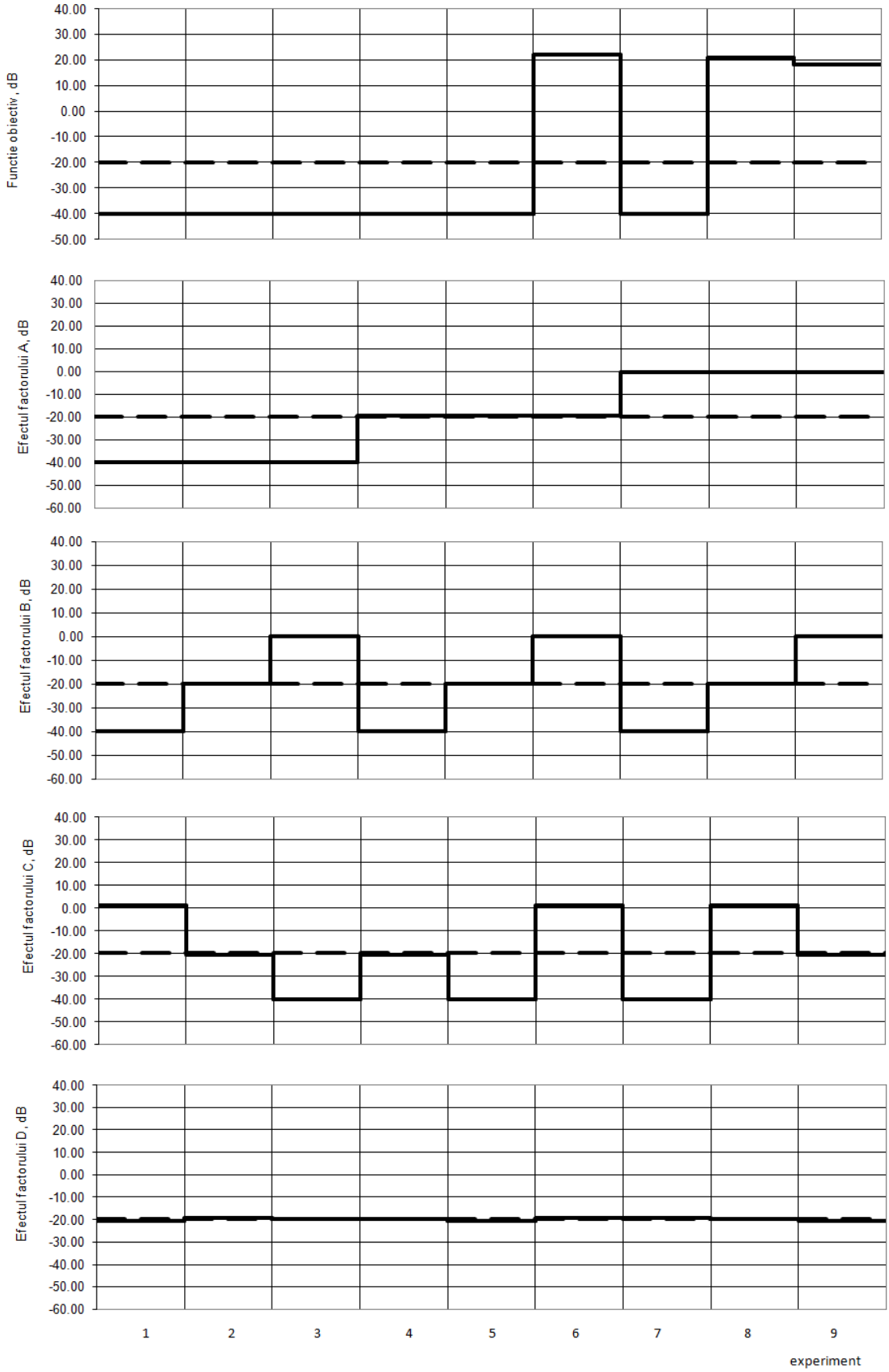

Fig. 6. *The influence of factor levels on all experiments*

THE ANNALS OF "DUNAREA DE JOS" UNIVERSITY OF GALATI
FASCICLE IX. METALLURGY AND MATERIALS SCIENCE
Nº. 2 - 2019, ISSN 2668-4748; e-ISSN 2668-4756
Article DOI: https://doi.org/10.35219/mms.2019.2.03

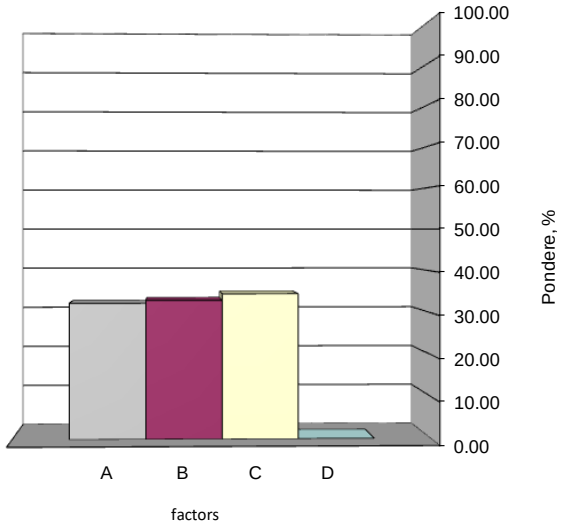

Fig. 7. *Weight of factors*

5. Results and Discussions

The measured result of the experiments was transformed into objective function with the relation (7). The results are rearranged in Table 7.

The best values obtained for the objective function, under the given experimental conditions correspond to the highest values of the average effect of each factor. Hence, the optimal recommended regime: A3B3C1D2. This corresponds to the practical situation where the experimental model was tested at the highest wind speed (A) (9 m/s), has the most blades (B) respectively 6 blades, has the width (C) the largest, respectively 70 mm and tilt angle (D) of 45 degree. The effect of each level of each factor was showed in Fig. 6.

6. Conclusions

The weight of the factors considered is shown in Fig. 7 and indicates that the factors A, B and C have an approximately equal weight and in sum they give 99.96%. The allure of influence of each factor is shown in Fig. 5.

References

[1]. Sorensen Brent, *Renewable energy*, 4ed. s.l., Elsevier, ISBN 978-0-12-375025-9, 2011.
[2]. Manwell J. F., McGowan J. G., Rogers A. L., *Wind Energy Explained. Theory, Design and Application*, s.l., John Wiley & Sons Ltd., p. 590, 2002.
[3]. Smulders P. T., *Rotors for wind power*, Eindhoven: University of Technology, Eindhoven, Faculty of Physics, 1st edition, October 1991, (revised edition January 2004).
[4]. Taguchi G., *Introduction to quality engineering into products and processes*., s.l.: Asian productivity organization, 1986.
[5]. Phadke M. S., *Quality engineering using robust design*, Englewood Cliffs, New Jersey: Prentice Hal, 1989.
[6]. Patel M. R., *Wind and Solar Power Systems*, s.l.: CRC Press, 1999.
[7]. Menet Jean-Luc, Bourabaa Nachida, *Increase in a savonius rotor efficiency*, 2003.
[8]. Matthews Clifford, *Aeronautical Engineer's Data Book*, s.l.: Butterworth-Heineman, 2002.
[9]. Burton Tony *et al.*, *Wind Energy Handbook*, s.l.: John Wiley & Sons, Ltd. p. 463, ISBN 0471489972, 2001.
[10]. Benesh A., *Wind turbine system using a vertical axis Savonius-type rotor*, US Patent 4784568, 1988.

THE ANNALS OF "DUNAREA DE JOS" UNIVERSITY OF GALATI
FASCICLE IX. METALLURGY AND MATERIALS SCIENCE
Nº. 2 - 2019, ISSN 2668-4748; e-ISSN 2668-4756
Article DOI: https://doi.org/10.35219/mms.2019.2.04

EXPERIMENTAL MODEL OF WIND TURBINE WITH VERTICAL AXIS, MULTI-STOREY AND WITH 2 PAIRS OF BLADES ON LEVEL COUPLED AERODYNAMIC

Nelu CAZACU
"Dunarea de Jos" University of Galati, Romania
e-mail: nelu.cazacu@ugal.ro

ABSTRACT

The concept presented in this paper tries to solve the torque uniformity of the wind turbine with vertical axis. The concept of multi-stage S-rotor without angular delay is used. At the floor level, two pairs of blades are used and the aerodynamic coupling of the opposing blades by overlapping. The tests were carried out in the wind tunnel at wind speeds of up to 9 m/s and the use of data acquisition systems. The results confirm the favourable behaviour of the experimental model and the validity of the concept.

KEYWORDS: VAWT, Savonius type, 2 pair of blades, multistage

1. Introduction

The vertical axis wind turbine Savonius type is one of the most known turbines due to its constructive simplicity [1]. Constructively, the Savonius turbine has in its simplest structure a pair of blades, hemispherical or semi-cylindrical, placed symmetrically with respect to a vertical axis of rotation. The semi-cylindrical blades have the axis of the cylinder parallel to the axis of rotation (Fig. 1) with the so-called active stroke from 0 to 180 degrees, and the reverse stroke from 180 to 360 degrees (Fig. 2).

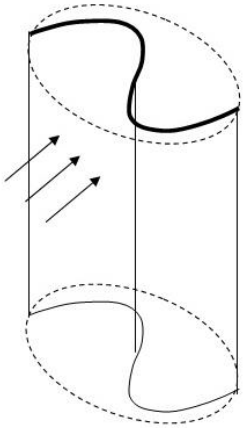

Fig. 1. *The rotation motion occurs due to the different behaviour of the blade against the airflow*

The aerodynamic resistance that the paddle opposes is different and can be found in the so-called coefficient of resistance (CD), which has a value of 1.2 for the active cup, and a value of 0.3 for the resistant cup.

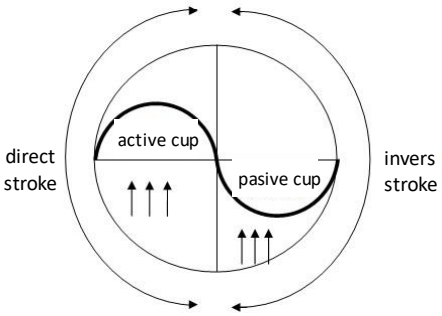

Fig. 2. *Rotation motion of the "S-rotor" turbine*

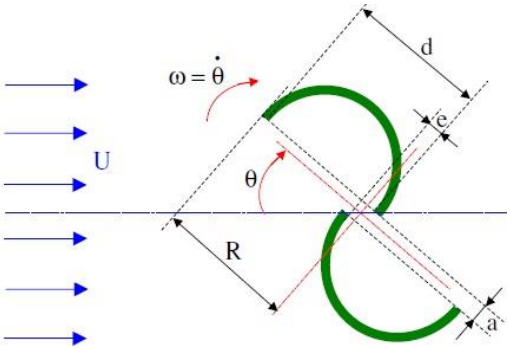

Fig. 3. *"S-Rotor"(Savonius Wind Turbine)* [2]

THE ANNALS OF "DUNAREA DE JOS" UNIVERSITY OF GALATI
FASCICLE IX. METALLURGY AND MATERIALS SCIENCE
N°. 2 - 2019, ISSN 2668-4748; e-ISSN 2668-4756
Article DOI: https://doi.org/10.35219/mms.2019.2.04

By integrating the pressure exerted on the surface of the blade, a resultant force is obtained that differs for each of the two blades, depending on the position relative to the zero point. The force differences between the active and the resistant race give rise to a rotating torque.

A rotor is called a conventional Savonius rotor if the geometric parameters *a* and *e* are equal to 0 and respectively, d/6. (Fig. 3).

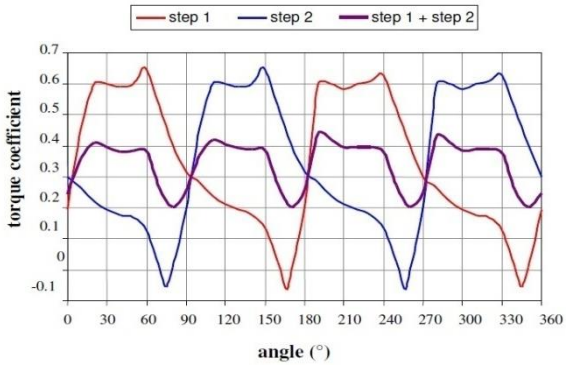

Fig. 4. *360-degree torque variation* [2]

The main disadvantage of the 2-blade Savonius vertical axis wind turbine is the unevenness of the rotation torque which is shown schematically in Fig. 4 to the 360-degree variation of the torque.

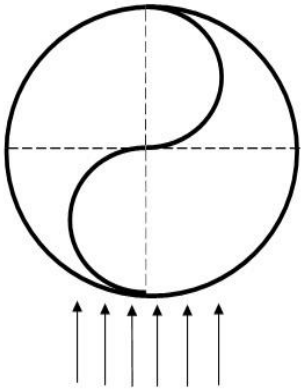

Fig. 5. *The position of the cups from the wind direction when the couple is very small*

There is a point where the couple is very small, that is when the blades are in the wind direction, a situation shown in Fig. 5.

In this case, the torque may be very small and the wind turbine may not start. If the wind is coupled to a mechanical load, respectively a generator, the unevenness of the couple is found in the unevenness of the power at the axis that the generator can cut.

Notations
σ - Indices of solidities
v - wind speed, m/s
ρ - air density, kg/m^3
L - mechanical work, J
x - distance, m
P - power, W
V - air volume, m^3
Δτ - time interval, s
A - swept aria, m^2
CD - drag coefficient
ω - angular speed, radians / s
g - gap, mm; (a)
o - overlap, mm; (e)
d - cup base diameter, m
R - S rotor radius, m
θ - instantaneous angle, degree
F - force, N
Δτ - time interval, s
m - mass of air, kg
V - air volume, m^3
L - Mechanical work, N

Abbreviations
HAWT - Horizontal Axis Wind Turbine
microWT - micro Wind Turbine
VAWT - Vertical Axis Wind Turbine
LED - Light Emitting Diode

Different conceptual models of vertical-axis wind turbine can be developed with improved starting torque:

- The simplest method of uniformity of torque and power respectively to the shaft is the use of a flywheel, which, however, has the disadvantage of increasing turbine inertia and a more difficult start;

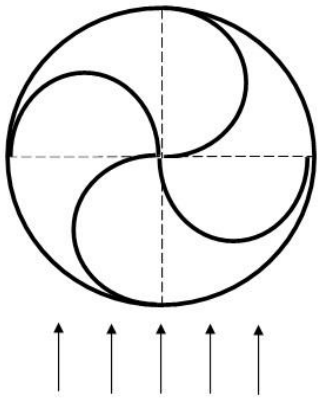

Fig. 6. *Wind turbine Savonius type with 4 blades*

- Another often used variant is to increase the number of wind blades to at least 4 (2 pairs). (Fig. 6);
- Construction of stages (Fig. 7). In this way, there is always at least one pair of blades in a

THE ANNALS OF "DUNAREA DE JOS" UNIVERSITY OF GALATI
FASCICLE IX. METALLURGY AND MATERIALS SCIENCE
N°. 2 - 2019, ISSN 2668-4748; e-ISSN 2668-4756
Article DOI: https://doi.org/10.35219/mms.2019.2.04

favourable position for which between forces and torque is large;

• Using twisted blades and approaching the vertical model Helix VAWT (3). This is achieved by dividing the blades into a number of n floors and offset each floor by 360 per n degrees. At this type of wind, the torque uniformity is high (the higher the n). In contrast, the degree of difficulty for the construction of the wind turbine increases (4).

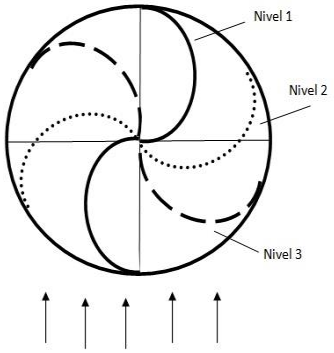

Fig. 7. *Wind turbine type Savonius with 3 stage*

The conceptual model is based on the idea that by using an aerodynamic profile commonly used in the aeronautical industry and HAWT, the operation of a Savonius type wind turbine can be improved by improving the operation of the wind turbine at the so-called "dead end"S (when the axis of the Savonius type turbine blades). Is in the same direction as the difference wind). Making floors in this way, there is always at least one pair of blades in a favourable position for which the difference between forces and torque is large.

There are several mathematical models to calculate the wind energy. The dynamic pressure of the wind, due to its displacement, is calculated according to the equation:

$$p = \rho \frac{v^2}{2} \quad (1)$$

where: ρ – air density, kg/m3; v - wind speed, m/s.

The larger the surface on which the wind acts, the greater the force produced by it [5]. In contact with a surface, the wind is broken, the kinetic energy transforming into potential pressure energy, respectively mechanical energy transferred to the surface that realized the braking. The force F developed by the wind on a surface A can be calculated:

$$F = pA \quad (2)$$

$$F = \rho \frac{v^2}{2} A \quad (3)$$

Mechanical work L when moving air over distance x, is calculated by the relation:

$$L = Fx \quad (4)$$

$$L = \rho \frac{v^2}{2} Ax \quad (5)$$

The power of the wind, over time Δt is calculated with the relation:

$$P = \frac{L}{\Delta\tau} \quad (6)$$

and by replacement:

$$P = \rho \frac{v^2}{2} A \frac{x}{\Delta\tau} \quad (7)$$

Where x/Δτ = v is wind speed, and relation became:

$$P = \rho \frac{v^3}{2} A \quad (8)$$

At the same distance x the volume of air moved is:

$$V = A\,x \quad (9)$$

From which results the mass of air that moves under the action of the wind determined with the relations:

$$m = \rho\, V \quad (10)$$

$$m = \rho A x \quad (11)$$

Where the kinetic energy of the air mass is calculated with the relations:

$$Ec = m \frac{v^2}{2} \quad (12)$$

$$Ec = \frac{1}{2} \rho A x v^2 \quad (13)$$

Or knowing that x = vτ results:

$$Ec = \frac{1}{2} \rho A v^3 \tau \quad (14)$$

The experimental models are presented in Fig. 8 and Fig. 9.

Wind Tunnel [6] is the equipment that underlies the measurements made on the experimental models

THE ANNALS OF "DUNAREA DE JOS" UNIVERSITY OF GALATI
FASCICLE IX. METALLURGY AND MATERIALS SCIENCE
N°. 2 - 2019, ISSN 2668-4748; e-ISSN 2668-4756
Article DOI: https://doi.org/10.35219/mms.2019.2.04

of the wind turbines. It is made of plywood, with dimensions 0.5 m x 0.5 m, with a length of equalization area of 2 m and recording a wind speed between 0 and 9.5 m/s.

The LCA 6000 anemometer has the following characteristics: measuring range: 0.25 ... 30 m/s, tolerance range: +/- 1%, +/- LSD, temperature range: -10 °C...50 °C, pressure range: 500 mbar…2 bar, integration time measurement: approx. 3 s.

Fig. 8. *Experimental model EM-C13*

Experimental frame with minimum friction with multiplier and generator made of two steel plates (lower and upper, with dimensions of 450 x 450 mm, height 480 mm), 6 columns (2 working and 4 supporting and stiffening). This framework allows fixing the experimental model and the measurement sensors, but also an easy change of the designed wind models. The models are supported on two 300 x 40 x 8 mm sleepers, which are adjusted on the work columns by means of nuts and washers. In the centre of these sleepers bearings and bearing devices are located on the discs of the experimental models. The experiments were carried out in the wind tunnel for the two experimental models and for different mechanical and electrical loads. When testing between peaks the only task acting on the model is friction in bearings (peaks). For the other tests, the model was fixed on the axis of a speed multiplier + DC electric generator, at its output electrical charges (LED, adjustable load resistance) can be connected. When testing between peaks the only task acting on the model is friction in bearings (peaks). For the other tests, the model was fixed on the axis of a speed multiplier + DC electric generator, at its output electrical charges (LED, adjustable load resistance) can be connected.

Fig. 9. *Experimental model EM-C12*

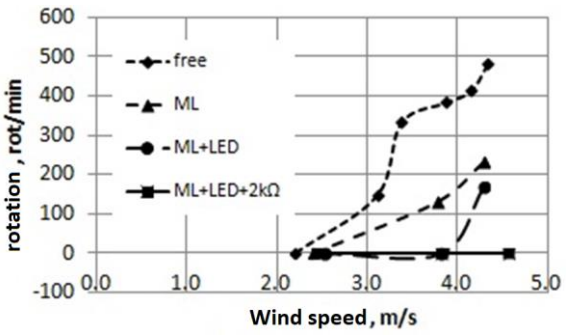

Fig. 10. *The influence of wind speed on the speed EM C12*

THE ANNALS OF "DUNAREA DE JOS" UNIVERSITY OF GALATI
FASCICLE IX. METALLURGY AND MATERIALS SCIENCE
Nº. 2 - 2019, ISSN 2668-4748; e-ISSN 2668-4756
Article DOI: https://doi.org/10.35219/mms.2019.2.04

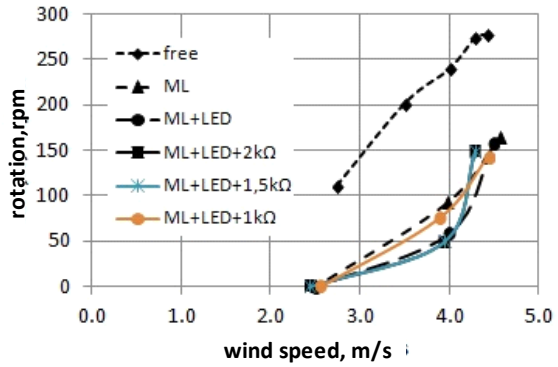

Fig. 11. *The influence of wind speed on the speed of EM- CI3*

2. Results and discussions

The graph in Figure 12. represent the influence of wind speed on the speed of the experimental model EM-CI2 for different load values. The rotations of the blades increase with the increase of the wind speed. When a mechanical load is applied, and gradually increasing its values, a significant decrease in blade speed is observed.

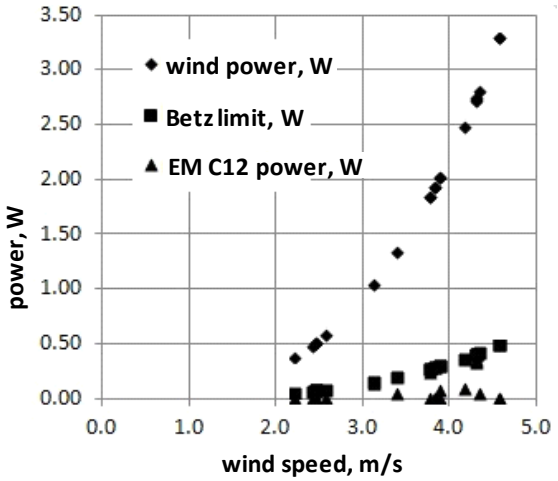

Fig. 12. *Variation of powers in the wind speed system (EM-CI2)*

In Fig. 15 was showed how the powers in the system vary with the wind speed, for different added load values. Having established the limit of Betz for the experimental model, it is observed that the power EM-CI2 is below this limit, reaching a maximum value of 0.343 W, at a wind speed of 4.3 m/s, has applied a LED.

The graph in Fig. 13 represent the influence of the specific speed on the Reynolds number for EM-C12.

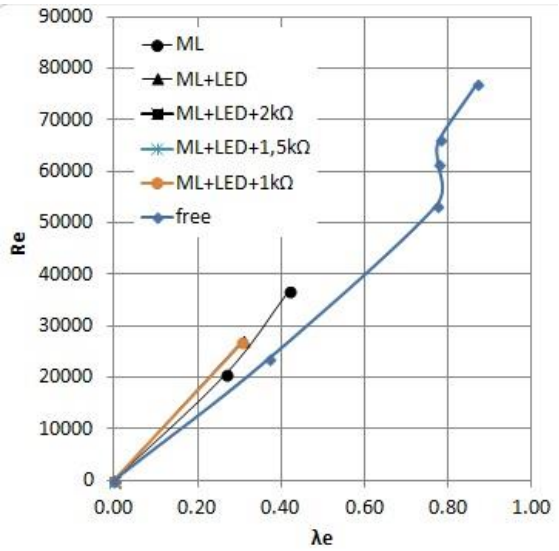

Fig. 13. *Reynolds number variation with specific speed for EM C12*

In the case of the experimental model CI3, the graph in Fig. 13 highlights how the wind speed influences the turbine speed in the wind tunnel, at different values of the applied mechanical load.

As the wind speed increases, the rotations of the blades of the experimental model EM-CI3 register a linear increase, if no load is applied to the so-called "idle", reaching a maximum value of 278 rotations per minute, at with a wind speed of 4.4 m/s. Since it is applied mechanical loads, the rotations decrease, but following the same linear growth curve, as the wind speed increases.

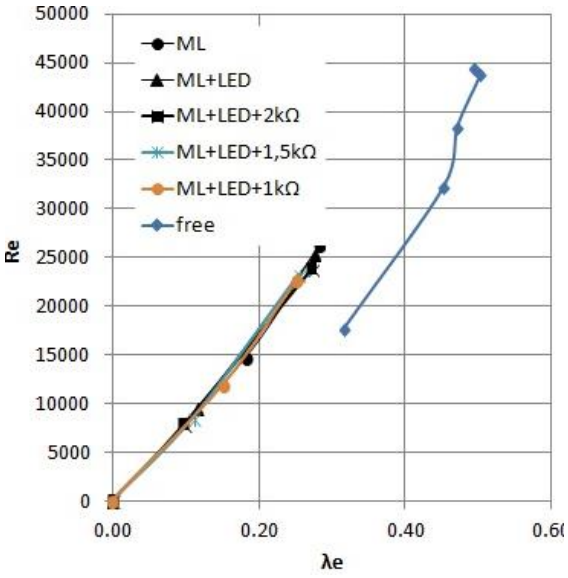

Fig. 14. *Reynolds number variation with specific speed for EM C13*

THE ANNALS OF "DUNAREA DE JOS" UNIVERSITY OF GALATI
FASCICLE IX. METALLURGY AND MATERIALS SCIENCE
N°. 2 - 2019, ISSN 2668-4748; e-ISSN 2668-4756
Article DOI: https://doi.org/10.35219/mms.2019.2.04

As it has been shown, increasing the wind speed increases its power, implicitly the power of the experimental turbine. Referring to the Betz limit set for the experimental model EM-CI3, it is observed that the turbine is approaching this value very well, reaching a maximum power of 0.405 W at a wind speed of 4.6 m/s but without any applied load. The graph in Fig. 14 shows the influence of the specific speed on the Reynolds number for the experimental model EM-CI3.

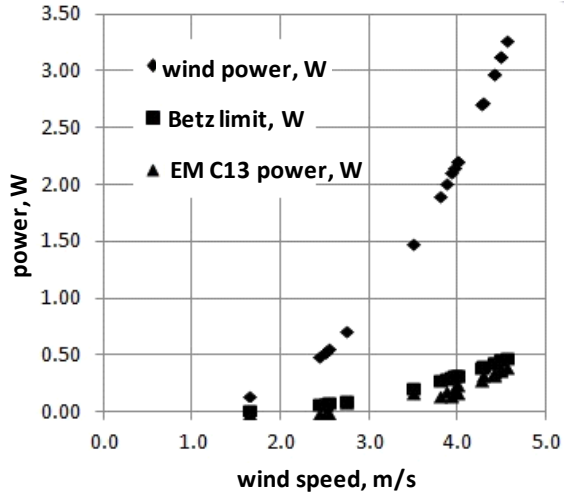

Fig. 15. *Variation of powers in the system with the wind speed EM-C13*

3. Conclusions

• The experimental models realized according to the concept of the theoretical part exposed at the beginning of the work show the validity of applying the aerodynamic profiles to the vertical turbines of the type Savonius.

• The experiments performed on the experimental model CI2 with two blades with aerodynamic profile and coupled (range and overlap), demonstrate the easy passage through the zero point (with a high speed).

• The uniformization of the wind movement is shown by the experimental model CI3, in which the operation is very uniform, due to the combination of the aerodynamic profiles (approximately NACA 4412) at the base of the model, and due to the extended surface in the middle of the model.

• Vertical, 6-level coupling of the pairs of blades allows efficient wind loading and uniformity of torque in operation.

• Testing the experimental model with 6 load levels shows an operation between 2.5 and 4.5 m/s wind speed and a decrease in load speed.

• The efficiency of the experimental models reached the maximum value of 13% for the operation of the model in a hollow, and for 2.7 m/s the wind speed.

• The maximum values of 12% for minimum loads, respectively mechanical loads and leads, and wind speeds exceeding 4 m/s were reached.

References

[1]. Hau Erich, *Wind Turbines, Fundamentals, Technologies, Applications, Economics*, s.l.: Springer, 2006.
[2]. Menet J. L., Bourabaa N., *Increase in a savonius rotor efficiency*.
[3]. Saha U. K., Rajkumar M. J., *On the performance analysis of Savonius rotor with twisted blades*, Renewable Energy, 31, 2006.
[4]. Zigman A., *Optimization of a Savonis Rotor Vertical-Axes wind turbine*, Massachussets: MIT, 2007.
[5]. Manwell J. V., McGowan J. G., Rogers A. L., *Wind Energy Explained. Theory, Design and Application*.
[6]. Nelson V., *Wind Energy. Renewable Energy and the Environment*, s.l.: Taylor & Francis Group LLC, 2009.

THE ANNALS OF "DUNAREA DE JOS" UNIVERSITY OF GALATI
FASCICLE IX. METALLURGY AND MATERIALS SCIENCE
No. 2 - 2019, ISSN 2668-4748; e-ISSN 2668-4756
Article DOI: https://doi.org/10.35219/mms.2019.2.05

IMPROVING THE PROPERTIES OF THE ASPHALT MIXTURE, BY CONTENT VARIATION OF THE BITUMEN

Beatrice Daniela TUDOR
"Dunarea de Jos" University of Galati, Romania
e-mail: btudor@ugal.ro

ABSTRACT

The paper presents a study, on several samples of asphalt mix, with different compositions, in order to investigate the influence of the composition, on the properties, which asphalt mix must fulfil. For all kinds of aggregates, the granulometric analysis was made, and the bitumen content was varied, to study the influence on the properties of the mixture.

KEYWORDS: asphalt mixture, bitumen, granulometry, filler, quality

1. Introduction

The asphalt mix is a mixture of filler, fine and coarse stone granules, as well as bitumen, as a binder.

The bitumens are natural or artificial materials, of organic nature, of variable consistency (from viscous liquid to brittle solids), and the colour is brown-black. Bitumen mixed with mineral powders is called asphalt.

The hot asphalt mixture is a building material, made by a technological process, which involves heating the natural aggregates and bitumen, mixing, transporting, and putting into operation, usually by hot compaction.

The asphalt mixes are used for the wear layer, the bonding layer, as well as for the base layer. The production of asphalt mixtures can be done, by "hot" or "cold" technologies, depending on the binder used in their composition [1].

The technological process for the manufacture of hot asphalt mixtures comprises the following phases: pre-aggregating, heating, dosing and mixing the aggregates with bitumen in the mixer, at high temperatures.

The drying, heating, and dust removal from the aggregates are very important operations, since, in order to achieve a good coating with bitumen, they must have a suitable temperature, so that the hot binder, in contact with the aggregate, not to cool, but to remain fluid, to coating all the granules as evenly as possible.

The main factors to be considered in the drying and heating process are:

- humidity of the aggregates;
- their granulosity;
- the temperature required for coating.

The dosing and mixing are done so that asphalt mixtures can be made, as homogeneous as possible, respecting the dosages, given by the laboratory. The sorter-doser, aims at sifting the hot aggregates, separating them into fractions, thus reconstituting a mixture, perfectly dosed. It consists of several sieves, which allow the fractions to be sorted.

The hot aggregates, weighed by the metering dispenser, are introduced into the mixer. It adds the cold filler, seeking to achieve a better homogenization of the aggregates with the filler. Then it adds the binder (bitumen), hot, at 150...170 °C, and continue mixing. For mixing, the bitumen must be heated to 150…170 °C, to ensure a good viscosity.

Insufficient mixing, results in a heterogeneous distribution of the binder. Too much mixing, does not improve the coating, and decreases the efficiency of the installation [2, 4].

The heating of the aggregates and the bitumen, at very high temperatures (over 200 °C), leads to transformations, which change the characteristics of the bitumen, being able to reach, at the "burning" of the bitumen, which is equivalent to the loss of adhesiveness and aging premature.

The quality control of the asphalt mix produced, is performed by the laboratory, which performs the analysis of the asphalt mix, determining the bitumen content and the granulosity of the aggregate.

2. Experimental research

For the research, I took into consideration, a number of 4 samples, in which I did the granulometric analysis, of the materials that enter the

THE ANNALS OF "DUNAREA DE JOS" UNIVERSITY OF GALATI
FASCICLE IX. METALLURGY AND MATERIALS SCIENCE
Nº. 2 - 2019, ISSN 2668-4748; e-ISSN 2668-4756
Article DOI: https://doi.org/10.35219/mms.2019.2.05

recipe of the mixture, and we varied the bitumen content, to study, how they influence the properties of the asphalt mixture, and which would be the optimum quantity of the bitumen, to obtain the best characteristics of the asphalt mixture [3].

Asphalt mixing, under laboratory conditions, involves the following steps:

Calculation of the dosages of material, for each variant of recipe, according to their characteristics.

The materials used in the preparation of the mixture are the following:

- Chippings with different degrees of size.

Fig. 1. *Chipping 5-10 mm*

Fig. 2. *Chipping 10-20 mm*

Fig. 3. *Sand crushing 0-5 mm*

Fig. 4. *Filler*

Fig. 5. *Cellulose fiber*

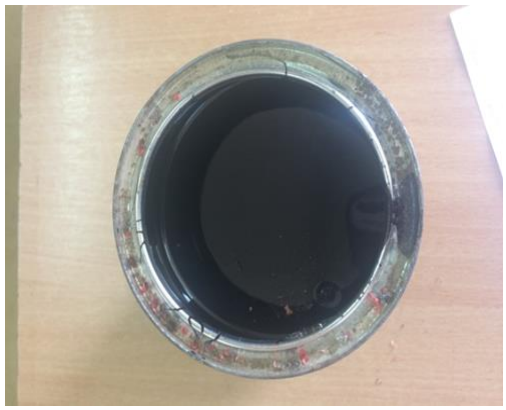

Fig. 6. Bitumen

Separately in a tray, the aggregates + the filler + fiber are weighing in the calculated dosages, for each sample and heat in the oven, at 160-170 °C.

The bitumen is heated, in a thermoreglable oven, at temperatures of 140-150 °C (Fig. 8).

Preparation of the asphalt mixture - The prepared asphalt mixture, is transferred from the mixer into a tray, and is introduced in the oven (Fig. 7), to reach the temperature necessary to make the samples.

THE ANNALS OF "DUNAREA DE JOS" UNIVERSITY OF GALATI
FASCICLE IX. METALLURGY AND MATERIALS SCIENCE
Nº. 2 - 2019, ISSN 2668-4748; e-ISSN 2668-4756
Article DOI: https://doi.org/10.35219/mms.2019.2.05

Fig. 7. *Oven with adjustable heating*

After all the steps of making asphalt samples are followed, they are subjected to tests, to see if they comply with the norms, then, the recipe of the mixture, is sent to the asphalt making station.

Fig. 8. *Heating of bitumen, in a thermoreglable oven*

The granulometric analysis of the materials is presented in the following tables.

Table 1. *Sand crushing tests sort 0/5 mm*

No	Characteristics	Results obtained
		Sample 1
1	Granulometry:	
	Passes% on the sieve 10.0	100.0
	Passes % on the sieve 5	97.8
	Passes % on the sieve 2.5	65.3
	Passes % on the sieve 1.25	49.4
	Passes % on the sieve 0.63	31.0
	Passes % on the sieve 0.315	18.7
	Passes % on the sieve 0.140	9.6
	Passes % on the sieve 0.071	5.3

Table 2. *Tests on the chippings, sort 5/10 mm*

No	Characteristics	Results obtained
		Sample 2
1	Granulometry:	
	Passes % on the sieve 40.0	
	Passes % on the sieve 20.0	100.0
	Passes % on the sieve 10.0	99.1
	Passes % on the sieve 7.5	66.3
	Passes % on the sieve 5	8.7
	Passes % on the sieve 2.5	1.6
	Passes % on the sieve 1.25	
	Passes % on the sieve 0.63	
	Passes % on the sieve 0.315	
	Passes % on the sieve 0.140	
	Passes % on the sieve 0.071	

Table 3. *Tests on the chippings, sort 10/20 mm*

No	Characteristics	Results obtained
		Sample 3
1	Granulometry:	
	Passes % on the sieve 40.0	100.0
	Passes % on the sieve 20.0	99.3
	Passes % on the sieve 10.0	65.2
	Passes % on the sieve 7.5	9.4
	Passes % on the sieve 5	0.9
	Passes % on the sieve 2.5	
	Passes % on the sieve 1.25	
	Passes % on the sieve 0.63	
	Passes % on the sieve 0.315	
	Passes % on the sieve 0.140	
	Passes % on the sieve 0.071	

Table 4. *Tests on the filler (sample 4)*

Granulometric analysis		
Sieve, mm	% Passes	Limit
1.25	100	100%
0.63	100	
0.315	99.9	
0.14	93.9	
0.071	77.2	min. 70%

In order to control the quality of the asphalt mix, the samples were subjected to the following determinations: mean density, water saturation, and swelling.

For this, the samples were weighed, after the following steps:

THE ANNALS OF "DUNAREA DE JOS" UNIVERSITY OF GALATI
FASCICLE IX. METALLURGY AND MATERIALS SCIENCE
N°. 2 - 2019, ISSN 2668-4748; e-ISSN 2668-4756
Article DOI: https://doi.org/10.35219/mms.2019.2.05

The dry test

- it leaves the sample in the water for one hour (Fig. 10);
- the sample is weighed in water;
- then, the sample is weighed in the air;
- the samples are placed in the suction vessel, with vacuum pump, for 3 hours (Fig. 9).

Fig. 9. *Suction vessel, with vacuum pump*

Fig. 10. *Preparation of the samples for the absorption test*

The results obtained are highlighted in the following graphs:

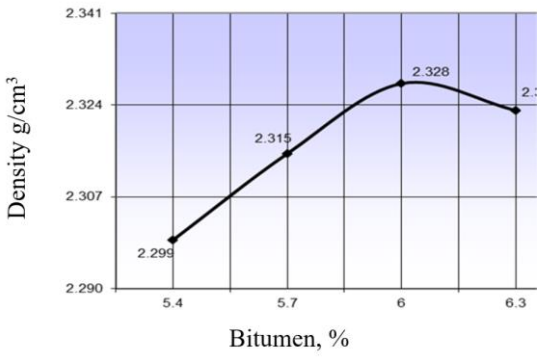

Fig. 11. *The average density, of the asphalt mixing samples*

A maximum of the average density, we found at the sample with 6% bitumen, and at the sample with 6.3% bitumen, the average density decreases (Fig. 11).

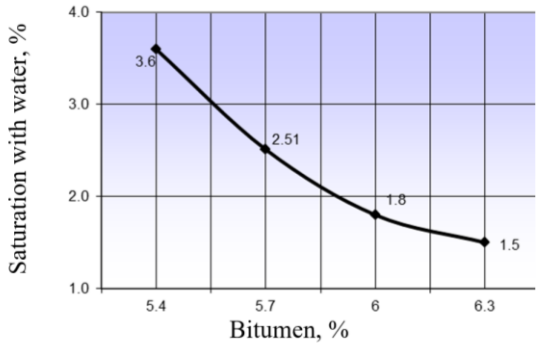

Fig. 12. *Saturation with water, of the samples of asphalt*

By studying the results at the 4 samples, with different content of bitumen, we found that the saturation with water of the samples decreases, with the increase of bitumen percentage (Fig. 12).

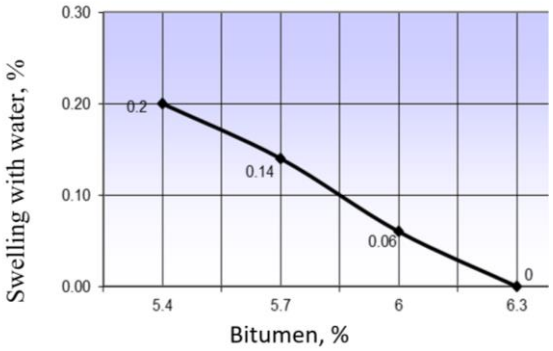

Fig. 13. *Swelling with water of the asphalt mixing samples*

The sample with a higher bitumen content, respectively 6.3%, has the lowest water absorption, which is an advantage, for the final composition, because the asphalt becomes more resistant to moisture (Fig. 13).

3. Conclusions

The quality of the materials used in an asphalt mix, plays an important role, in the subsequent behavior and in the exploitation of the mix, so that for make up the mix should be used aggregates with high mechanical strength, bitumen with low susceptibility

THE ANNALS OF "DUNAREA DE JOS" UNIVERSITY OF GALATI
FASCICLE IX. METALLURGY AND MATERIALS SCIENCE
N°. 2 - 2019, ISSN 2668-4748; e-ISSN 2668-4756
Article DOI: https://doi.org/10.35219/mms.2019.2.05

to the temperature variations, and an optimum percentage of filler [5, 6].

- Is establishing an optimum binder content, which ensures for the asphalt mix, the best characteristics, and a good behavior in operation.

-The most important problems, in the case of making good quality asphalt mixtures, is to establish, with an optimal bitumen content, and a rigorous particle size analysis at all the materials that make up the mix's recipe.

- The quality of the asphalt mixtures is one of the important factors, which determines the quality of the works for road construction, which first of all implies, satisfying the requirements of resistance, and safety in operation.

- For all kinds of aggregates, granulometric analysis was performed.

- For all 4 samples, we varied the bitumen content, for see, how was influenced the properties of the mixture.

- Following the tests, on the mixtures of asphalt mix, prepared in the laboratory, with the following bitumen dosages: 5.4%; 5.7%; 6.0%; 6.3%, determinations were made, of some physical-mechanical characteristics.

- For each test, the variation curve was drawn, with the increase of the bitumen dosage.

- The best properties were obtained at the sample with 6.0% bitumen.

References

[1]. West R. C., Watson D. E., Turner P. A., Casola J. R., *Mixing and Compaction Temperatures of Asphalt Binders in Hot-Mix Asphalt*, NCHRP Report 648, Transportation Research Board, 2010.

[2]. Błażejowski K., Styk S., *Technologia warstw asfaltowych*, Wydawnictwa Komunikacji i Łączności, 2004.

[3]. ***, *CONCAWE: Chemical Safety Report. Part B. "Bitumen" and "Oxidized Asphalt"*.

[4]. ***, *Development in Asphalt Binder Specifications. Transportation Research Circular E-C147*, Transportation Research Board, December 2010.

[5]. ***, *Physical differentiation between air-rectified and oxidised bitumens*, Technical Committee Task Force, Eurobitume, 15.04.2011.

[6]. ***, *Une méthode ameliorèe de caractérisation des bitumes par leurs propriétés mechaniques*, Heukelom W., Bull. Liaison Labo. P. et Ch., 76, p. 55-64, 1975.

THE ANNALS OF "DUNAREA DE JOS" UNIVERSITY OF GALATI
FASCICLE IX. METALLURGY AND MATERIALS SCIENCE
N°. 2 - 2019, ISSN 2668-4748; e-ISSN 2668-4756
Article DOI: https://doi.org/10.35219/mms.2019.2.06

FIBER ORIENTATION AND FILLERS EFFECTS ON SPECIFIC HEAT OF FABRIC REINFORCED HYBRID EPOXY COMPOSITES

Marina BUNEA, Mihaela Claudia GOROVEI, Claudia Veronica UNGUREANU, Vasile BRIA
"Dunarea de Jos" University of Galati, Romania
e-mail: marina.bunea@ugal.ro

ABSTRACT

In this investigation, the specific heat of four fabric reinforced hybrid composite materials with filled stratified epoxy matrix was analysed. All hybrid composite materials were made of 17 layers, for which were used carbon, aramid, glass and hybrid fabrics. The stratified filled epoxy matrix of fabric reinforced hybrid composites represents a matrix, in whose structure it was used three types of fillers mixtures between certain plies. The investigation of specific heat of hybrid composite materials was performed by using of Differential Scanning Calorimetry instrument. It was analysed the effects of fiber orientation at various angles on specific heat of fabric reinforced hybrid composites with filled stratified epoxy matrix and the influence of fillers mixtures on these thermal properties of epoxy matrix. Also, it was studied the specific heat of hybrid epoxy composites in dependence of carbon and aramid plies number in studied materials structure.

KEYWORDS: hybrid stratified composites; filled epoxy matrix; fiber orientation; specific heat

1. Introduction

The thermosetting composite materials reinforced with fibers or fabrics are widely used in many applications, which are carried out under conditions with high or low temperatures, or under conditions with temperature variations. So, the temperature increasing or decreasing leads to volume deformation of the composite materials, which affects the structural stability. Thus, the thermal investigations of the composite materials are important, because their mechanical performance depends on their thermal deformations [1].

The thermal behaviour of the fiber reinforced thermosetting composites can be carried out by the investigation of specific heat, thermal conductibility, coefficient of thermal linear expansion, etc. [2]. In case of composite materials reinforced with fibers, the polymeric matrix and the fibers exhibits different temperature fluctuations due to their different thermoelastic constants [3]. The epoxy systems are the thermosetting polymers most widely used as matrix for fiber reinforced composite materials, due to their thermal stability, chemical resistance, mechanical properties and high adherence to all fiber types and inorganic fillers [4].

Considering the thermal properties of the reinforcement and matrix of the composites structures, it can be predicted their thermal behaviour and their mechanical resistance under conditions with temperature variations. In order to increase the structural stability, for example, for different types of constructions, it can be used the hybrid composites reinforced with different types of fibers and with filled polymeric matrix. Through hybridization it can be obtained the composite materials with desired properties, considering the properties of each constituent component, their compatibility and the quality of the fiber-matrix and filler-matrix interfaces [5].

For this study it was made an experimental investigation of specific heat of the hybrid composite materials reinforced with plain fabrics and with stratified filled epoxy matrix, which were formed, actually, in order to obtain multifunctional advanced composite materials. The stratified filled epoxy matrix represents an epoxy matrix modified with three types of fillers mixtures used for certain layers of the laminates. In order to obtain the stratified epoxy matrix, it was used the fillers such as potatoes starch, carbon black, aramid powder, ferrite, carbon and glass whiskers.

THE ANNALS OF "DUNAREA DE JOS" UNIVERSITY OF GALATI
FASCICLE IX. METALLURGY AND MATERIALS SCIENCE
N°. 2 - 2019, ISSN 2668-4748; e-ISSN 2668-4756
Article DOI: https://doi.org/10.35219/mms.2019.2.06

In ref. [6] it was established that the 10 wt.% of corn starch had no influence on thermal stability (specific heat and coefficient of thermal expansion) in the temperature range of 70-110 ºC. The thermal conductivity of the epoxy composites increases with the increasing of the carbon black content [7, 8]. The specific heat of the nano-ferrites epoxy composites increase with the increasing of the nano-ferrite content in the temperature range of 70-120 ºC [9], but by adding 50 wt. % of clay in epoxy matrix the values of specific heat in the temperature range of 90-150 ºC decrease with the increase of ferrite content from 20 to 50 wt.% [10]. The thermal conductibility through thickness of the composites reinforced with fibers can be improved, also, by addition of fillers in polymeric matrix such as graphene nanoplatelets [11–13], carbon nanotubes [14, 15], graphite [16], metallic nanoparticles as TiO_2 nanoparticles [17], nickel particles [18], up to 2 wt.% of ZnO nanoparticles [19] and another filler types. For example, in ref. [20] it was found that the thermal conductivity through thickness without affecting the mechanical resistance of carbon fiber reinforced composite laminates increased with 40% by addition of graphene nanoplatelets (1 vol.%) together with silver nanoparticles and nanowires (0.5 vol.%).

In this paper the influence of the fillers on specific heat of the epoxy matrix, fiber orientation and aramid/carbon plies number on specific heat of the hybrid composite materials was investigated.

2. Materials and experimental method

2.1. Materials

As epoxy matrix of fabric reinforced hybrid composites with stratified filled matrix, it was selected EPIPHEN 4020 system (DE resin and RE hardener) with 100:30 ratio, due to its properties before and after polymerization. After 14 days the complete polymerization is reached at laboratory conditions (temperature of 23 °C and humidity of 50%). This used epoxy system exhibits a high adherence to all fiber types and to the most filler types.

As reinforcements for hybrid stratified composites it was used five plain fabric types: carbon fabric with 160 g/m^2 density, denoted C; aramid fiber fabric with 173 g/m^2 specific density, denoted A; glass fiber fabric with 163 g/m^2 specific density, denoted 1G; glass fiber fabric with 390 g/m^2 specific density, denoted 2G; hybrid fabric with 270 g/m^2 specific density, denoted M.

In order to obtain the hybrid fabric M, it was used a carbon aramid fiber mixed fabric with 205 g/m^2 specific density, whose weave geometry represents an alternated carbon fiber by two aramid fibers in the weft direction and alternated aramid fiber by two carbon fibers in the warp direction. Each second aramid fiber in the weft direction of mixed fabric was replaced by a tin covered copper wire with diameter of 0.2 mm and a glass fiber with linear density of 200 tex [21–23].

In order to improve the quality of matrix-fiber interface of fabric reinforced hybrid epoxy plates, which depends on the adherence properties of the fibers, all used fabrics were treated with detergent, sodium hydroxide and perchloric acid solutions by uniform spaying and they were cleaned after each treatment with water. After that the fabrics were dried and they were covered by uniform spraying with a thin film made of nitro diluent and used EPIPHEN epoxy system mixture.

The fillers such as aramid powder, carbon black, potatoes starch, barium ferrite and carbon and glass whiskers were selected in order to obtain the stratified epoxy matrix of multifunctional hybrid composite plates. The potatoes starch was mixed with another types of fillers due to experimental results obtained in ref. [24], which showed that the 10 wt.% of corn starch can be used without affecting the electrical, thermal and mechanical properties of the epoxy composites, but it lead to an increase of the prepolymeric liquid viscosity by its swelling. So, it was ensured the uniform distribution of other selected fillers into prepolymeric mixtures and it was avoided their sedimentation. The carbon black and barium ferrite were used to improve the thermal and electromagnetic properties. In order to improve the mechanical properties and impact performance, it was used the aramid powder, carbon whiskers and glass whiskers.

It was formed four hybrid composites made of 17 layers, which were denoted in this paper H1, H2, H3 and H4. The hybrid composites H1 and H3 are the laminates with fiber orientation at 0°, whose structure represents a symmetrical arrangement of the layers relative to the medial one. The hybrid composites H2 and H4 are the laminates with fiber orientation at various angles, whose structure represents an anti-symmetrical balanced arrangement of the layers relative to the medial one. The plies configuration of the fabric reinforced hybrid epoxy composite with 0° fiber orientation H1 is [$C_0/A_0/A_0/1G_0/2G_0/1G_0/C_0/A_0/M_{90}/A_0/C_0/1G_0/2G_0/1G_0/A_0/A_0/C_0$]. The plies configuration of composite material H2 is similar to that of composite material H1, but with fiber orientation at various angles, as [$C_0/A_{-15}/A_{15}/1G_{-30}/2G_0/1G_{30}/C_{45}/A_0/M_{90}/A_0/C_{45}/1G_{45}/2G_0/1G_{45}/A_{15}/A_{-15}/C_0$]. The layers configuration of the hybrid composite H3 is [$C_0/C_0/A_0/1G_0/2G_0/1G_0/A_0/C_0/M_{90}/C_0/A_0/1G_0/2G_0/1G_0/A_0/C_0/C_0$]. As in case of hybrid epoxy composite H1

THE ANNALS OF "DUNAREA DE JOS" UNIVERSITY OF GALATI
FASCICLE IX. METALLURGY AND MATERIALS SCIENCE
N°. 2 - 2019, ISSN 2668-4748; e-ISSN 2668-4756
Article DOI: https://doi.org/10.35219/mms.2019.2.06

and H2, the plies configuration of composite material H4 is similar to that of composite material H3, but with fiber orientation at various angles, as [C_0/C_{-15}/A_{15}/$1G_{-30}$/$2G_0$/$1G_{30}$/A_{45}/C_0/M_{90}/C_0/A_{45}/$1G_{45}$/$2G_0$/$1G_{45}$/A_{15}/C_{-15}/C_0].

The epoxy matrix of the fabric reinforced hybrid plates is a stratified filled matrix made of three types of fillers mixtures, such as: MF1 - polymeric mixture with 10 wt.% of potatoes starch and 10 wt.% of carbon black, which was used for layers 01 to 03 and 15 to17; MF2 - polymeric mixture with 5 wt.% of potatoes starch, 5 wt.% of aramid powder, 5 wt.% of glass whiskers and 5 wt.% of carbon whiskers, which was used for layers 04 to 06 and 12 to 14; MF3 - polymeric mixture with 10 wt. % of aramid powder and 10 wt.% of barium ferrite, used for layers 07 to 11.

The hybrid epoxy composites reinforced with fabrics and with stratified filled matrix were formed by wet lay-up method. By this method each layer of the plates was placed into a glass mould and imbued with the prepolymeric and fillers mixtures. After complete polymerization the plates were cured thermally according to technical specifications and the water jet machine was used to extract the specimens for specific heat measurements.

2.2. Experimental method

The specific heat of these hybrid epoxy composites reinforced with fabrics and stratified filled matrix was measured using Differential Scanning Calorimetry (DSC 1) instrument from Mettler Toledo and data acquisition and evaluation software STARe. For these thermal tests were used specimens with diameter of 3 mm. The specific heat of the hybrid composite materials was investigated by heating in the temperature range of 30-330 ºC and by cooling in the temperature range of 330-30 ºC with 20 ºC/min. In order to study the influence of filled mixtures on specific heat of the formed composites, it was measured the specific heat for unfilled epoxy matrix (ME) and for each filled epoxy matrices (MF1, MF2 and MF3) in the similar temperature ranges. As example, the averaged values of the heat flow and specific heat measured in the temperature range of 30-330 ºC for hybrid composite material H1 are presented in Figure 1.

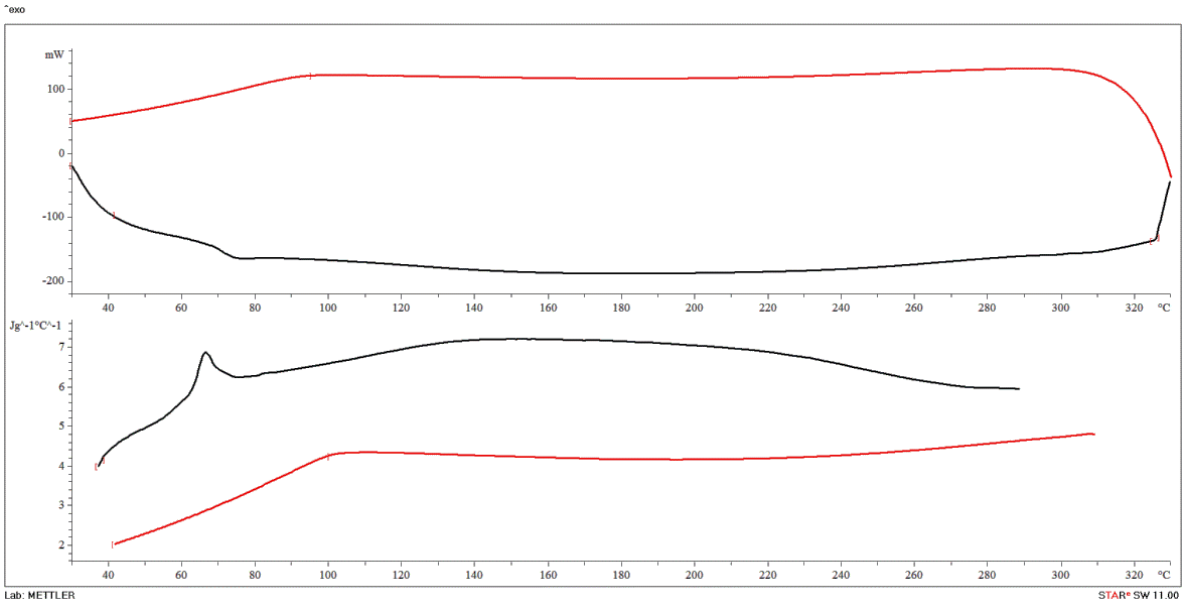

Fig. 1. *Heat flow vs temperature (above) and specific heat vs temperature (below) curves for hybrid composite H1*

3. Results and discussion

The investigation of specific heat was performed on the limits of the linear portions of both specific heat vs temperature curves (heating and cooling curves showed in Fig. 1). So, the specific heat of epoxy matrices and hybrid epoxy composites reinforced with fabrics and with stratified filled matrix was analysed in the heating and cooling temperature ranges of 50-60 ºC, 80-100 ºC, 100-150 ºC, 160-200 ºC and 200-240 ºC. The average values of the specific heat of unfilled epoxy matrix (ME) and filled epoxy matrices (MF1, MF2 and MF3) determined in the heating temperature ranges are presented in Fig. 2 and those determined in the cooling temperature ranges are showed in Fig. 3. It

THE ANNALS OF "DUNAREA DE JOS" UNIVERSITY OF GALATI
FASCICLE IX. METALLURGY AND MATERIALS SCIENCE
N°. 2 - 2019, ISSN 2668-4748; e-ISSN 2668-4756
Article DOI: https://doi.org/10.35219/mms.2019.2.06

can be observed that the values of specific heat in the cooling temperature ranges are, generally, lower than those in the heating temperature ranges, excepting specific heat evaluated in the temperature range of 50-60 ºC. The addition of 20 wt.% of potatoes starch and carbon black into epoxy matrix led to a decreasing of specific heat values in all temperature ranges. Regarding the specific heat of the filled epoxy matrices measured in the heating temperatures ranges (Fig. 2), it can be seen that the epoxy matrix filled with 20 wt.% of aramid powder and barium ferrite showed in all temperatures ranges almost the same values with those obtained in case of epoxy matrix filled with 20 wt.% of potatoes starch and carbon black. The amount of 20 wt.% of potatoes starch, aramid powder and glass and carbon whiskers showed no influence on the specific heat values of epoxy matrix in the temperature ranges of 50-60 ºC, 80-100 ºC and 100-150 ºC, but it led to an increasing of the values in the temperature ranges of 160-200 ºC and 200-240 ºC.

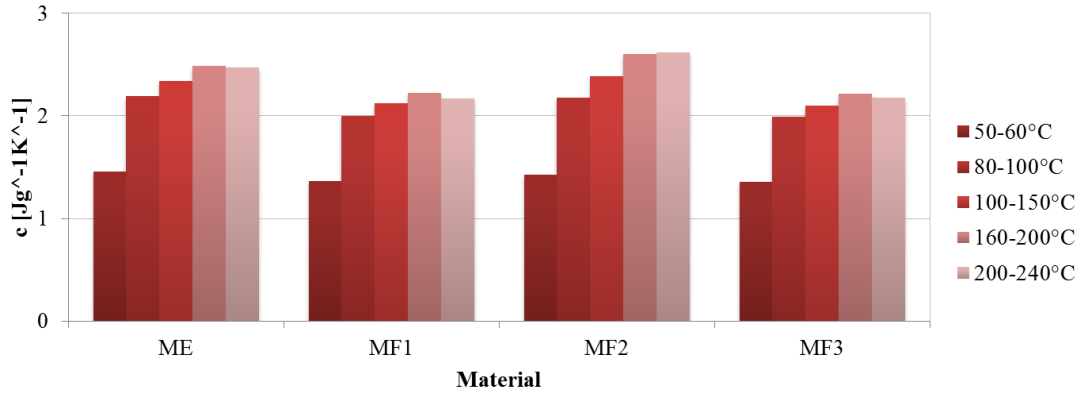

Fig. 2. *Specific heat of epoxy matrices measured in the heating temperature ranges*

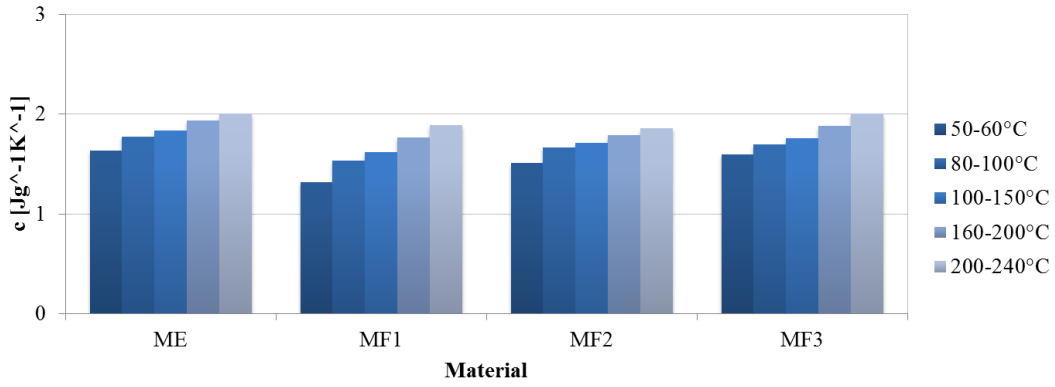

Fig. 3. *Specific heat of epoxy matrices measured in the cooling temperature ranges*

In the cooling temperature ranges (Fig. 3), it can be seen that the specific heat of filled epoxy matrices exhibited lower value in comparison with those of unfilled epoxy matrix. The epoxy matrix filled with 20 wt.% of aramid powder and barium ferrite (MF3) showed in all temperatures ranges the values close to those presented by unfilled epoxy matrix (ME). The lowest values of specific heat were obtained in case of epoxy matrix filled with 20 wt.% of potatoes starch and carbon black (MF1) in the temperature ranges of 50-60 ºC, 80-100 ºC, 100-150 ºC and 160-200 ºC, but the lowest values in the temperature range of 200-240 ºC were determined in case of epoxy matrix filled with 20 wt.% of potatoes starch, aramid powder and glass and carbon whiskers (MF2).

In Figures 4 and 5 are plotted the average values of specific heat measured for hybrid epoxy composites reinforced with fabrics and stratified filled matrix in the same temperature ranges as in case of filled matrices. It can be observed that the hybrid epoxy laminates presented, also, higher values of specific heat determined in the heating temperature ranges compared to those determined in the cooling temperature ranges. Thus, the hybrid epoxy laminates need a larger amount of heat to increase their temperature with a unit, while for their temperature

THE ANNALS OF "DUNAREA DE JOS" UNIVERSITY OF GALATI
FASCICLE IX. METALLURGY AND MATERIALS SCIENCE
N°. 2 - 2019, ISSN 2668-4748; e-ISSN 2668-4756
Article DOI: https://doi.org/10.35219/mms.2019.2.06

reduction with a unit it is necessary a lower amount of heat to release. Regarding the number of aramid and carbon plies in structure of hybrid epoxy composite materials, it can be seen in Fig. 4 that the hybrid epoxy composites with more aramid layers (H1 and H2) showed higher values of the specific heat in all heating temperature ranges as compared to those obtained in case of hybrid epoxy composites with more carbon layers (H3 and H4). The fiber orientation at various angles (±15°, ±30° and ±45°) led to a significant increase of specific heat values in all heating temperature ranges.

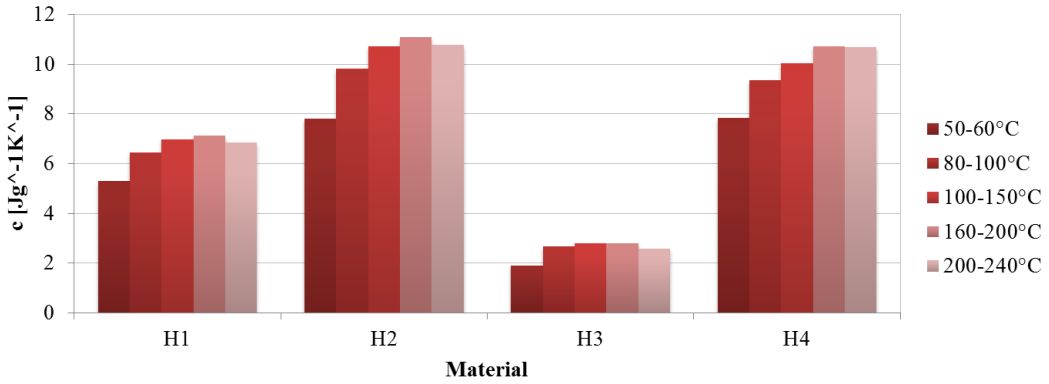

Fig. 4. *Specific heat of hybrid composite materials measured in the heating temperature ranges*

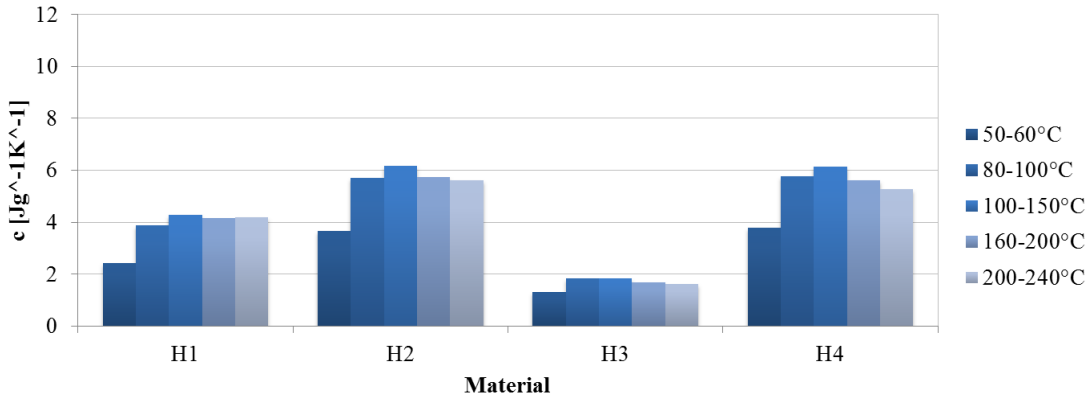

Fig. 5. *Specific heat of hybrid composite materials measured in the cooling temperature ranges*

The values of specific heat measured in the cooling temperature ranges of 50-60 ºC, 80-100 ºC, 100-150 ºC, 160-200 ºC and 200-240 ºC for hybrid epoxy composites reinforced with fabrics and stratified filled matrix (Fig. 5) showed that the fiber orientation at various angles led to a significant increase, as in case of those measured in the heating temperature ranges. If we compare the composites with fiber orientation at 0°, it can be seen that the ones with more aramid plies presented much higher values of specific heat as compared to the ones with more carbon plies.

But if we compare the composites with fiber orientation at various angles, it can be observed that the ones with more carbon plies showed higher value of specific heat in the temperature ranges of 50-60 ºC and 80-100 ºC as compared to the ones with more aramid plies. But in the temperature ranges of 100-150 ºC, 160-200 ºC and 200-240 ºC the highest values of specific heat were obtained in case of hybrid composite material with more aramid plies.

4. Conclusions

The influence of filler mixture types, number of carbon and aramid layers and fiber orientation at various angles (±15°, ±30° and ±45°) on specific heat of hybrid epoxy composites reinforced with fabrics and with filled stratified matrix measured in the in the heating and cooling temperature ranges of 50-60 ºC, 80-100 ºC, 100-150 ºC, 160-200 ºC and 200-240 ºC was investigated. It can be made the following conclusions by analysis of obtained and plotted above experimental data:

• The investigation of the influence of filler mixtures on specific heat of epoxy matrix showed that the amount of 20 wt.% of potatoes starch, aramid powder and glass and carbon whiskers had no influence in the heating temperature ranges of 50-60 ºC, 80-100 ºC and 100-150 ºC, but it led to an increase of the values in the temperature ranges of 160-200 ºC and 200-240 ºC. The epoxy matrix filled with 20 wt.% of aramid powder and barium ferrite and that filled with 20 wt.% of potatoes starch and carbon black showed in all heating temperatures ranges almost the same values, but lower as compared to the ones of unfilled epoxy matrix.

• In the cooling temperature ranges of 50-60 ºC, 80-100 ºC, 100-150 ºC and 160-200 ºC the lowest values of specific heat were obtained in case of epoxy matrix filled with 20 wt.% of potatoes starch and carbon black, but in the temperature range of 200-240 ºC the lowest values was determined in case of epoxy matrix filled with 20 wt.% of potatoes starch, aramid powder and glass and carbon whiskers.

• The hybrid epoxy composites with more aramid layers exhibited much higher values of the specific heat in all heating and cooling temperature ranges as compared to the ones determined in case of hybrid epoxy composites with more carbon layers.

• The fiber orientation at various angles led to a significant increase of specific heat values in all heating temperature ranges, especially, for hybrid epoxy composites with more carbon layers. The composite materials with more carbon plies exhibited the highest value of specific heat in the cooling temperature ranges of 50-60 ºC and 80-100 ºC. But the composite material with more aramid layers presented the highest values in the temperature ranges of 100-150 ºC, 160-200 ºC and 200-240 ºC.

Acknowledgements

This work has been funded by the European Social Fund through the Sectoral Operational Programme Human Capital 2014-2020, through the Financial Agreement with the title „Burse pentru educaţia antreprenorială în rândul doctoranzilor şi cercetătorilor postdoctorat (Be Antreprenor!)" (in English: "Scholarships for entrepreneurial education among doctoral students and postdoctoral researchers (Be Entrepreneur!)", Contract no. 51680/09.07.2019 - SMIS code: 124539.

References

[1]. Vidal P., Gallimard L., Ranc I., Polit O., *Thermal and thermo-mechanical solution of laminated composite beam based on a variables separation for arbitrary volume heat source locations*, Applied Mathematical Modelling, 46, p. 98-115, https://doi.org/10.1016/j.apm.2017.01.064, 2017.

[2]. Saba N., Jawaid M., *A review on thermomechanical properties of polymers and fibers reinforced polymer composites*, Journal of Industrial and Engineering Chemistry, 67, p. 1-11, https://doi.org/10.1016/j.jiec.2018.06.018, 2018.

[3]. Melvin A. D., Lucia A. C., Solomos G. P., *The thermal response to deformation to fracture of a carbon/epoxy composite laminate*, Composites Science and Technology, 46, p. 345-351. https://doi.org/10.1016/0266-3538(93)90180-O, 1993.

[4]. Karnati S. R., Agbo P., Zhang L., *Applications of silica nanoparticles in glass/carbon fiber-reinforced epoxy nanocomposite*, Composites Communications, 17, p. 32-41, https://doi.org/10.1016/j.coco.2019.11.003, 2020.

[5]. Praveen R. S., Jacob S., Murthy C. R. L., Balachandran P., Rao Y. V. K. S., *Hybridization of carbon–glass epoxy composites: An approach to achieve low coefficient of thermal expansion at cryogenic temperatures*, Cryogenics, 51, p. 95-104. https://doi.org/10.1016/j.cryogenics.2010.12.003, 2011.

[6]. Birsan I. G., Roman I., Bria V., Ungureanu V., Circiumaru A., *Starch-Epoxy Composites*, Annals of DAAAM for 2011 & Proceedings of the 22nd International DAAAM Symposium, 22 p. 285-286, 2011.

[7]. Abdel-Aal N., El-Tantawy F., Al-Hajry A., Bououdina M., *Epoxy resin/plasticized carbon black composites. Part I. Electrical and thermal properties and their applications*, Polymer Composites, 29, p. 511-517, https://doi.org/10.1002/pc.20401, 2008.

[8]. Bera T., Acharya S. K., Mishra P., *Synthesis, mechanical and thermal properties of carbon black/epoxy composites*, International Journal of Engineering, Science and Technology, 10, p. 12-20, https://doi.org/10.4314/ijest.v10i4.2, 2018.

[9]. Muntenita C., Ungureanu C., Bria V., Graur I., *Specific heat of nano-ferrites modified composites*, MATEC Web of Conferences, 112, 04016, 2017.

[10]. Birsan I. G., Bria V., Circiumaru A., Roman I., *Characterization of particulate epoxy composites*, The Annals of University "Dunărea de Jos" of Galati, Fascicle VIII, XV, p. 83-87, 2009.

[11]. Jarosinski L., Rybak A., Gaska K., Kmita G., Porebska R., Kapusta C., *Enhanced thermal conductivity of graphene nanoplatelets epoxy composites*, Materials Science-Poland, 35, p. 382-389, https://doi.org/10.1515/msp-2017-0028, 2017.

[12]. Zhu D., Qi Y., Yu W., Chen L., Wang M., Xie H., *Enhanced Thermal Conductivity for Graphene Nanoplatelets/Epoxy Resin Composites*, Journal of Thermal Science and Engineering Applications, 10, 2018.

[13]. Wang F., Drzal L. T., Qin Y., Huang Z., *Mechanical properties and thermal conductivity of graphene nanoplatelet/epoxy composites*, Journal of Materials Science, 50, p. 1082-1093, https://doi.org/10.1007/s10853-014-8665-6, 2015.

[14]. Park J. G., Cheng Q., Lu J., Bao J., Li S., Tian Y., Liang Z., Zhang C., Wang B., *Thermal conductivity of MWCNT/epoxy composites: The effects of length, alignment and functionalization*, Carbon, 50, p. 2083-2090, 2012.

[15]. Yang S. Y., Ma C. C. M., Teng C. C., Huang Y. W., Liao S. H., Huang Y. L., Tien H. W., Lee T. M., Chiou K. C., *Effect of functionalized carbon nanotubes on the thermal conductivity of epoxy composites*, Carbon, 48, p. 592-603. https://doi.org/10.1016/j.carbon.2009.08.047, 2010.

[16]. Caradonna A., Badini C., Padovano E., Pietroluongo M., *Electrical and Thermal Conductivity of Epoxy-Carbon Filler Composites Processed by Calendaring*, Materials, 12, 1522, https://doi.org/10.3390/ma12091522, 2019.

[17]. Majeed N. S., Salih S. M., Abdulmajeed B. A., *Effect of nanoparticles on thermal conductivity of epoxy resin system*, IOP Conference Series: Materials Science and Engineering, 518, 062006, https://doi.org/10.1088/1757-899X/518/6/062006, 2019.

[18]. Li X., Park W., Chen Y. P., Ruan X., *Effect of Particle Size and Aggregation on Thermal Conductivity of Metal–Polymer Nanocomposite*, Journal of Heat Transfer, 139, https://doi.org/10.1115/1.4034757, 2017.

[19]. Thipperudrappa S., Ullal Kini A., Hiremath A., *Influence of zinc oxide nanoparticles on the mechanical and thermal responses of glass fiber-reinforced epoxy nanocomposites*, Polymer Composites, https://doi.org/10.1002/pc.25357, 2019.
[20]. Kandare E., Khatibi A. A., Yoo S., Wang R., Ma J., Olivier P., Gleizes N., Wang C. H., *Improving the through-thickness thermal and electrical conductivity of carbon fibre/epoxy laminates by exploiting synergy between graphene and silver nano-inclusions*, Composites Part A: Applied Science and Manufacturing, 69, p. 72-82, 2015.
[21]. Bunea M., Cîrciumaru A., Buciumeanu M., Bîrsan I. G., Silva F. S., *Low velocity impact response of fabric reinforced hybrid composites with stratified filled epoxy matrix*, Composites Science and Technology, 169, p. 242-248. https://doi.org/10.1016/j.compscitech.2018.11.024, 2019.
[22]. Bunea M., Bosoanca R., Eni C., Cristache N., Stefanescu V., *The impact characteristics of fabric reinforced hybrid composites*, Materiale Plastice, 54, p. 286-290, 2017.
[23]. Bunea M., Bosoanca I., Bosoanca R., Bodor M., Circiumaru A., *Bending and Compressive Properties of Fabric Reinforced Composites*, Materiale Plastice, 52, p. 368-372, 2015.
[24]. Bria V., Cîrciumaru A., Bîrsan I. G., *Some Properties of Starch/Epoxy Composites*, Materiale Plastice, 48, p. 189-194, 2011.

THE ANNALS OF "DUNAREA DE JOS" UNIVERSITY OF GALATI
FASCICLE IX. METALLURGY AND MATERIALS SCIENCE
N°. 2 - 2019, ISSN 2668-4748; e-ISSN 2668-4756
Article DOI: https://doi.org/10.35219/mms.2019.2.07

STUDIES AND RESEARCH ON THAT ELECTROMAGNETIC FIELDS IN PUBLIC AREAS

Tudor Andrei RUSU, Marius LOBONȚIU, Tiberiu RUSU
Technical University of Cluj-Napoca, Faculty of Materials and Environmental Engineering
Department Environmental Engineering and Sustainable Development Entrepreneurship
103-105, Muncii Boulevard, Postal code 400641, Cluj-Napoca
e-mail: Andrei.Rusu@im.utcluj.ro

ABSTRACT

The society development in the new era of technologies led to increasing demands of electricity needs. For this reason, the distribution networks had extended significantly. A key factor affecting global warming is energy production and consumption. This affects the natural ecosystems and biodiversity, having adverse effects on human, animal and environment health. To keep pace with social evolution in every household the number of electrical and/or electronic devices have increased significant. All these devices lead to Complex Electromagnetic Radiations that are directly loaded into the environment, even in the places where people rest and sleep. The lack of information, research and depth analysis about electromagnetic emissions or radiation effects on human health on long time exposure, compels us to use the precautionary principle. As in any scientific work, we will present the results of measurements on electromagnetic radiation for several public places in different cities. For frequency measurements we focused on low and high frequency. The measurements reveal us, that in several places the values exceed legal limit admitted on long time exposure.

KEYWORDS: electromagnetic fields; radiation; Non-ionizing Radiation; Environment; human exposure

1. Aspects relating electromagnetic fields

Rapid rate industrialization using electrical power led to serious electrical networks extension on global scale. Electric power consumption and production are generating considerable pressures on the Environment, with negative impact on natural ecosystems and human health.

The variety of electric/electronic products and devices used in transport sector, trade market, industry, telecommunications, medicine, agriculture, education, domestic activities alongside with all electric networks are generating around us a bundle of electromagnetic fields (EMF).

An experiment without aim can be called, the submission of human populations to electromagnetic radiation in the last 80 years. Concerns arise from the lack of information about the effects on human health and/or the environment by radiations.

An electromagnetic field (radiation or electromagnetic waves) contains an electrical field (E) and a magnetic field (H), mutually perpendicular and at the same time perpendicular on the propagation direction that oscillate sinusoidal from positive to negative (as value) with a f Frequency.

The distance between two maximum positive values (or negative) is called wavelength, inversely proportional with f Frequency.

The field may be divided in two main components: reactivate component and radiant component. The reactive component refers to the energy stored near the source region being responsible for effects on humans.

The region is found around the source, till a distance of approximately 1/6 m~2 m also known as close field region.

The measurements for close field are demanding, because even by introducing the inlet probe into the field, we are interfering significantly the field.

The reactive component is found at larger distances than one wavelength. The electromagnetic wave is described as a plane wave, with a constant

THE ANNALS OF "DUNAREA DE JOS" UNIVERSITY OF GALATI
FASCICLE IX. METALLURGY AND MATERIALS SCIENCE
N°. 2 - 2019, ISSN 2668-4748; e-ISSN 2668-4756
Article DOI: https://doi.org/10.35219/mms.2019.2.07

ratio between electric and magnetic field strength, also known as distant field.

This unique feature is important, because it make it possible to measure the component field (electric or magnetic) with a single measurement.

In between these two regions there is a transitional region, where the radiant component is prevailing.

As the wavelength is inversely proportional with frequency, the region may vary. Magneto electric fields are totally invisible, being all over around us.

There are two types of radiation: ionizing radiation (have the capacity to break the molecules) and non-ionizing radiations depending on the quantity of energy delivered.

In addition to the existing natural electromagnetic non-ionizing radiation fields (Earth's magnetic and electric field, lightning magneto electric fields, solar radiation) in which the living organisms have developed over decades and millennia, human activity by developing technologies over the last 40 years generated numerous sources of non-ionizing electromagnetic radiations with different frequency and intensities.

Although are classified by their frequency, the electromagnetic waves with frequency between 0-300 Hz in the academic literature are called extreme low frequency fields (ELF).

The main cause of their existence is the transmission and distribution systems of electric energy (including households, electrical or electronic equipment's).

Every day surround us various types of intermediate frequency radiation (IF 300 Hz – 100 kHz) such as: video displays, anti-theft devices, card readers, metal detectors, electro surgery; Radiofrequencies (RF) (100 kHz to 300 GHz) used in wireless communications such as GSM, UMTS, Wireless LAN and RFID for both mobile devices and base stations, hospital applications, radio and TV broadcasting.

2. Impact on the environment by electromagnetic fields

Through the interaction between living organisms and electromagnetic fields are generated negative influences such as electromagnetic pollution and benefits like human therapy's using electromagnetic waves.

A key factor responsible for destroying environment quality is electromagnetic fields. Long-time excessive exposure to electromagnetic fields in buildings and outdoor public places can cause illness on human and environment as well.

Is well known that electromagnetic fields are causing non-thermal dramatic effects to human cells, tissue and organs, but currently nobody takes consideration about long-time exposure.

Several experiments have confirmed that microwave radiations, magnetic and electric radiations at very low frequency are causing human body stress reactions. Stress is the precursor phase for human illness determining the immune system to perform its functions.

The human body has an extremely adaptable capacity, but submitting the body to permanent aggression day by day is leading him to weakness with unknown harmful effects on health. The symptoms observed are hard to be awarded to other environmental factors, which operate simultaneously across urban environment.

Living organisms feel any modification in the magnetic field. That is perfectly normal because living organisms have polar molecules which interact with electric fields. Physiological process can be affected by the magnetic field, depending on the type, value or time period of exposure.

The ionic component of living organisms (Sodium, Chlorine, Potassium) under variable magnetic fields give rise through induction to micro-currents influencing biochemical reactions.

The studies carried out in past 15 years have revealed that animal's exposure to electric and magnetic fields (sinusoidal or static) for short or long periods reduce the maximum nocturnal levels of melatonin from blood.

After more than 30 years of research, WHO (World Health Organization) have published various studies and revealed that those persons who live close to high-voltage power lines present an increased risk of contracting cancerous diseases, leukaemia, cardiovascular diseases, mental, nervous or emotional problems, depression or suicides problems.

BioInitiative report concluded that there is a reasonable suspicion risk based on clear evidence about the negative impact on the environment caused by the bio-effect and after prolonged exposure is capable to have effects on human health as well.

As regards to ELF, a new public safety limit for inhabited areas should be established for all new buildings. A lower limit should be established for areas where are children or pregnant women.

A limit value for precaution should be adopted, cumulative for radioactive radiation and internal RF-fields, with considerably lower limits admitted than those existing now.

The IARC (International Agency for Research on Cancer, part of the WHO) evaluated the risks for cancer due to radio frequency radiation (RF).

THE ANNALS OF "DUNAREA DE JOS" UNIVERSITY OF GALATI
FASCICLE IX. METALLURGY AND MATERIALS SCIENCE
N°. 2 - 2019, ISSN 2668-4748; e-ISSN 2668-4756
Article DOI: https://doi.org/10.35219/mms.2019.2.07

Epidemiological human studies highlighted a suspected increased risk of glioma and neuroma acoustic.

RF radiations were classified as Group 2B, a possible human carcinogen agent [2].

On the other hand, there are evidences showing that long-term exposure to some CEM`s is a key risk factor for cancer, Alzheimer and male infertility [3].

In the case where scientific investigation is not conclusive, it is therefore appropriate to adopt the precautionary principle.

In these conditions, having the current rules and concerning we must think for a little bit where we are.

3. Equipment's used for measuring electromagnetic field

To measure the electric and magnetic fields values we used a NFA1000-3D Low Frequency Analyzer. The professional equipment is capable to measure simultaneous electric and magnetic fields at the same time.

Electric fields are generated by the present tension using the measurement unit in volts per meter (V/m). Magnetic fields are generated by flows of electricity in conductors, electric equipment's/devices and other metal pipes networks (water, gas network facilities). The unit used in the case is MilliGauss (mG) or MicroTesla (μT).

The measuring instrument NFA 1000 carries out automatic measurement and detection in real time offering frequency values for networks (50 Hz or 60 Hz) and their harmonics up to 2 kHz

Measurement data is stored on a memory card slot SD for analysis. The time limits set up to record data is 10 data sets/second.

The device is capable to record simultaneously all values of the three axis fields and in addition it records the automatic field E on an extra channel.

The reading of the counter and the recordings can be directly compared with the values obtained from the Classifications Recommendation of organizations/experts in buildings biology.

Furthermore, harmonic 3D frequency is recorded:

- 100/120 Hz 3D - second ununiformed harmonic;
- 150/180 Hz 3D – third ununiformed harmonic.

The harmonics frequencies are integral multiples of fundamental frequency supply, (ex: for a harmonic frequency of 50 Hz third rank the frequency will be 150 Hz).

Graphic colour assignment corresponds to standards for biological measurement of buildings SBM2015) [5]:

- Green for no concerns;
- Yellow for light concerns;
- Red for sever concerns;
- Purple for extreme concern.

4. Measurements results

The measurements were done in two different cities, different in size and development.

The measurements were done reached on foot, with a relative constant speed, at different hours, repeating the route in the same way.

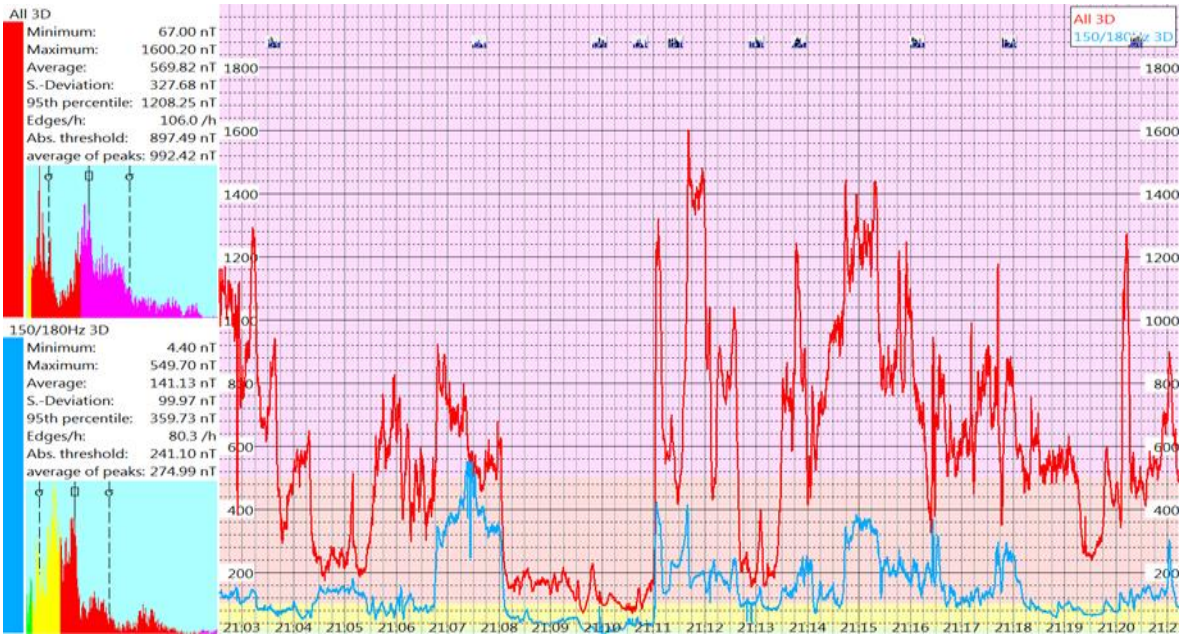

Fig. 1. *Graphic results at Griviția Boulevard area*

THE ANNALS OF "DUNAREA DE JOS" UNIVERSITY OF GALATI
FASCICLE IX. METALLURGY AND MATERIALS SCIENCE
N°. 2 - 2019, ISSN 2668-4748; e-ISSN 2668-4756
Article DOI: https://doi.org/10.35219/mms.2019.2.07

Fig. 2. *Measurement surface Griviţa Boulevard between Gheorghe Duca Boulevard and Grant Bridge*

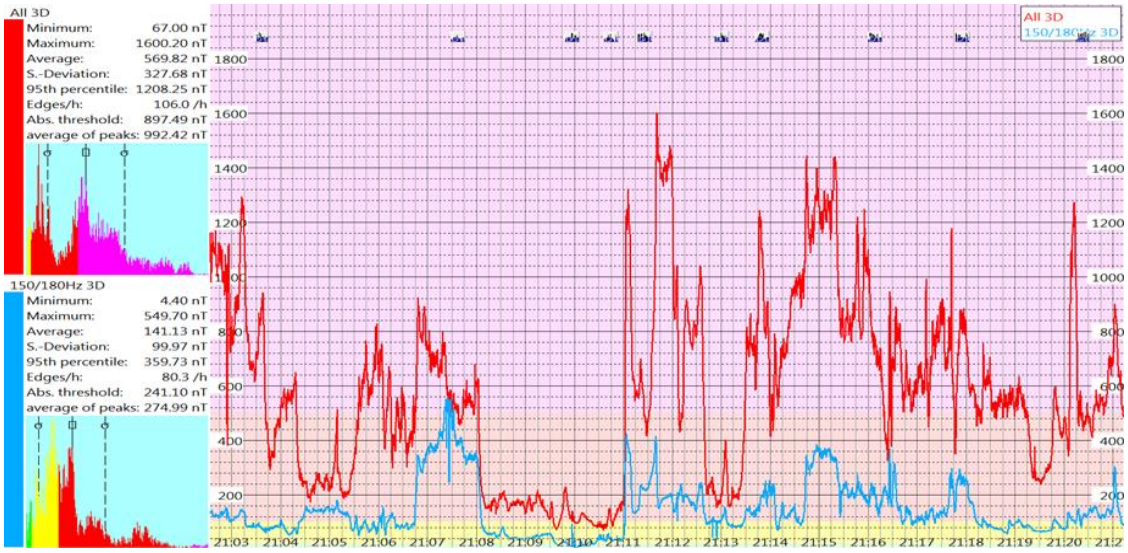

Fig. 3. *Graphic results at Grănicerilor Boulevard area*

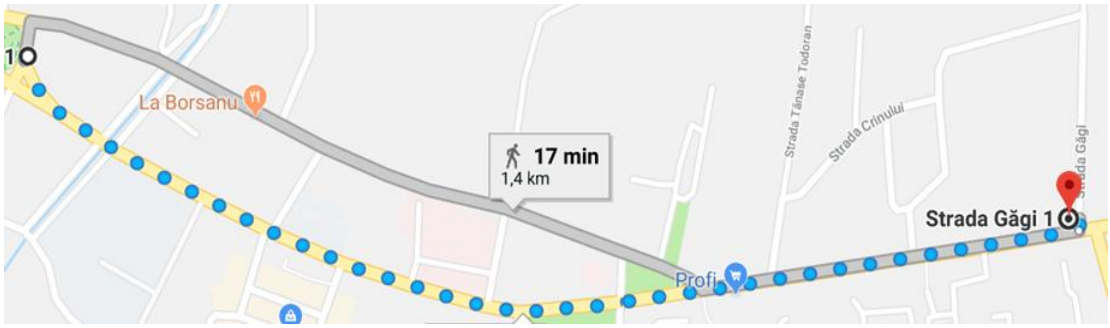

Fig. 4. *Measurement surface Grănicerilor Boulevard*

5. Conclusions

The measurements done in high traffic density shows that some electromagnetic fields values do exceed the accepted limits. The reason for exceeding the limit is the position of the: electric networks, switchboards, transformers or other electromagnetic devices too close to urban areas.

In this particular case is necessary to place warning signs, and second to build protection panels against electromagnetic fields.

References

[1]. ***, Rev Environ Health., 31(3), p. 363-97. doi: 10.1515/reveh-2016-0011, 1 sep. 2016.
[2]. Belyaev I., Dean A., Eger H., Hubmann G., Jandrisovits R., Kern M., Kundi M., Moshammer H., Lercher P., Müller K., Oberfeld G., Ohnsorge P., Pelzmann P., Scheingraber C., Thill R., *Guideline 2016 for the prevention, diagnosis and treatment of EMF-related health problems and illnesses*, Europaem EMF.
[3]. ***, *Ergänzung zum Standard der baubiologischen Messtechnik*, Institut für Baubiologie + Nachhaltigkeit IBN Richtwerte, SBM-2015 Baubiologische Richtwerte, Baubiologie Maes.
[4]. ***, www.bioinitiative.org, 2007.
[5]. ***, www.iarc.fr/en/media-centre/pr/2011/pdfs/pr208_E.pdf.
[6]. ***, www.gigahertz-solutions.de/en/custom/index/sCustom/74.

THE ANNALS OF "DUNAREA DE JOS" UNIVERSITY OF GALATI
FASCICLE IX. METALLURGY AND MATERIALS SCIENCE
N°. 2 - 2019, ISSN 2668-4748; e-ISSN 2668-4756
Article DOI: https://doi.org/10.35219/mms.2019.2.08

SUSCEPTIBILITY TO INTERGRANULAR CORROSION OF AA2024 ALUMINUM ALLOY USED IN AEROSPACE INDUSTRY

Vasile HOTEA
Technical University of Cluj Napoca – North University Center of Baia Mare
e-mail: vasilehotea50@yahoo.com

ABSTRACT

Idea in this work has been performed the susceptibility to intergranular corrosion of high strength aluminum alloy 2024 in aggressive corrosion environments. Intergranular corrosion is limited to the immediate area of the grain boundary and is not apparent by simple visualization and the resistance to intergranular corrosion of aluminum alloys in the Al-Cu-Mg system is related to the heating conditions applied during the solution treatment. This is can be an important source of limiting the life of the aircraft body where alloys from the 2xxx series are used, which is why they are systematically subjected to intergranular corrosion tests in dedicated laboratories.

KEYWORDS: AA2024 aluminum alloy, intergranular corrosion, metallography, optical microscopy

1. Introduction

The 2024 Al alloy (AA2024) is widely used in aviation industry due to its high strength to weight ratio, its high mechanical properties resulting from alloying elements such as copper [1, 2]. However, alloying elements generate a heterogeneous microstructure leading to an increase of the susceptibility of the alloy to localized corrosion such as intergranular corrosion [3].

The susceptibility to intergranular corrosion (IGC) depends mainly on the alloy composition and the thermal treatment applied. This form of corrosion can be very dangerous because the attack can be undetectable through the material and can damage the mechanical properties of the metal and cause rupture without visible external corrosion alloys. In the presence of seawater, the phenomenon of corrosion can occur, which consists in an attack on the anode area at the grain boundary. This attack may be relatively rapid and may exist without visible evidence [4].

The microstructure of metals and alloys is made up of grains, separated by grain boundaries. Intergranular corrosion is localized attack along the grain boundaries, or immediately adjacent to grain boundaries, while the bulk of the grains remain largely unaffected. This form of corrosion is usually associated with chemical segregation effects (impurities have a tendency to be enriched at grain boundaries) or specific phases precipitated on the grain boundary [5].

The type of treatment according to the ANSI H35 standard and the definitions used in the United States and Europe, through the European standard EN 515 and internationally through the standard ISO 2107, standard used for heat treated aluminum alloys is temper T3 and means solution treatment followed by natural aging and during the heat treatment, the aluminum alloy (AA2024-T3) is heated to a temperature at which the alloying elements dissolve [6].

The AA2xxx series of alloys are among the most complicated to analyse. While there have been several reports of the compositions of different phases within this group, most have focused on the legacy alloy AA2024-T3, which, unfortunately, is one of the most complex of the 2xxx series of alloys. To begin to understand the microstructure and its influence on corrosion it is important to know compositions of second phase intermetallic particles. Heat treatment dissolves mainly much of the Al_2Cu and Al_2CuMg [7].

Boag *et al.* showed that only the most intermetallic compounds on the surface of AA2024-T3 were associated with chloride signals drawing a strong link between clustering and stable pitting. The subsurface attack at these sites was almost exclusively intergranular, penetrating as much as 60 μm in 120 minutes exposure to 0.1M NaCl [7, 8].

THE ANNALS OF "DUNAREA DE JOS" UNIVERSITY OF GALATI
FASCICLE IX. METALLURGY AND MATERIALS SCIENCE
N°. 2 - 2019, ISSN 2668-4748; e-ISSN 2668-4756
Article DOI: https://doi.org/10.35219/mms.2019.2.08

Standard Practice for Evaluating Intergranular Corrosion Resistance of Heat Treatable Aluminum Alloys by Immersion in alkaline environments is ASTM G110-92 (2009) [9].

The purpose of this paper was to obtain more complete and clear information on the influence of the corrosion medium on the 2024-T3 alloy and also the influence of microstructure and heat treatment on the corrosion resistance. The corrosion behaviour was evaluated by intergranular corrosion tests, regarding the ASTM standard G110 - 92 for the evaluation of intergranular corrosion resistance of the thermally treated aluminum alloys by immersion in sodium chloride solution and hydrogen peroxide.

2. Experimental procedure

2.1. Materials and method

In this paper, the aluminum alloy 2024 - T3 extruded according to the classification of the American Aluminum Association was considered. This high strength alloy is commonly used in the aerospace industry and samples was received from UAC Europe SRL (Romania). The composition of the alloy is shown in Table 1.

Table 1. *Chemical composition of extruded aluminum alloy 2024 T3* [10]

Element	Al	Mg	Si	Mn	Cu	Zn	Fe	Cr	Ti	Other
(% w.)	Balance	1.2-1.8	0.5	0.3-0.9	3.8-4.9	0.25	Max 0.5	0.10	0.15	0.15

As can be seen from Table 1, the main alloying element for alloy 2024-T3 is copper with magnesium that plays an important role in this alloy class.

For the IGC corrosion test according to ASTM G110-92, a sample of the previous month is taken from the largest thickness extrusion profile (<0.25 "). The preparation of samples is shown schematically in Figure 1.

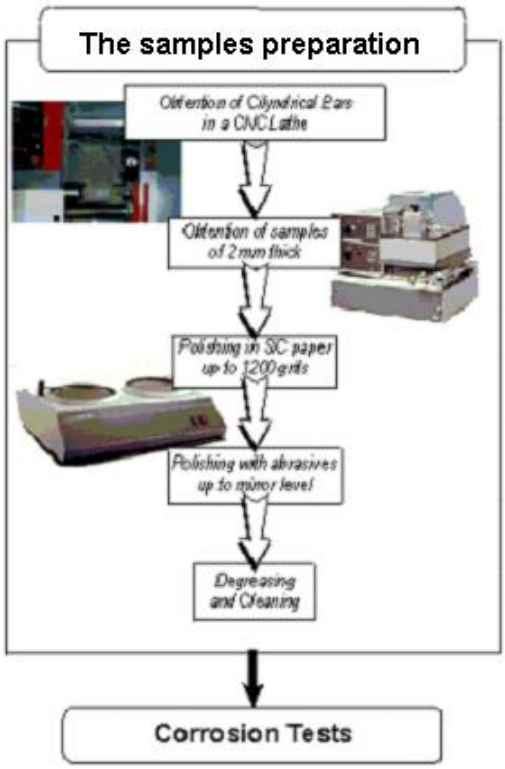

Fig. 1. *The samples preparation*

Samples must have clean surfaces, free of impurities, oils or any other kind of residue. Removal was performed by immersion of the sample in a 5% sodium hydroxide solution and 60 °C temperature, followed by immersion for 1 min in a concentrated nitric acid solution.

The samples exposed in the corrosion solution should be carried out at 30 ± 3 °C. The samples were identified in such a way as to ensure the traceability of the test material. The test specimen was machined by grinding / milling so that 10% of the test surface was removed. All solutions used for the test are prepared using chemical reagents and deionized water. Prior to intergranular corrosion testing, the samples were degreased by immersion for one minute in the degreasing solution.

Fig. 2. *Place the samples in the vessel with the corrosion solution*

The intergranular corrosion test solution consisted of 57 grams of sodium chloride (NaCl),

THE ANNALS OF "DUNAREA DE JOS" UNIVERSITY OF GALATI
FASCICLE IX. METALLURGY AND MATERIALS SCIENCE
N°. 2 - 2019, ISSN 2668-4748; e-ISSN 2668-4756
Article DOI: https://doi.org/10.35219/mms.2019.2.08

oxygenated water (H_2O_2) 10 mL and deionized water 945 mL.

In the case of the use of several samples, they will be immersed in the same vessel with the corrosive solution, as seen in Figure 2, taking care to be arranged separately so that they do not touch each other. The container in which the samples are to be tested must be made of plastic or glass.

3. Optical microscopy

The corroded samples were embedded and analysed metallographically on a Leica DM2500 optical microscope, with 100 W bright illumination, high quality, optical performance, as well as last-minute accessories.

It is coupled to a Windows operating system, determining the microstructure of the sample surface, after having previously been pre-treated by grinding, polishing and chemical attack with 5% orthophosphoric acid for 5 minutes. After a 6-7 hour immersion, the specimens are removed from the corrosive solution, washed, brushed with a soft brush to remove corrosion products and dried with compressed air. Each specimen is examined at a magnification of 10x for the location of the corroded surface.

After locating the corroded surface, it is cut from the corroded sample at a distance of approximately 20 mm (¾″) from the edge length. The samples thus taken are prepared for the assessment of susceptibility to intergranular corrosion (IGC). The sample preparation is done according to the laboratory methodology, and the image of the corroded and clean samples are shown in Figure 3.

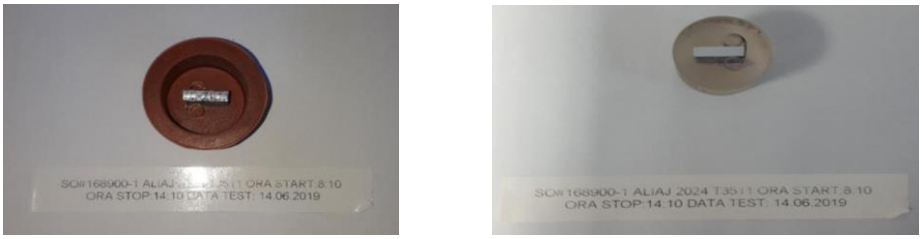

Fig. 3. *Sample taken (left) and embedded in cross section (right)*

3.1. Metallographic evaluation

The procedure for the metallographic evaluation of corrosion damage was in accordance to ASTM G46-94 (2018) [11]. The maximum depth of intergranular corrosion is investigated in the cross section by examination under the optical microscope, and the degree of susceptibility to intergranular corrosion can be of maximum 0.01″ (0.254 mm) or according to the client's specification.

Figures 4 and 5 show the optical micrographs at a magnification of 200x and at different times regarding the intergranular corrosion of the 2024-T3 alloy.

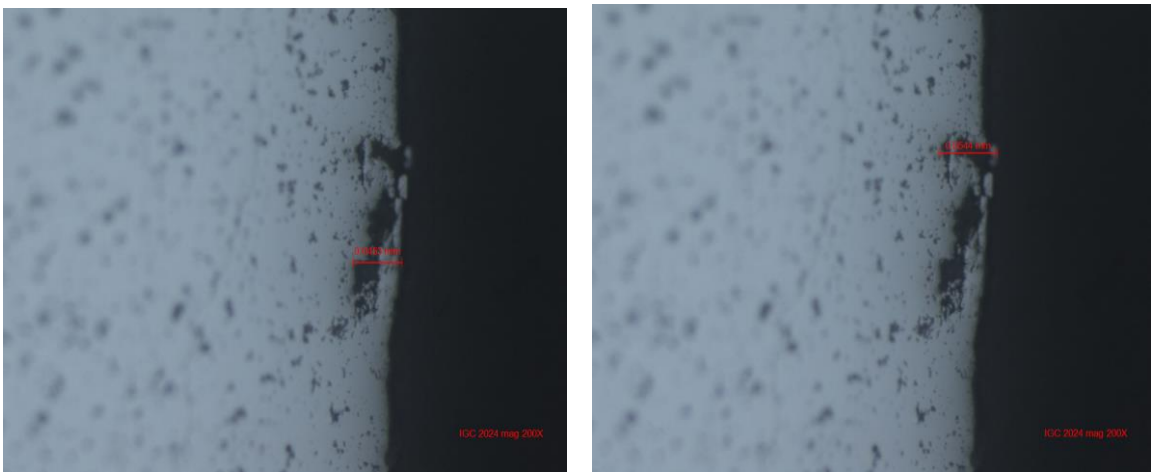

Fig. 4. *Corrosion after 2 hours (left) and Corrosion after 4 hours (right)*

THE ANNALS OF "DUNAREA DE JOS" UNIVERSITY OF GALATI
FASCICLE IX. METALLURGY AND MATERIALS SCIENCE
N°. 2 - 2019, ISSN 2668-4748; e-ISSN 2668-4756
Article DOI: https://doi.org/10.35219/mms.2019.2.08

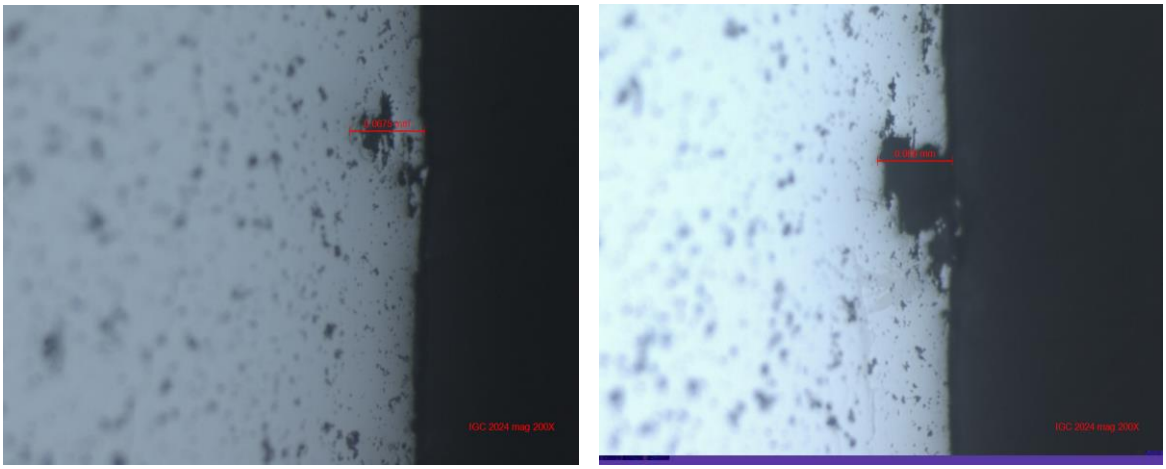

Fig. 5. *Corrosion after 6 hours (left) and Corrosion after 8 hours (right)*

After 4 hours of exposure, even if the average depth of corrosion increased slightly to 0.054 mm, most of the developed corrosion points are still a little shallow, where their distribution is observed in terms of their depth.

The results regarding the metallographic examination on the depth of the samples are centralized in Table 2.

Table 2. *Metallographic examination of the corrosion samples on their depth*

Exposure time [h]	2	4	6	8
Characterization of corrosion	Pits	Pits	Intergranular corrosion	Exfoliation corrosion

The metallographic evaluation of the corrosion on the top surface is summarized in Table 2 and the corrosion damage evolution in Figure 4.-5. The results indicate that corrosion damage evolves from pitting to exfoliation progressively.

By increasing the corrosion exposure time from 6 hours to 8 hours, the pits become deeper and wider, and the cross sections have shown that the most pronounced shape is mainly quoted at 0.069 mm leading to a stratification and exfoliation which is a severe form of intergranular corrosion.

In extruded products, if the crystalline grains are flattened and elongated in the extrusion direction, the presence of intergranular corrosion can lead to stratification and exfoliation, as seen in Figure 6.

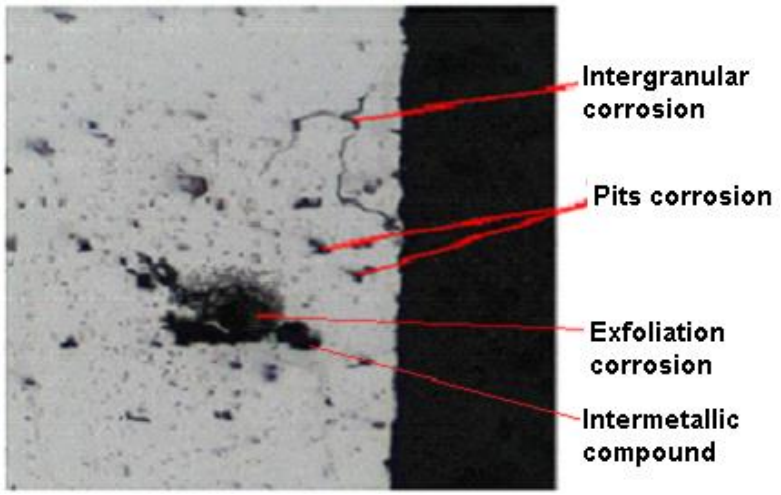

Fig. 5. *Intergranular corrosion at 2024-T3 alloy (500x)*

THE ANNALS OF "DUNAREA DE JOS" UNIVERSITY OF GALATI
FASCICLE IX. METALLURGY AND MATERIALS SCIENCE
N°. 2 - 2019, ISSN 2668-4748; e-ISSN 2668-4756
Article DOI: https://doi.org/10.35219/mms.2019.2.08

From a corrosion perspective, the dominant characteristics of the high strength alloy microstructure of the 2xxx series are the granular structure and the distribution of the intermetallic compounds (Al_3Fe, Al_2Cu), which include components and particles of impurities and dispersoids that precipitate. On a larger scale, the corrosion is observed around the constituents and impurities of the particles that result from a severe corrosion attack by points as observed in the above image [12, 13].

The high-strength 2024 -T3 alloy has a phase distribution ranging in size from about 0.1 microns to a few nanometres in diameter. These particles (as the secondary phase) are enriched in different alloying elements, particles that form during the initial solidification of the moulded blank and do not dissolve to a large extent during the heat treatment. This is why aluminum alloys with copper content (from the 2xxx series), with heat treatments in temper T3, are susceptible to intergranular corrosion.

4. Conclusions

In this paper, an extensive metallographic investigation was carried out to evaluate the corrosion damage of the aluminum alloy AA2024-T3 after exposure to corrosion in strongly corrosive environments with NaCl solution and oxygenated water (H_2O_2). The defects were quantified in terms of the metallographic characteristics of the corrosion, namely the depth of the corrosion points and their thickness.

The susceptibility to intergranular corrosion depends mainly on the composition of the alloy and the heat treatment applied. This form of corrosion can be very dangerous, as the attack can go undetected in the material and cause cracking and tearing, with no visible signs of corrosion in the alloy.

Corrosion damage has been found to progressively evolve, from pits to intergranular corrosion and exfoliation, with exposure time.

The cross sections of the embedded samples showed that the lateral surfaces of the material accumulated a significant amount of deep sample damage compared to the damage detected on the surface of the samples.

As a result, this can be an important source of limiting the life of the aircraft body where alloys from the 2xxx series are used, which is why they are systematically subjected to intergranular corrosion tests in dedicated laboratories.

References

[1]. ***, *Aging of U.S. AirForce Aircraft: Final Report*, Commission on Engineering and Technical Systems, Committee on Aging of U.S. Air Force Aircraft, National Research Council, Division on Engineering and Physical Sciences and National Materials Advisory Board, National Academies Press, Washington, 1997.
[2]. ***, *Success stories: air force; material substitution and new sealing*, vol. 7, no. 4, 2003.
[3]. M.-L. de Bonfils Lahovary *et al.*, Corrosion Science, 119, p. 60–67, 2017.
[4]. Roberge P. R., *Handbook of corrosion engineering*, New-York. McGraw-Hill, Inc. 2000.
[5]. ***, https://www.nace.org/resources/general-resources/corrosion-basics/group-2/intergranular-corrosion.
[6]. ***, *American National Standard Alloy Temper Designation System for Aluminum, Secretariat, The Aluminum Association*, Inc., ANSI H35.1/H35.1(M) – 2009 Revision of H35.1/H35.1(M) – 2006approved April 7, 2009.
[7]. Zaki Ahmad, *Recent Trends in Processing and Degradation of Aluminium Alloys, Chapter 10 - High Strength Al-Alloys: Microstructure*, Corrosion and Principles of Protection, ISBN: 978-953-307-734-5, DOI: 10.5772/741, 2011.
[8]. Boag A., A. E. Hughes, *et al.*, *Corrosion of AA2024-T3 Part I. Localised corrosion of isolated IM particles*, Corrosion Science, 53(1), p. 17-26, 2011.
[9]. ***, *Standard Practice for Evaluating Intergranular Corrosion Resistance of Heat Treatable Aluminium Alloys by Immersion in Sodium Chloride and Hydrogen Peroxide Solution*, ASTM International, West Conshohocken, PA, ASTM G110-92, 2009.
[10]. ***, http://asm.matweb.com.
[11]. ***, *Standard Guide for Examination and Evaluation of Pitting Corrosion*, DOI: 10.1520/G0046-94R18, ASTM G46-94, 2018.
[12]. Vargel C., Jacques M., Schmidt M. P., *Types of Corrosion on Aluminium, in Corrosion of Aluminium*, Elsevier: Amsterdam. p. 113-146, 2004.
[13]. Glenn M., Muster T. H., *et al.*, *Corrosion of AA2024-T3 Part III: Propagation*, Corrosion Science, 53(1), p. 40-50, 2011.

THE ANNALS OF "DUNAREA DE JOS" UNIVERSITY OF GALATI
FASCICLE IX. METALLURGY AND MATERIALS SCIENCE
N°. 2 - 2019, ISSN 2668-4748; e-ISSN 2668-4756
Article DOI: https://doi.org/10.35219/mms.2019.2.09

ASSESSMENT OF VISUAL EXAMINATION FOR WIRE ROPE SLINGS USING THE ATTRIBUTIVE MEASUREMENT SYSTEM ANALYSIS

Carmen SIMION
University Lucian Blaga from Sibiu, Faculty of Engineering, Romania
e-mail: carmen.simion@ulbsibiu.ro

ABSTRACT

Wire ropes are used for a variety of day-to-day job operations. They have a finite service life and therefore requires consistent, thorough and documented examinations to identify component degradation before a failure. Conducting regular examinations is the most effective way to detect, monitor and respond to wire rope sling fatigue failures. Thorough routine examinations should be carried out by a capable and experienced person so the assessment of the visual examination for wire ropes is crucial to obtain the confidence in the inspection process.

The purpose of this paper is to determine if the persons using the sling in a day-to-day job have sufficient training and practical experience to perform visual examination of wire rope slings, using the method of attributive measurement system analysis. This method looks at how effective or capable a person is in accepting good products and sorting out bad products repeatedly and looks also at the probability of a bad product being missed and a good one rejected. The results were processed with MINITAB software.

KEYWORDS: wire rope slings, visual examination, discard criteria, attributive measurement system analysis

1. Basics of wire rope sling

Wire rope is a very complex machine having the primary function to move, which in turn is where it obtains its source of strength. It has three basic components: wires, strands and core (Fig. 2) [1, 2]:

- the wires are single and continuous lengths of metal materials including steel, iron, stainless steel, monel and bronze; they can be manufactured in a variety of grades that relate to the strength, resistance to wear, fatigue resistance, corrosion resistance and curve of the wire rope. The wires form the strands and together provide the rope's strength;
- the strands consist of two or more wires arranged and twisted in a specific arrangement; the individual strands are then laid in a helical pattern around the core of the rope. Strands made of larger diameter wires are more resistant to abrasion, while strands of smaller diameter wires are more flexible;
- the core, which forms a foundation for the strands, runs through the center of the rope and supports the strands and helps to maintain their relative position under loading and bending stresses. Cores can be made from different materials including natural or synthetic fibers and steel to give the rope support and flexibility.

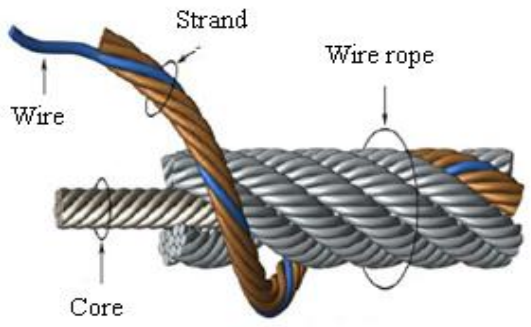

Fig. 1. *Components of a wire rope* [2]

Therefore, a wire rope is essentially numerous metal strands spiralled around the wire core. The construction of the wire rope is primarily specified by the number of strands and the number of wires in each strand. The arrangement of wires in the strand,

THE ANNALS OF "DUNAREA DE JOS" UNIVERSITY OF GALATI
FASCICLE IX. METALLURGY AND MATERIALS SCIENCE
N°. 2 - 2019, ISSN 2668-4748; e-ISSN 2668-4756
Article DOI: https://doi.org/10.35219/mms.2019.2.09

type of lay and outer and core material depend on the rope's indispensable application for its usage. The main uses are running ropes, stationary (stay) ropes, track ropes and wire rope slings.

Wire rope sling (Fig. 2) is a preferred lifting device because it is one of the most reliable ways to secure a load to lifting equipment. Wire rope slings are light, strong, and durable and they can be used in a variety of ways for many different kinds of lifts. They are popular in the construction, automotive, oil and gas and general manufacturing industries where a variety of heavy loads and rugged conditions exist and also very popular in steel mills and forging facilities where the durability of the rope is really put to the test [2].

Traditional single-part wire rope slings are constructed from multiple steel wires that form individual strands laid in a helical pattern around a fiber or steel core. Different configurations of the material, wire and strand structure will provide different benefits for the specific lifting application, including: strength, flexibility, abrasion resistance, crushing resistance, fatigue resistance, corrosion resistance and rotation resistance [2].

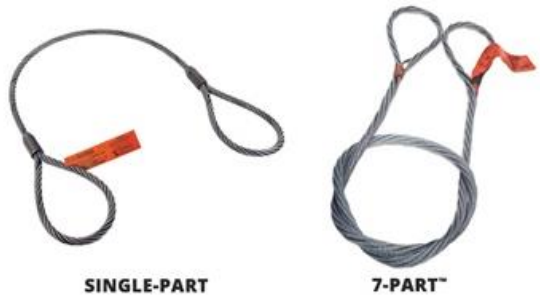

Fig. 2. *Wire rope slings* [2]

1.1. Visual examination of wire rope slings

Better performance of wire rope slings is achieved if and only if they are healthy. This is assured when maintenance and inspection are carried out at regular interval of time by a capable person.

Wire rope sling is a consumed item and therefore requires consistent, thorough and documented inspections to identify component degradation before a failure. Detailed inspection requirements for wire rope slings are described in the international standards such as ISO 8792, federal regulations such as OSHA 1910.184 and applicable industry standards such as ASME B30.9.

There are two major non-destructive inspection methods: visual examination (the most effective) that is useful for detecting external deterioration and electromagnetic inspection for the detection of internal damages.

To ensure that all wire rope slings are properly inspected, it is important to know how frequently inspections should be performed, who should perform the inspections and what criteria should be examined to pass an inspection.

During service, wire rope slings are subjected to conditions which affect their safe working characteristics. It is necessary therefore to ensure that the sling is safe for continued use. The sling shall be inspected for damage or deterioration before each period of use and therefore shall be checked for obvious defects at suitable intervals during service. In addition, thorough routine examinations (visual examination) shall be carried out, at intervals not exceeding six months and this interval shall be less where deemed necessary or where required by statutory requirements, by a competent person. Where necessary, the thorough examinations shall be supplemented by other means such as non-destructive testing in order to detect damage or deterioration which might affect the firmness for use of the wire rope sling [3].

A specific procedure for wire rope sling inspection is the best safeguard against injury, death and property damage. To detect possible damage, it is necessary to perform a visual inspection throughout their entire length.

All wire rope slings should be inspected at regular intervals and it is important to employ a three-stage level of inspection to ensure that slings are inspected with appropriate frequency [2, 4, 5]:

- Initial inspection (prior to initial use) upon receiving from the manufacturer. Double-check the sling tag to make sure it's what you ordered and that the rated capacity meets all of your project specifications and lifting requirements.

- Frequent (daily at the beginning of each work period or prior to use): a designate competent person must also determine that the wire rope sling is proper for the intended use, hitch, load and environment. Any condition that may result in a hazard shall cause the sling to be removed from service.

The designated person is selected or assigned by the employer or employer's representative as being competent to perform specific duties.

All running ropes and slings in service should be visually inspected once each working day.

- Periodic inspection, performed by either a professional service provider or by a qualified person.

Qualified person is a person, who by possession of a recognized degree or certificate of professional standing in an applicable field, or who, by extensive knowledge, training and experience, has successfully demonstrated the ability to solve or resolve problems relating to the subject matter and work.

The interval of periodic inspection is based upon: the frequency of use, severity of the service

THE ANNALS OF "DUNAREA DE JOS" UNIVERSITY OF GALATI
FASCICLE IX. METALLURGY AND MATERIALS SCIENCE
Nº. 2 - 2019, ISSN 2668-4748; e-ISSN 2668-4756
Article DOI: https://doi.org/10.35219/mms.2019.2.09

conditions, the nature of the work being performed and experience gained during the inspection of slings.

At least one periodic inspection is required annually, but ASME provides these additional periodic inspection guidelines based on the service of the wire rope sling: normal service – yearly, severe service – monthly to quarterly and special service – as recommended by a qualified person.

The visual examination should be carried out by appropriately qualified, capable, experienced person using the wire rope in a day-to-day job who has learned through special training or practical experience what to look for and who knows how to judge the importance of any abnormal conditions they may discover. It is the responsibility of the person making the inspection to follow the proper inspection criteria for each application [4].

1.2. Basic inspection criteria

While inspecting (examination) a wire rope sling there are certain important considerations that need to be kept in mind. Once such consideration is of course the frequency of it use, but some other important aspects include: application of the wire rope sling, operational conditions like weather etc., manufacturer recommendations and statutory requirements and analysis of wire rope sling history of its previous used for the same application.

An inspection (examination) consists of observation of all wire ropes and end connections which can reasonably be expected to be in use during daily operations.

ISO, OSHA and ASME specific that wire rope slings shall be removed from service if any of the following mainly discard criteria are visible [3, 6, 7]:

- missing or illegible sling identification (tag);
- broken wires/localized faults (LFs);
- corrosion of the rope or end attachments;
- distortion/deformation: kinking, crushing, bird caging (basket deformation), doglegs or any other damage resulting in distortion of the structure;
- mechanical damage at end attachments;
- heat damage (including electric arcing) which is evident by wire discoloration, burn marks, weld splatter, etc.;
- decrease (reduction) in rope diameter/loss of metallic area (LMA);
- other conditions, including visible damage that cause doubt as to be continued use of the wire rope sling.

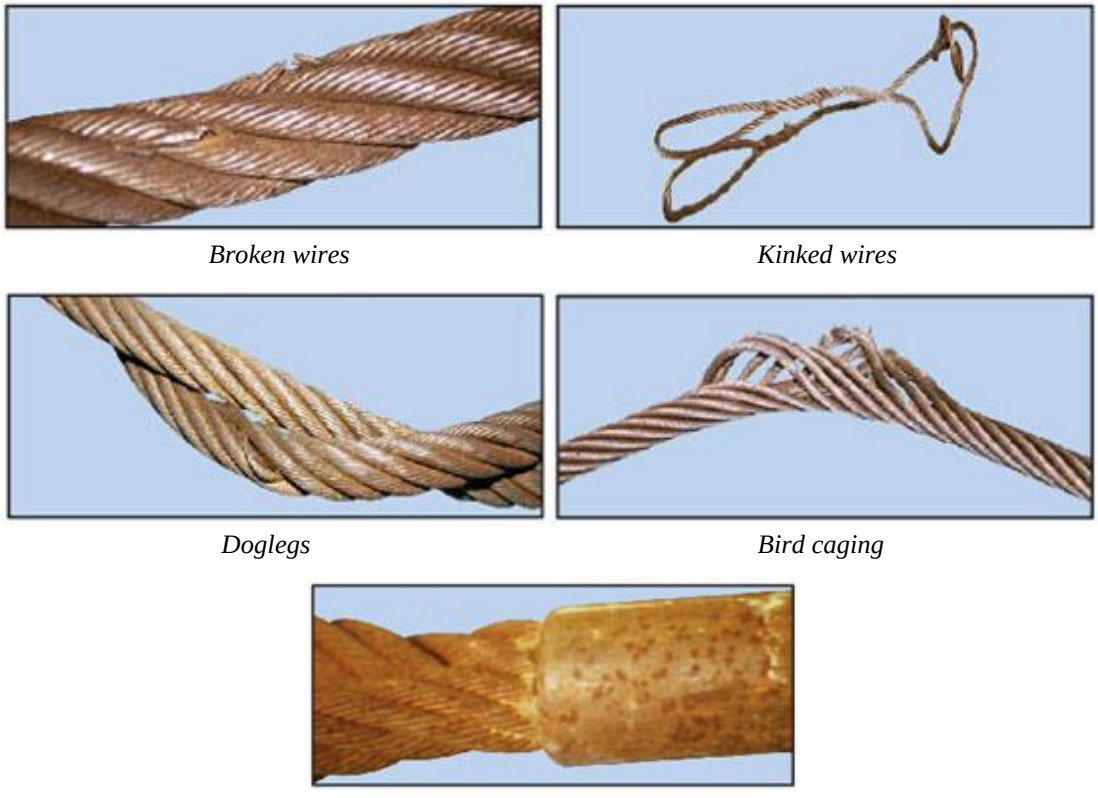

Broken wires *Kinked wires*

Doglegs *Bird caging*

Corrosion

***Fig. 3**. Basic inspection criteria* [5]

THE ANNALS OF "DUNAREA DE JOS" UNIVERSITY OF GALATI
FASCICLE IX. METALLURGY AND MATERIALS SCIENCE
N°. 2 - 2019, ISSN 2668-4748; e-ISSN 2668-4756
Article DOI: https://doi.org/10.35219/mms.2019.2.09

Abraded/worn wire

Heat damage

Damaged fittings

***Fig. 3**. Basic inspection criteria - continued* [5]

2. About attributive measurement system analysis

A measurement system is a collection of operations, procedures, gages and other equipment, software and personnel used to assign a number or a qualificative to the characteristic being measured or categorized [8]. Measurement system can be divided into two categories: variable (for continuous data) and attribute measurement system (for discrete data).

Most problematic measurement system issues come from measuring discrete data, which are usually the result of human judgment when categorizing products "good" or "bad" as a result of the visual inspection. This is because it is very difficult for all inspectors/appraisers to apply the same operational definition of what is "good" and what is "bad". However, such measurement systems are seen everywhere so it is important to quantify how well they are working [9].

The attributive measurement system analysis is a set of trials conducted to assess the inspector ability to categorize products. The methodology involves multiple inspectors (two or more) that categorize, independently and in a random order, multiple products (usually between 20 and 30) multiple number of times (two or more trials). Measures are calculated based on how often the inspectors correctly characterize each product (agreement with the standard) and how frequently they agree with themselves and each other.

The methodology uses two primary methods of assessing the agreement of the attribute with the standard: the percentage or extent to which the inspectors agree with the standard and Kappa statistics (the percentage or extent to which adjustment is made between the agreement between the appraisals and the standard, after chance agreement has been removed) [8-10]:

- agreement within inspector: the percentage or extent to which each inspector agrees with himself or herself on all trials when each inspector conducts more than one trial;
- agreement between inspectors: the percentage or extent to which all inspectors agree with each other on all trials when more than one inspector makes one or more trials;
- agreement of each inspector versus standard: the percentage or extent to which each inspector agrees with himself or herself as well as with the standard when a known standard is specified;
- agreement of all inspectors versus standard: the percentage or extent to which inspectors agree with each other on all trials as well as with the standard when a known standard is specified;
- kappa statistic indicating the degree of agreement of the assessments made by multiple inspectors when evaluating the same products; Fleiss's kappa - statistic used for assessing the reliability of agreement when inspectors are selected at random from a group of available inspectors; Cohen's kappa - statistic used for assessing the reliability of agreement when the inspectors are specifically chosen and are fixed.

The key in all measurement systems is having a clear assessment method and clear criteria for what to accept and what to reject. The hypothesis test analysis method, used in this analysis, consists mainly of qualificative/classification counting and division and the results are evaluated using acceptability criteria from AIAG MSA reference manual presented in

THE ANNALS OF "DUNAREA DE JOS" UNIVERSITY OF GALATI
FASCICLE IX. METALLURGY AND MATERIALS SCIENCE
N°. 2 - 2019, ISSN 2668-4748; e-ISSN 2668-4756
Article DOI: https://doi.org/10.35219/mms.2019.2.09

Table 1 [8]. For any marginally acceptable or unacceptable measurement system, corrective action is required and when corrective action is completed, the attribute MSA must be redone.

Table 1. *Decision criteria* [8]

Measures	Excellent	Acceptable	Not acceptable
Within Appraisers	> 90%	80%-90%	< 80%
Appraiser vs. Standard	> 90%	80%-90%	< 80%
Disagreement G/NG	< 2%	2%-5%	> 5%
Disagreement NG/G	< 5%	5%-10%	> 10%
Between Appraisers	> 90%	80%-90%	< 80%
Appraisers vs Standard	> 90%	80%- 90%	< 80%

A general rule of thumb is that values of kappa greater than 0.75 indicate good to excellent agreement (with a maximum kappa = 1); values between 0.40 and 0.75 indicate marginal agreement and values less than 0.40 indicate poor agreement [8].

3. Case study

Because it is important that all inspections must be done by appropriately qualified and capable personnel, the purpose of the paper is to determine if the persons using the wire rope slings in a day-to-day job have sufficient training and practical experience to perform their visual examination.

In order to assess the inspection process, the attributive MSA method was used. This looks at how effective or capable a person (appraiser) is in accepting good products and sorting out bad products repeatedly and looks also at the probability of a bad product being missed and a good one rejected.

The results were processed using MINITAB software with its module called Attribute Agreement Analysis [11].

Analysing results of the research, presented in Figure 4 and Tables 2 to 6, the conclusions are:

- Within Appraisers (Individual Repeatability of inspectors) is above 90%, so excellent (Fig. 5 – left side and Table 2): this means that inspectors are consistently with themselves; also, Fleiss's values of kappa statistic indicate very good (for appraiser 3) to excellent agreement (for appraiser 1 and 2);

- Each Appraiser vs. Standard (Individual Effectiveness of inspectors) is also above 90%, so excellent (Fig. 5 – right and Table 3): this means that inspectors are in agreement with the true status (standard) of the wire rope sling; also, Fleiss's values of kappa statistics indicate very good (for appraiser 2 and 3) to excellent agreement (for appraiser 1);

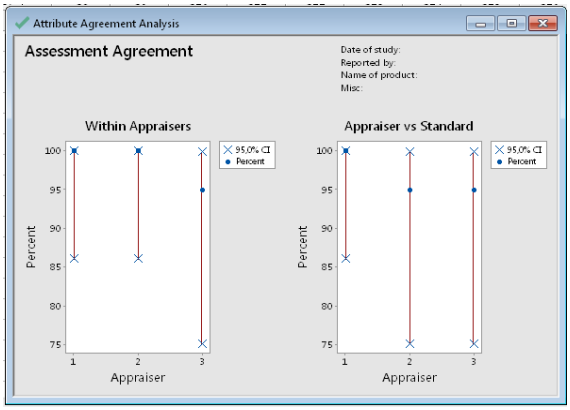

Fig. 4. *Minitab graphs*

Table 2. *Within appraisers' results*

Appraiser	# Inspected	# Matched	Percent
1	20	20	100.00
2	20	20	100.00
3	20	19	95.00

Matched: Inspector agrees with him/herself across trials

Fleiss' Kappa Statistics		
Appraiser	Response	Kappa
1	G	1.00000
	NG	1.00000
2	G	1.00000
	NG	1.00000
3	G	0.85663
	NG	0.85663

Table 3. *Each appraiser vs. standard results*

Appraiser	# Inspected	# Matched	Percent
1	20	20	100,00
2	20	19	95,00
3	20	19	95,00

Matched: Inspector's assessment across trials agrees with the hnown standard

Fleiss' Kappa Statistics		
Appraiser	Response	Kappa
1	G	1.00000
	NG	1.00000
2	G	0.85663
	NG	0.85663
3	G	0.92832
	NG	0.92832

- Assessment Disagreement (Table 4) results show that inspector 2 classified a good wire rope

THE ANNALS OF "DUNAREA DE JOS" UNIVERSITY OF GALATI
FASCICLE IX. METALLURGY AND MATERIALS SCIENCE
N°. 2 - 2019, ISSN 2668-4748; e-ISSN 2668-4756
Article DOI: https://doi.org/10.35219/mms.2019.2.09

sling as a bad one on 1 occasion and inspector 3 was inconsistent in his judgments on 1 occasion;

- Between Appraisers (Reproducibility of Measurement System), shows that all three inspectors agreed with each other on both assessments to 90% (on 18 out of 20 inspected wire rope slings), so acceptable; Fleiss's values of kappa statistic indicate good agreement, too (Table 5).

Table 4. *Assessment disagreement results*

Person	# NG/G	%	# G/NG	%	# Mixed	%
1	0	0	0	0	0	0
2	0	0	1	20	0	0
3	0	0	0	0	1	5

NG/G: Assessment across trials =NG / standard=G
G/NG: Assessment across trials =G / standard=NG
Mixed: Assessment across trials are not identical

Table 5. *Between appraisers' results*

# Inspected	# Matched	Percent
20	18	90.00

Matched: All inspectors' assessments agree with each other

Fleiss' Kappa Statistics		
Response	Kappa	SE Kappa
G	0.875747	0.0577350
NG	0.875747	0.0577350

Table 6. *All appraisers versus standard results*

# Inspected	# Matched	Percent
20	18	90.00

Matched: All inspectors' assessments agree with the known standard

Fleiss' Kappa Statistics		
Response	Kappa	SE Kappa
G	0.928315	0.0912871
NG	0.928315	0.0912871

- All Appraisers versus Standard (overall Effectiveness of the Measurement System) tells that for 18 out of 20 wire rope slings inspected all three inspectors agreed with the true status, which represents 90%, so acceptable;

Fleiss's values of kappa statistics indicate also a very good agreement (Table 6).

In conclusion, the visual examination of wire rope slings is carried out by appropriately qualified, capable and experienced personnel and conducting regular examinations is the most effective way to detect, monitor and respond to wire rope sling fatigue failures.

4. Conclusions

Human measurement systems are often used to perform visual inspection, so their assessment is important to see where the problems are and eliminate them. The attribute MSA study is just one of many such tools that may be used to verify the validity of the data collected through a measurement system.

Because most processes require at least some form of subjective judgment, visual inspection must be carried out by a trained person, in which any product defect is detected by the aid of a naked eye.

Good practice requires that all wire rope slings should be subject to a frequent inspection to ensure that they are proper for the intended use.

The paper demonstrated an effective mean by which to evaluate inspection personnel capability to assess the quality of the wire rope slings through visual examination, using attributive measurement analysis technique.

References

[1]. ***, https://www.osha.gov/dts/shib/shib011917.html.
[2]. ***, https://www.mazzellacompanies.com/Resources/Blog/.
[3]. ***, *Wire rope slings - Safety criteria and inspection procedures for use*, ISO 8792, 1986.
[4]. ***, https://www.spanco.com/wire-rope-sling-inspection/.
[5]. ***, https://www.lift-it.com/info-wire-rope-considerations, https://www.rentlgh.com/blog/how-to-inspect-wire-rope-slings/.
[6]. ***, ASME B30.9, Slings, 2018.
[7]. ***, OSHA 1910.184, Slings.
[8]. ***, Automotive Industry Action Group (AIAG), Measurement Systems Analysis, 4th edition, Detroit-Michigan, 2010.
[9]. ***, http://www.isixsigma.com/tools-templates/measurement-systems-analysis-msa-gage-rr/making-sense-attribute-gage-rr-calculations/.
[10]. **Durivage M. A.**, *Practical attribute and variable measurement system analysis (MSA): a guide for conducting gage R&R studies and test validations*, Quality Press, ISNB 978-0-87389-915-4, 2016.
[11]. ***, *Minitab 17 Statistical Software, State College*, PA: Minitab, Inc., 2010.

THE ANNALS OF "DUNAREA DE JOS" UNIVERSITY OF GALATI
FASCICLE IX. METALLURGY AND MATERIALS SCIENCE
No. 2 - 2019, ISSN 2668-4748; e-ISSN 2668-4756
Article DOI: https://doi.org/10.35219/mms.2019.2.10

VARIATION OF THE FORCES WITH THE WIND DIRECTION TO AN EXPERIMENTAL MODEL OF AERODYNAMIC PROFILE OF WIND TURBINE

Nelu CAZACU
"Dunarea de Jos" University of Galati, Romania
e-mail: nelu.cazacu@ugal.ro

ABSTRACT

The work is based on wind tunnel experiments on an experimental turbine blade model. The vertical force (Lift) and the resisting force (Drag, in the wind direction) are measured. The tests can be considered under static conditions because the experimental model rotates with a hexadecimal degree per second. The measurement range is 180 (-90...+90) at the maximum wind speed of 9 m/s. The results confirm the importance of the position of the blade with respect to the wind direction and its speed.

KEYWORDS: wind tunnel, lift force, drag force

1. Introduction

The phenomenological understanding of lift (lift), drag force (drag), aerodynamic fineness of the profile and the influence of the angle of attack on the behaviour of the aerodynamic profile, is the basis for designing small wind turbines. The aerodynamic profile is the cross section through a wind turbine such as the NACA 4412 profile is shown in Fig. 1 [1]. Under certain conditions of air flow in addition to this profile, the load-bearing force appears in the blade and which is large enough to generate a couple of forces.

The wind blades have similar aerodynamic profiles, because the working principle is the same as in the wing of the plane, the resultant being the carrying force and the resistant force. This time the air mass is naturally moving in the form of air currents (wind) that are generated by the pressure differences between two geographical points at different distances. Mainly the local pressure at these points is given by the density of the air (atmosphere) the hot air having a lower density than the cold air.

Much of the energy of radiation from the sun is found in the kinetic energy of the wind [2, 3].

A specialized profile for the three-blade wind turbine downstream is SG6050 (Selig / Giguere), where the name retains the inventors' initials.

Aerodynamic profiles are still considered to be a combination of art and science. Profiles are constructed by coordinates (x, y) for a large number of points). Performance verification is usually done under laboratory conditions, based on experiments in the wind tunnel on experimental models, after which the main curves characterizing the behaviour of the profile are constructed.

Small wind turbines occupy an important area in wind energy conversion like night lighting. A common application of such wind turbines is to illuminate the parking spaces at night [4]. This application is widespread and due to the development of white LEDs that have very low consumption compared to lighting methods considered classic for such applications the small wind turbines must be adapted to the annual wind values in the location area and equipped with a DC or AC multiplier and electric generator.

In both generator situations the voltage and DC current used to charge a battery (battery) are obtained by intercalating some converters. For example, you can use a DC: DC converter that has a large input range and 12 V, or 24 V or 48 V at the output. The diameter of small residential wind turbines has values between 1...2.5 m, the number of blades is 2...6, the output power being 300 W...2.5 kW, for low wind speeds, the method of widening the blade is used by increasing the gas-dynamic length of the profile. A reduction of the wind speed by half can be associated with a two-fold increase in the airflow length, to maintain the same Re.

THE ANNALS OF "DUNAREA DE JOS" UNIVERSITY OF GALATI
FASCICLE IX. METALLURGY AND MATERIALS SCIENCE
No. 2 - 2019, ISSN 2668-4748; e-ISSN 2668-4756
Article DOI: https://doi.org/10.35219/mms.2019.2.10

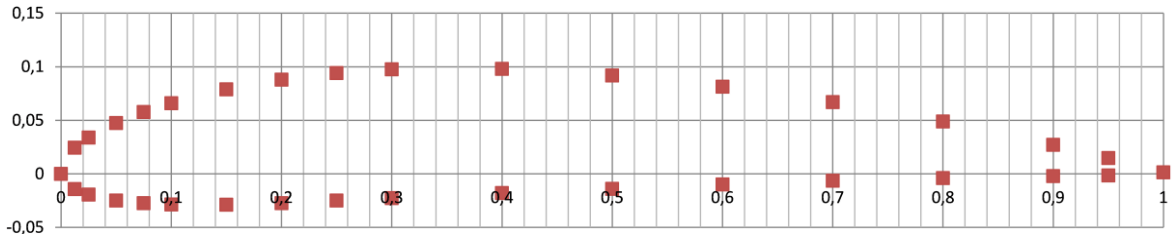

Fig. 1. *NACA4412 airfoil* [1]

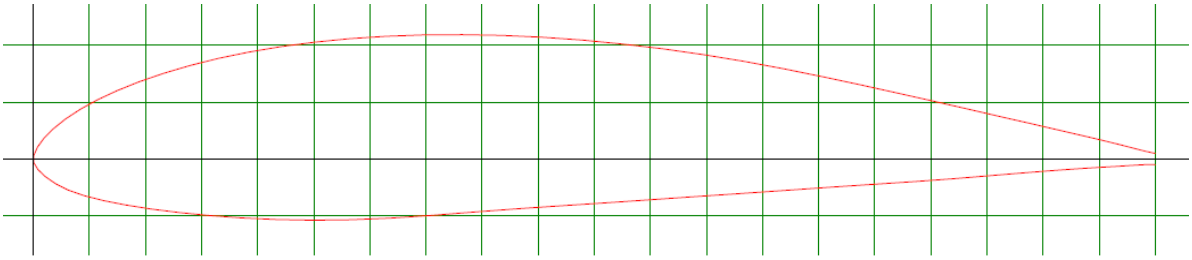

Fig. 2. *SG6050 (Selig/Giguere) airfoil for HAWT blade* [1]

2. Experimental conditions

The use of aerodynamic profiles (airfoil) when making blades for small wind turbines with three blades (upstream, turbine before the tower), is based on their special behaviour, respectively the lift force and drag force with an L / D ratio as high as possible [5].

An air-dynamic profile was used for which the angle of the chord of the profile with the wind direction from -90 to + 90 ° was changed, L and D are measured with sensors and plotted L and D for different positioning angles.

Abbreviations:
NACA - National Advisory Committee for Aeronautics (SUA)
UIUC - University of Illinois at Urbana-Champaign, (SUA)
NREL - National Renewable Energy Laboratory (SUA)

Notations:
v - wind speed, m/s;
v_a - apparent wind speed, m/s;
v_{tip} - tip speed of blade, m/s;
A - aria, m^2;
α - angle of attack, °;
φ - apparent wind angle with turbine plane, (base disk), °;
β - pitch angle of blade, °;
L - Lift force, N;
D - Drag force, N;
T - Thrust force, N;
DV - Driving Force, N;
k - quality airfoil coefficient
Re - Reynolds number, ad;

An experimental model (EM) is used in the form of an area of a wind turbine blade [3]. The experimental model is showed in Fig. 2 and has the following characteristics: blade length: 0.158 m, blade width: 0.158 m, maximum thickness: 0.030 m, chord: 0.158, length on intrados: 0.164 m, length on extrados 0.172 m: chord/ high ratio: 5.26.

For experiments we used: wind tunnel with maximum wind speed of 9 m/s, and measurement section of 0.5 m x 0.5 m x 1.25 m, anemometer LCA6000, balance for measuring forces at two points (with measuring cell and film resistors). The experimental measurement system also contains the following elements: SAD Arduino UNO, anemometer (2^{nd}), force cell type sensors for L and D, A/N converters with HC711, Futaba S3003 servomotor, program (code).

For experiments we have two independent variables: the wind speed and the positioning angle of the model. The dependent variables are: the lift force, the drag force [3]. The choice of model testing at different fixed wind speeds was chosen: 0 m/s, 3 m/s, 5 m/s and 9 m/s. For each of these, a graph showing the variation L and D with the rotating angle of the model is recorded (the angle of placement of the blade). The actuator rotates by 1 °/s and therefore it is considered static determinations.

THE ANNALS OF "DUNAREA DE JOS" UNIVERSITY OF GALATI
FASCICLE IX. METALLURGY AND MATERIALS SCIENCE
N°. 2 - 2019, ISSN 2668-4748; e-ISSN 2668-4756
Article DOI: https://doi.org/10.35219/mms.2019.2.10

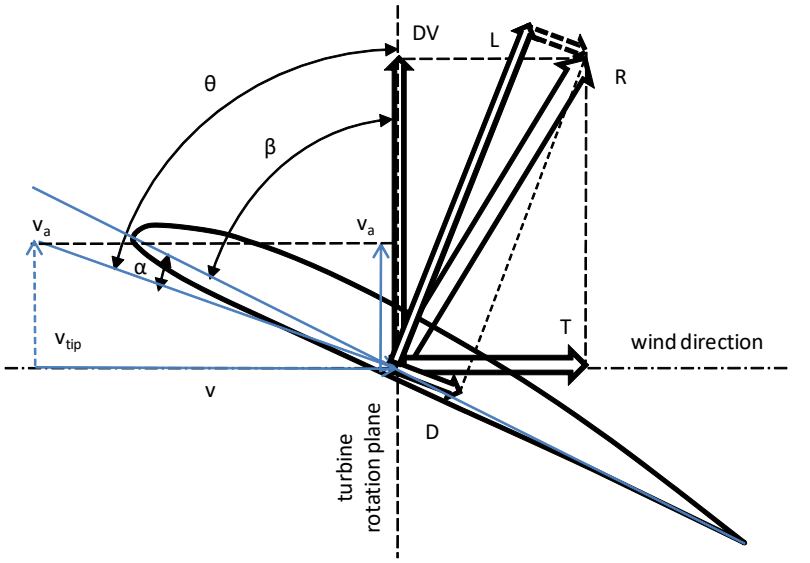

Fig. 3. *Principle diagram of the arrangement of velocity and force vectors for a three-blade wind turbine* [2]

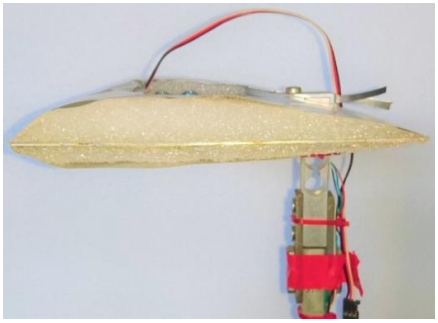

Fig. 4. *Experimental model at 0° angle*

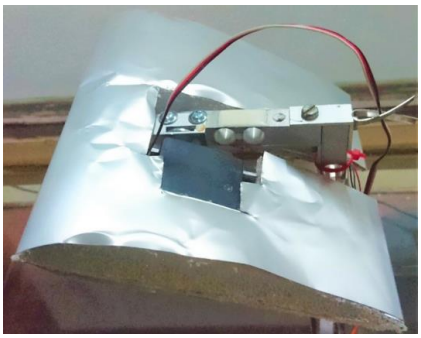

Fig. 5. *Experimental model in attack angle 0...15°*

3. Results and discussion

The variation L and D is tracked with the wind speed and for different values of the angle of attack. For this, for each wind speed (0 m/s, 3 m/s, 5 m/s and 9 m/s) a graph is recorded on the interval -90°... +90°. Below we analyse each graph. For the speed 0 m/s of the wind a variation of L and D caused by the change of the model's position with respect to the axis of rotation is observed, given that the axis of rotation is not exactly in the mass center.

The force is between -0.3...+0.5 N At speed v = 3 m/s it is found that L and D have distinct variations depending on the position of the blade, both have an approximately sinusoidal appearance with a phase gap between them. D is maximum at 0 degrees and 180 degrees on the graph which corresponds to the angles of -90° and +90°. The force L has a special variation in the sense that at -90° it has a small negative value (1 N) and then it increases to about +3 N. In this interval, the favourable angle of attack is also taken 5...15°, at the maximum value the area also showing a vortex variation. L / D = 3 (in absolute values).

At v = 5 m/s the curves L and D have the same allure on 180° range of variation. The values and slopes of the curves are changed. L has the maximum value 2N and at the same value D = -4N. The L / D ratio becomes small and its value is approx. 0.5. This shows a reduced fineness of the experimental model. D reaches -4N at about 90°. The positioning of the sensors makes the measured sheets not pure forces. For example, sensor D also adds a torque when the angle is different from zero. An exact calculation introduces corrections that take into account the true composition of forces and moments.

The behaviour of the model at v = 9 m/s. This is the maximum speed that the wind tunnel can develop. L reaches maximum 7 N at D = 10 N. That is L / D = 0.7 which shows a poor aerodynamic profile. Usual L / D = 5...10. When rotating from 90° to 0° L it increases and D is almost constant, around zero.

THE ANNALS OF "DUNAREA DE JOS" UNIVERSITY OF GALATI
FASCICLE IX. METALLURGY AND MATERIALS SCIENCE
No. 2 - 2019, ISSN 2668-4748; e-ISSN 2668-4756
Article DOI: https://doi.org/10.35219/mms.2019.2.10

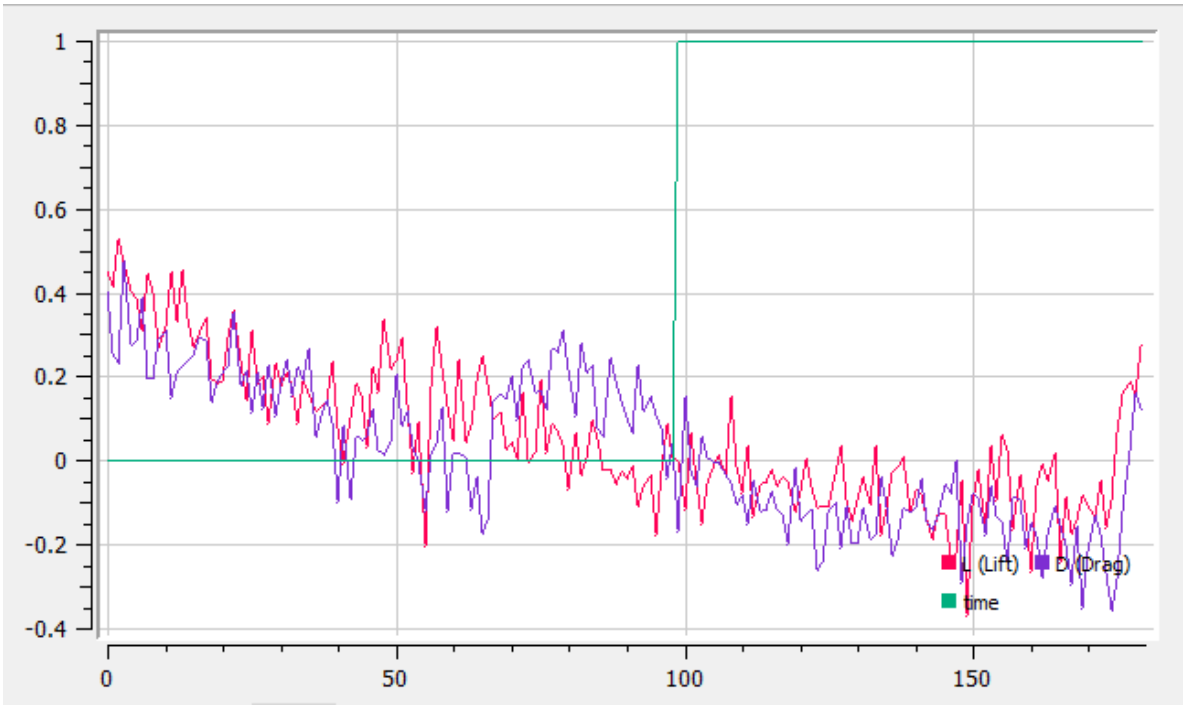

Fig. 6. *Variation of forces L and D (measured in N) at a cycle of 180° (-90°...+90°), without wind*

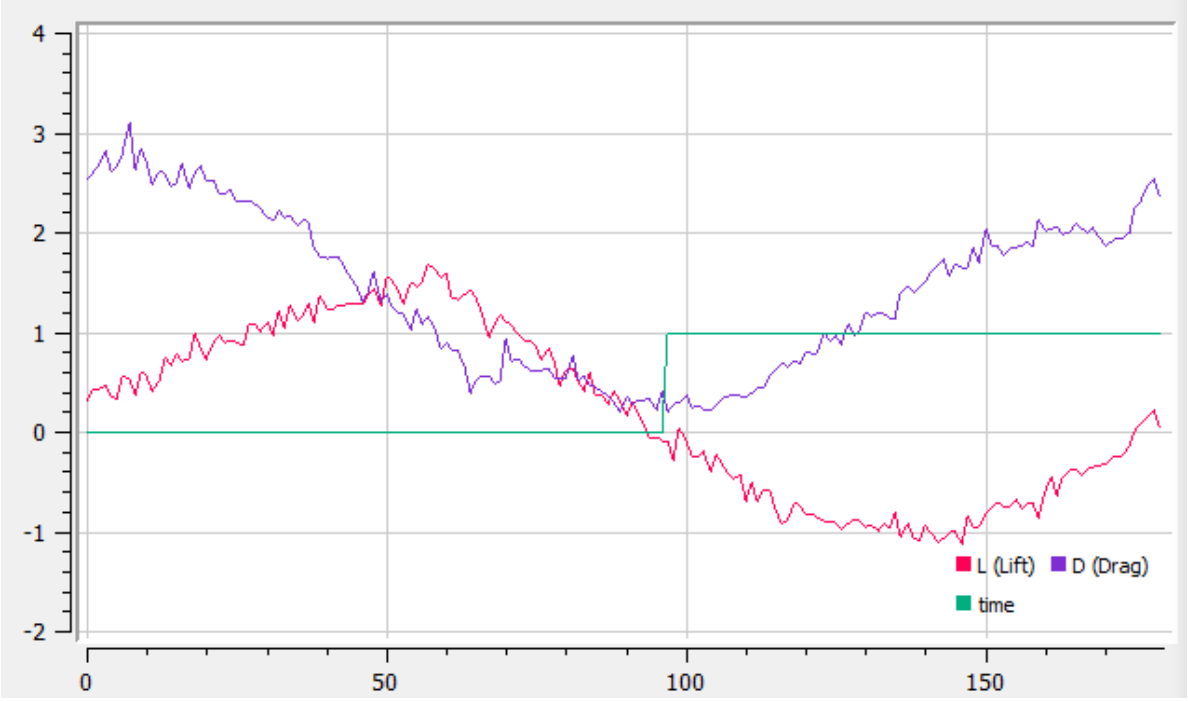

Fig. 7. *Variation of forces L and D (measured in N) at a cycle of 180° (-90°...+90°), for the wind speed of 3 m/s*

THE ANNALS OF "DUNAREA DE JOS" UNIVERSITY OF GALATI
FASCICLE IX. METALLURGY AND MATERIALS SCIENCE
No. 2 - 2019, ISSN 2668-4748; e-ISSN 2668-4756
Article DOI: https://doi.org/10.35219/mms.2019.2.10

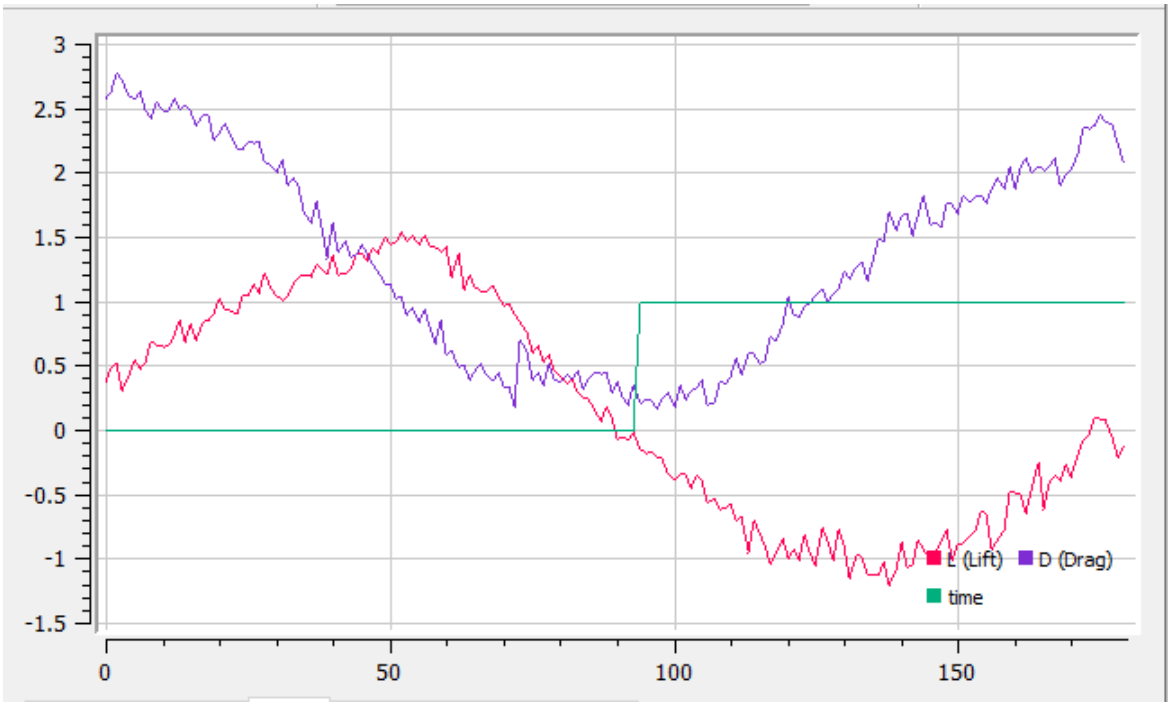

Fig. 8. *Variation of forces L and D (measured in N) at a cycle of 180° (-90°...+90°), at a wind of 5 m/s*

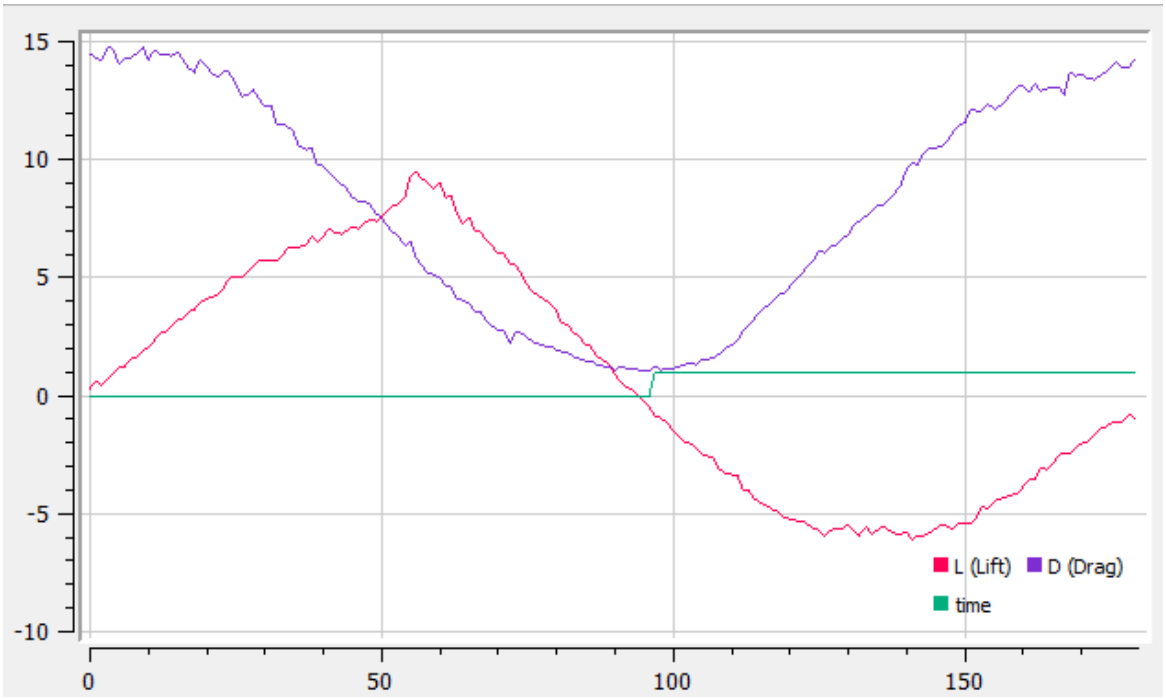

Fig. 9. *Variation of forces L and D (measured in N) at a cycle of 180° (-90°...+90°), at a wind of 9 m/s*

This shows that the resisting force overrides the mass of the model. Then at 90° a maximum of resistance and a minimum of lift is reached.

4. Conclusions

According to the figures Fig. 6…Fig. 9 analysed above, the proposed airfoil has a good behaviour at

THE ANNALS OF "DUNAREA DE JOS" UNIVERSITY OF GALATI
FASCICLE IX. METALLURGY AND MATERIALS SCIENCE
N°. 2 - 2019, ISSN 2668-4748; e-ISSN 2668-4756
Article DOI: https://doi.org/10.35219/mms.2019.2.10

high wind speeds (9 m/s) for which it has an attack angle range of approx. 40 degrees.

The axis of rotation must be placed in the center of mass of the experimental model to reduce errors (Fig. 6).

The quality coefficient of the L / D profile is 3 to 3 m/s (maximum value).

The lift force has a maximum value of 10 N at 9m/s and the values of the drag force increase with the speed, t and reach a maximum of 15 N. When the profile is placed with the chord in the wind direction the drag force had minimum values for all experiments with wind speed greatest than zero.

References

[1]. ***, http://airfoiltools.com/airfoil/details?airfoil=naca4412-ilAirfoil Tools.
[2]. Dumitrescu H., Georgescu A., *Calcului elicei, Cap.4 Elicea eoliana*, s.l.: Editura Academiei Romane, 1990.
[3]. Selig Michael S., McGrahan Brian D., *Wind Tunnel Aerodynamic Tests of Six Airfoils for Use on Small Wind Turbines*, Urbana, Illinois: NREL, vol. NREL/SR-500-34515, 2004.
[4]. Hau Erich, *Wind Turbines, Fundamentals, Technologies, Applications, Economics*, s.l.: Springler, 2006.
[5]. Smulders P. T., *Rotors for wind power*, Eindhoven: University of Technology, Eindhoven, Faculty of Physics, 1st edition October 1991, (revised edition January 2004).
[6]. Manwell J. V., McGowan J. G., Rogers A. L., *Wind Energy Explained. Theory, Design and Application*.
[7]. Mathew Sathyajith, *Wind Energy_Fundamentals, Resource Analysis and Economics*, s.l.: Springer, 2006.

MANUSCRISELE, CĂRŢILE ŞI REVISTELE PENTRU SCHIMB, PRECUM ŞI ORICE CORESPONDENŢE SE VOR TRIMITE PE ADRESA:

MANUSCRIPTS, REVIEWS AND BOOKS FOR EXCHANGE COOPERATION, AS WELL AS ANY CORRESPONDANCE WILL BE MAILED TO:

LES MANUSCRIPTS, LES REVUES ET LES LIVRES POUR L'ECHANGE, TOUT AUSSI QUE LA CORRESPONDANCE SERONT ENVOYES A L'ADRESSE:

MANUSCKRIPTEN, ZIETSCHRITFTEN UND BUCHER FUR AUSTAUCH SOWIE DIE KORRESPONDENZ SID AN FOLGENDE ANSCHRIFT ZU SEDEN:

After the latest evaluation of the journals by the National Center for Science Policy and Scientometrics (**CENAPOSS**), in recognition of its quality and impact at national level, the journal will be included in the B^+ category, 215 code (http://cncsis.gov.ro/userfiles/file/CENAPOSS/Bplus_2011.pdf).

The journal is already indexed in:

SCIPIO-RO: http://www.scipio.ro/web/182206

EBSCO: http://www.ebscohost.com/titleLists/a9h-journals.pdf

Google Academic: https://scholar.google.ro

Index Copernicus: https://journals.indexcopernicus.com

The papers published in this journal can be viewed on the website of "Dunarea de Jos" University of Galati, the Faculty of Engineering, pages: http://www.sim.ugal.ro, http://www.imsi.ugal.ro/Annals.html.

Name and Address of Publisher:
Contact person: Elena MEREUȚĂ
Galati University Press - GUP
47 Domneasca St., 800008 - Galati, Romania
Phone: +40 336 130139
Fax: +40 236 461353
Email: gup@ugal.ro

Name and Address of Editor:
Prof. Dr. Eng. Marian BORDEI
"Dunarea de Jos" University of Galati, Faculty of Engineering
111 Domneasca St., 800201 - Galati, Romania
Phone: +40 336 130208
Phone/Fax: +40 336 130283
Email: mbordei@ugal.ro

AFFILIATED WITH:

- THE ROMANIAN SOCIETY FOR METALLURGY
- THE ROMANIAN SOCIETY FOR CHEMISTRY
- THE ROMANIAN SOCIETY FOR BIOMATERIALS
- THE ROMANIAN TECHNICAL FOUNDRY SOCIETY
- THE MATERIALS INFORMATION SOCIETY (ASM INTERNATIONAL)

Edited under the care of the FACULTY OF ENGINEERING

Annual subscription (4 issues per year)

Fascicle DOI: https://doi.org/10.35219/mms

Volume DOI: https://doi.org/10.35219/mms.2019.2

Editing date: 15.06.2019
Number of issues: 200
Printed by Galati University Press (accredited by CNCSIS)
47 Domneasca Street, 800008, Galati, Romania